Functional characterisation of the mechano-electrical transduction complex of the auditory hair cells

Ménélik Labbe

Université Pierre et Marie Curie

Ecole doctorale Complexité du Vivant

Unité de Génétique et Physiologie de l'Audition

Caractérisation fonctionnelle du complexe de transduction mécano-électrique des cellules ciliées du système auditif

Functional characterisation of the mechano-electrical transduction complex of the auditory hair cells

Par Ménélik LABBÉ

Thèse de doctorat de Neurosciences

Dirigée par le Professeur Christine PETIT

Présentée et soutenue publiquement le 12 avril 2016

Devant un jury composé de :

Serge PICAUD	Professeur	Président
Fabrice GIRAUDET	Maître de conférences	Rapporteur
Christophe VINCENT	Professeur	Rapporteur
Christine PETIT	Professeur	Directrice de thèse

Acknowledgements

Firstly, I would like to thank Christine Petit for giving me the opportunity to undertake my PhD in her lab, and by the same token, allowing me to meet and discuss with a number of passionate scientists on campus at the Institut Pasteur in Paris. Secondly, I would like to express my sincere gratitude and appreciation to my supervisor, Nicolas Michalski, on whom I have been able to count for any matter, whether it be scientific or personal.

I would also like to thank Serge Picaud for accepting to be the president of the jury of my thesis committee, as well as Fabrice Giraudet and Christophe Vincent for accepting to be the “rapporteurs” of my thesis committee.

Contents

MATERIALS & METHODS

RESULTS

DISCUSSION

List of figures

List of abbreviations

ABR	auditory brainstem response
Adgrv1	adhesion G protein-coupled receptor v1
BAPTA	1,2-bis(o-aminophenoxy)ethane-N,N,N’,N’-tetraacetic acid
Cdh23	cadherin-23
CIB2	calcium and integrin binding family member-2
DFNB	autosomal-recessive for of deafness
DPOAE	distorsion product otoacoustic emission
IHC	inner hair cell
MET	mechano-electrical transduction
OHC	outer hair cell
PBM	PDZ binding motif
Pcdh15	protocadherin-15
PCP	planar cell polarity
PDZ	postsynaptic density 95/disc large/zonula occludens-1 domain
PDZD7	PDZ domain containing 7
SEM	scanning electron microscopy
SPL	sound pressure level
TM	transmembrane domain
USH	Usher syndrome
Whrn	whirlin

INTRODUCTION

I. The human ear

I.1 Anatomy and function of the mammalian inner ear

The mammalian ear is composed of three distinct parts: the outer ear, the middle ear and the inner ear (**Figure 1**). The external ear's function is to capture and channel sound waves along the external auditory meatus. The waves then propagate through the middle ear, an air-filled cavity delimited by two membranes: the tympanum (or eardrum) and the oval window. Upon sound stimulation, the tympanum vibrates, transforming the airborne acoustic waves into solid mechanical waves, capable of propagating through the three ossicles located in the middle ear: the malleus (or hammer), the incus (or anvil) and the stapes (or stirrup). Through the lever action of the ossicles and a reduction in the area of force distribution, the sound wave is amplified. Amplification at this level allows the sound wave to cross the oval window and into inner ear. Because the inner ear is a fluid-filled cavity, if the sound wave were to arrive at the oval window, an air/liquid interface, without amplification, it would almost entirely be reflected back towards where it came from. The role of the middle ear is thus to act as an impedance adaptor, by compensating the loss of energy resulting from the changes in medium that occur between the external and inner ear.

While the external and middle ears are solely dedicated to auditory functions, the inner ear however is involved in auditory as well as equilibration functions. It is composed of the vestibule, the organ responsible for equilibration, and the cochlea, the organ responsible for hearing (**Figure 1**).

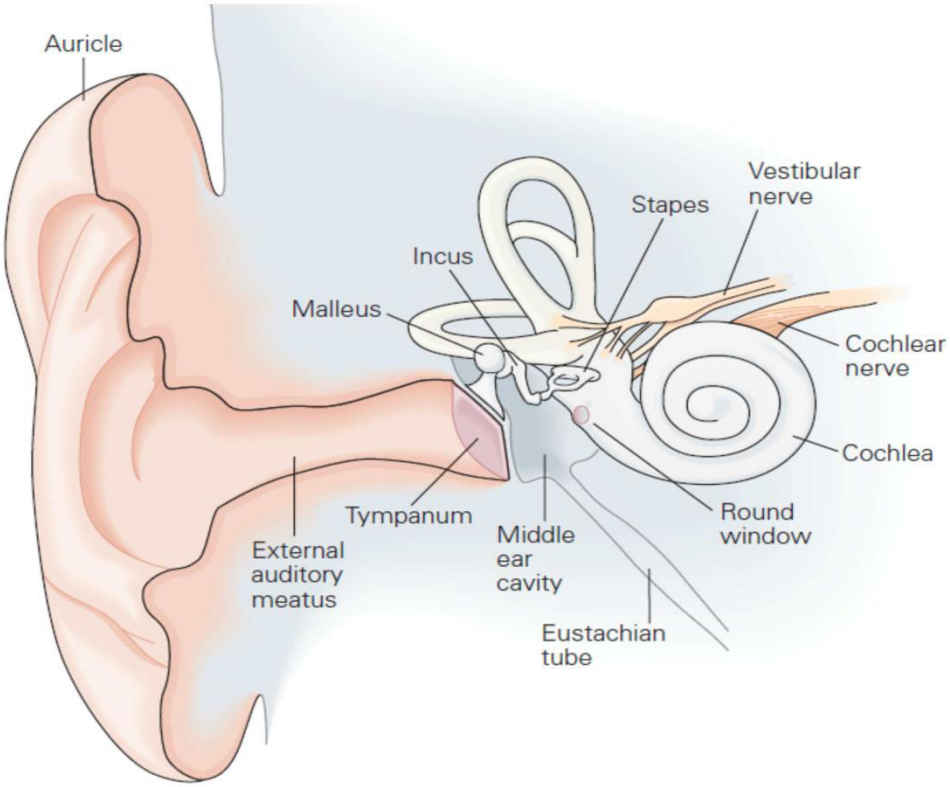

Figure 1. The human ear (adapted from Kandel et al., 2000)

I.2. Anatomy and physiology of the vestibule

The vestibule is the organ responsible for equilibration. Just like the cochlea, the vestibule uses highly specialised sensory cells, called hair cells, to detect the linear accelerations and rotational movements of the head. Hair cells are equipped at their apex with a mechanical antenna, called the hair bundle, where the transformation from mechanical to chemical signal is initiated. The information is sent to the central nervous system which coordinates head and eye movements, as well as body posture, to maintain balance.

In the vestibule, hair cells are grouped into 5 distinct neuroepitheliums: the saccule and the utricule, that detect linear accelerations, and the three ampullæ, that detect the angular accelerations of the head. The utricule is responsible for the detection of linear

accelerations on the horizontal plane, while the saccule is responsible for detecting accelerations on the vertical plane. The ampullæ detect angular movements of the head in the three possible axes: from left to right, up and down and the tilting of the head. They are situated in the three semi-circular canals and are orthogonal to one another.

Each one of these neuroepitheliums contains a sensory epithelium, called the macula, which is composed of sensory hair cells surrounded by supporting cells. Sensory hair cells are capable of producing electrical signals, although they are bereft of any axon or dendrites. The hair bundles of the hair cells are covered by the otoconial membrane, a gelatinous structure, formed by intertwined filaments organised in a mesh-like pattern, and the otoconial membrane is covered by calcite crystals, called otoconies, which play an important role in the sensitivity of the maculæ. When acceleration occurs, a force is exerted on the otoconies, and because of their inertia, this leads to a synchronised movement of the hair bundles. Depending on their orientation, certain hair cells are depolarised or hyperpolarised and the resulting information is then transmitted to the brain through the vestibular nerves.

I.3. Anatomy and physiology of the cochlea

The cochlea is a bony tube coiled around a conical bony core called the modiolus. A human cochlea consists of slightly less than three coils whereas in mice it is 1.75 coils long. The cochlea contains three fluid-filled compartments: the *scala vestibuli*, the *scala media* (or cochlear duct) and the *scala tympani* (**Figure** 2). The *scala vestibuli* and *scala tympani* are filled with a classic extracellular medium, rich in Na^+ ions (140 mM) and poor in K^+ ions (3- 5

mM), called the perilymph. The *scala media*, however, is filled with a very specific liquid called the endolymph. This liquid is abnormally rich in K^+ ions (150 mM) and poor in Na^+ ions (1mM). These unexpected extracellular concentrations are possible thanks to the *stria vascularis* which lines the external wall of the *scala media* and reabsorbs the Na^+ and secretes K^+ against their gradients (Figure 3). Because of the differences in ionic concentrations and the electrical isolation of the *scala media*, the endolymph has an electric potential of approximately +80 mV with respect to the perilymph. This electric potential is called the endocochlear potential and is crucial to the mechano-electrical transduction process which I will describe a little further in the manuscript.

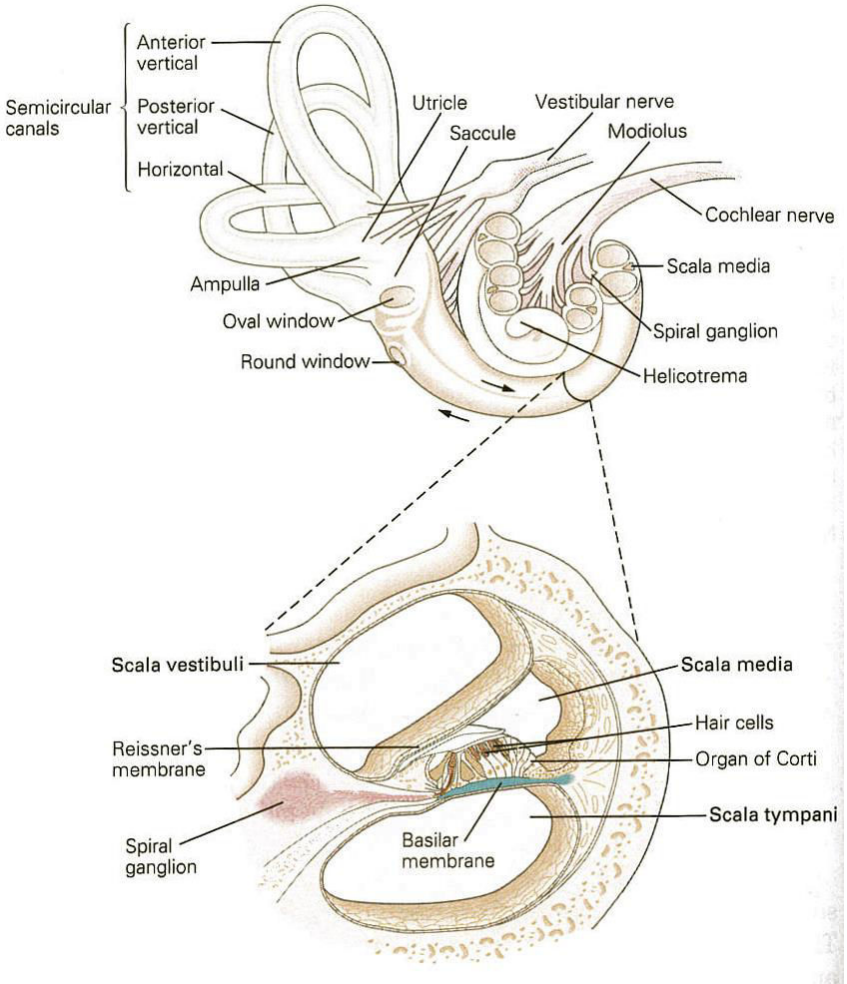

Figure 2. Cross-section of mammalian cochlea (adapted from Kandel et al., 2000)

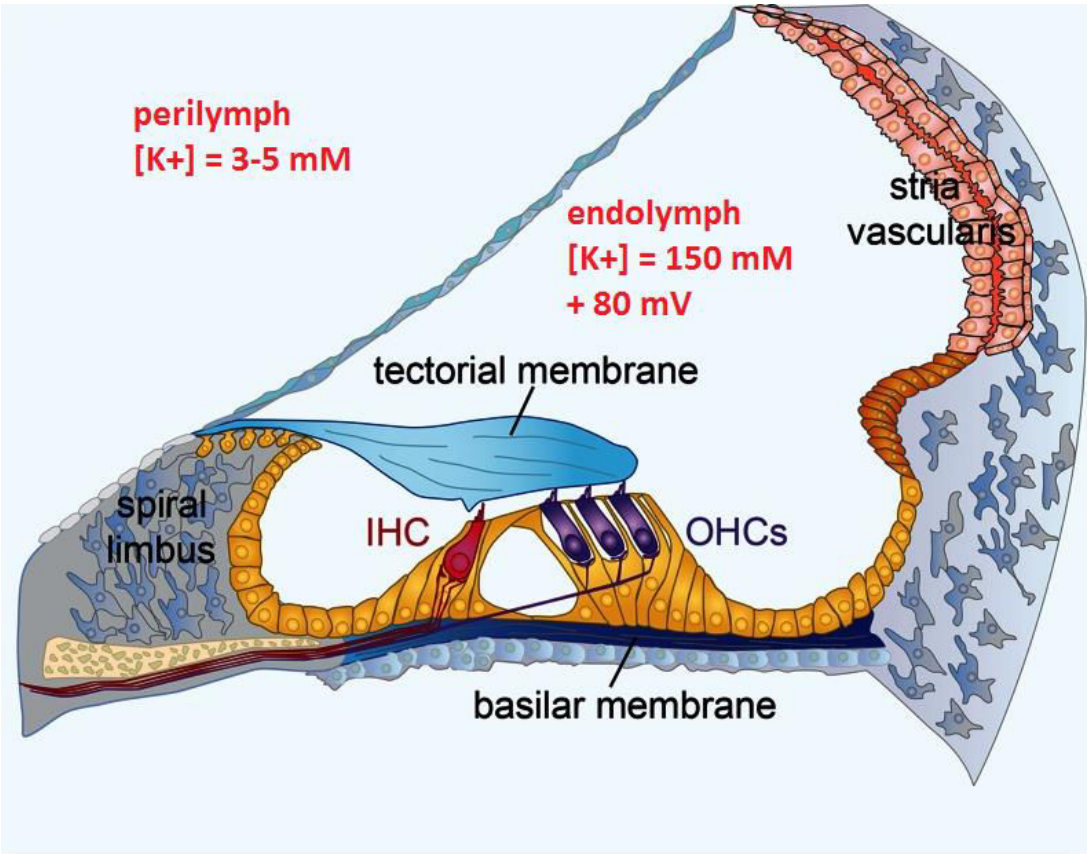

Figure 3. Ionic concentrations in the perilymph and endolymph (figure adapted from Michalski & Petit, 2015)

I.3.A. The basilar membrane

The *scala vestibuli* and the *scala media* are separated by a thin membrane, called the Reissner membrane, whereas the *scala media* and the *scala tympani* are separated by the basilar membrane, upon which the auditory neurosensory epithelium, the organ of Corti, rests. The basilar membrane possesses very particular mechanical properties which are responsible for the frequency discrimination capabilities characteristic of the cochlea. The work of von Bekesy (**Von Bekesy, 1954**) has shown that a pure tone does not provoke the oscillation of the basilar membrane in a unique position, but rather that there is a wave that

reaches a maximum amplitude at a specific characteristic frequency position, before rapidly petering out in direction of the cochlea apex. In humans, and in other species including mice, the basilar membrane is larger and more flexible at the apex than at base. High-frequency sounds reach their maximum amplitude in the basal region of the basilar membrane, whereas low frequency sounds reach their maximum amplitude in the apical region. This frequency gradient is known as the tonotopic organisation of the cochlea, and it determines the audible frequency range for a given species.

I.3.B. The organ of Corti and the hair cells

The organ of Corti, the hearing sensory neuro-epithelium, rests upon the basilar membrane, and is covered by an acellular gel called the tectorial membrane (Figure 3). It is composed of two families of cells: the auditory sensory hair cells and the supporting cells.

Supporting cells are non-sensory cells that form tight junctions with the auditory sensory hair cells. These tight junctions are located at the apex of the cells and act as a barrier between the two extracellular media, the endolymph and the perilymph. In this way, hair bundles of the sensory hair cells bathe in endolymph whereas the cell bodies bathe in perilymph. This compartmentalisation of the organ of Corti is essential to the mechano-electrical transduction (MET) process, even though MET solely occurs in sensory hair cells.

In the cochlea, hair cells subdivide into two categories: the inner hair cells (IHCs) and the outer hair cells (OHCs). There are approximately 3000 to 3500 IHCs, and 9000 to 12000 OHCs in humans which, compared to other sensory epitheliums in the body, represents a very small number. For example, the sensory organ of vision, the retina, contains several

million photoreceptor cells. Furthermore, following a gradient from the base to the apex of the cochlea, the cell body diameter of the hair cells varies from 10 to 20 μm and their length, from 10 to 50 μm. Hair cells of the cochlea are organised in such a way that IHCs form a single row of cells on the neural side (modiolus) of the organ of Corti, whereas OHCS form 3 rows of cells, situated toward the abneural side of the organ (**Figure 4**). IHCs and OHCs are separated by the pilar cells, which form the tunnel of Corti, and contribute to the overall stiffness of the organ. IHCs receive 95% of the organ of Corti's afferent nerve fibres while OHCs on the other hand, mainly receive efferent nerve fibres. IHCs are the genuine auditory sensory cells, whereas OHCs play a major role in sound amplification. This is possible thanks to a protein located in the membrane of the OHC cell body, called prestin. Prestin possesses piezo-electric properties which allow OHCs to contract or extend their cell body length in response to a modification of their membrane potential. OHC contraction/extension movements are transmitted to the basilar membrane through the Deiter cells, thus contributing to cochlear amplification.

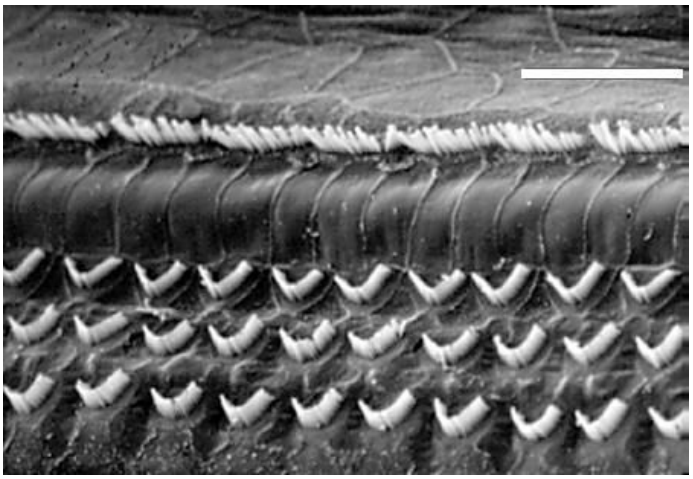

Figure 4. Scanning electron micrograph illustrating the 3 rows of OHCs, and the single row of IHCs in the organ of Corti

I.3.C. The hair bundle and mechano-electrical transduction (MET)

I.3.C.1. Morphological aspects of the hair bundle

The first studies on the development of the hair bundle were conducted on the chicken (**Tilney et al., 1992**), but with the introduction of genetics to the study of hearing deficits, mice then became the preferred animal model, and results obtained in mice mirrored those first found in the chicken.

There are three main phases in hair bundle development. During the first phase, several small microvilli appear at the apex of the hair cells and aggregate around a central cilium, called the kinocilium. In a second phase, the kinocilium and the growing microvilli then migrate to the periphery of the apical surface and the microvilli situated closest to the kinocilium begin to increase in length. Subsequently, the microvilli situated a little further from the kinocilium also increase in length. In the third phase, the kinocilium and the growing microvilli settle in their final position (**Figure 5**).

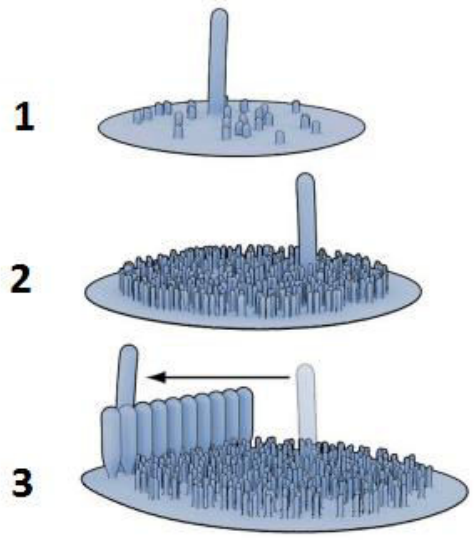

Figure 5. Schematic representation of sequential stages of hair bundle development (adapted from Schwander et al., 2010)

The final position of the kinocilium, and thus the proper orientation of the hair bundle, is of the utmost importance, and there are several planar cell polarity genes implicated in this crucial process. These genes include *Vangl1, Vangl2, Frizzled-3, Frizzled-6, Disheveled-1, Disheveled-2, Disheveled-3,* as well as genes responsible for Usher syndrome type 1, a syndrome I will detail later in the manuscript, as it is an important part of my PhD work. Furthermore, GTP-binding protein αi subunits (Gαi) control mitotic spindle orientation (**Walsh et al., 2010; Doherty et al., 2012**) and were recently found to be involved in kinocilium migration, and in hair bundle shape and orientation (**Ezan et al., 2013; Tarchini et al., 2013**). These proteins are located in the apical region of the hair cell, on its abneural side, between the cell junction and the hair bundle, forming a crescent-shaped domain (**Figure 6**). The role of Gαi in hair bundle shape was confirmed in *Gαi3* mutant mice that display flattened hair bundle shapes and mislocalised kinocilia (**Lefevre et al., 2008; Ezan et al., 2013**).

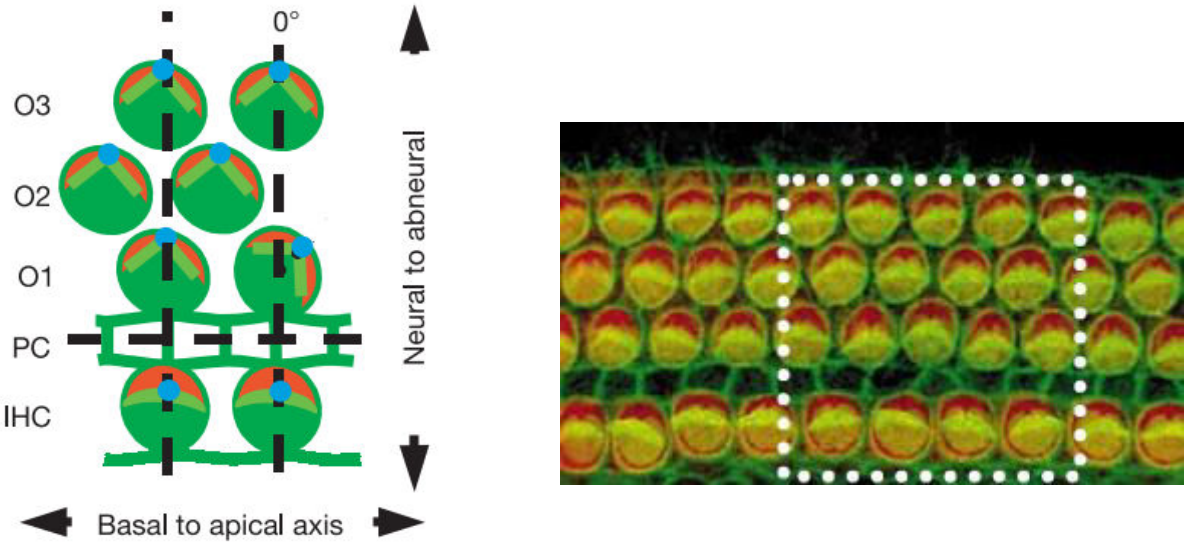

Figure 6. Schema and immunofluorescent image illustrating the crescent-shape disposition of PCP proteins in wild-type mice
(adapted from Montcouquiol et al., 2003)

The formation of the staircase pattern, typical of the hair bundle, is initiated by the elongation of the microvilli closest to the kinocilium. During a 2- to 3-day period, depending on the species, the number of actin filaments inside each microvilli (or stereocilium) increases simultaneously across the whole cochlea. During the final phase of stereocilia growth, all the rows grow at the same rate but the stereocilia from the shortest row stop growing first and the ones from the tallest row stop last. The difference in elongation time is also the reason behind the difference in stereocilia length between the apex (long stereocilia) and the base of the cochlea (short stereocilia). The shorter the stereocilia are, the higher their resonance frequency will be, and in this way their sensitivity to high-frequency sound stimuli is increased. Hair bundles come in all shapes and sizes, with variations observed from one species to another, from one organ to another and even differences within the same neuroepithelium. Hair bundles can be of different lengths, have stereocilia of different widths or have an altogether different shape. The explanation for these differences lies within the fact that different hair bundles process different types of information. For example, vestibular hair bundles in mice form a very compact hexagonal structure and have a kinocilium located next to the tallest stereocilia, which persists at adult stages (**Figure 7**).

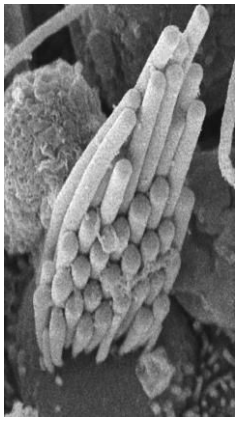

Figure 7. Scanning electron micrograph of a normal vestibular hair bundle (image courtesy of Vincent Michel)

This is not the case in the mouse cochlea, where the kinocilium disappears approximately a week-to-10 days after birth. In the cochlea, IHC and OHC hair bundle structures are very distinct. Both types of hair bundles are composed of three rows of stereocilia but IHC hair bundles are U-shaped and progressively become linear along the tonotopic axis. OHC hair bundles on the other hand are a V-shaped structure, pointing towards the abneural side of the cochlea (**Figure 4**). The tallest row of OHC stereocilia is directly coupled to the tectorial membrane (**Verpy et al., 2011**), and during acoustic stimulation, when the basilar membrane vibrates, the movement leads to tension at the stereocilia/tectorial membrane junction along the apex-to-base axis of the cochlea as well as along the radial (neural-to-abneural) axis. The V-shape of the OHC hair bundles plays a critical role, as it allows the stereocilia to take into account both components of the movement simultaneously.

The formation of the hair bundle and the maintenance of its cohesiveness are orchestrated by several types of links that come into play at different developmental stages. In 1984, using the guinea pig as a model, and by using both scanning and transmission electron microscopy, Pickles and collaborators showed the existence of an array of cross-links between stereocilia. Most notably, they observed that the tip of each shorter stereocilium on the hair cell gave rise to a single, upwards-pointing link, which connected with the stereocilium of the adjacent taller row. This link was called the tip link and it was suggested that its distortion lead to sensory transduction (**Pickles et al., 1984**). It was only in 1991 however, through biochemical experiments, that Assad J.A. and collaborators were able to show that the tip link was indeed physiologically implicated in the MET process. The different types of cochlear links were first biochemically characterised by testing their relative resistance to chemical treatments. The two main chemical products used are 1,2-

bis(o-aminophenoxy)ethane-N,N,N',N'-tetraacetic acid (BAPTA), which is a high-affinity calcium chelator, and a protease called subtilisin. It was shown that tip links were disrupted by BAPTA but not by subtilisin. In the presence of BAPTA, MET currents could no longer be measured, but if sufficient time was given after BAPTA treatment, tip links and MET currents reappeared (**Assad et al., 1991; Crawford et al., 1991; Zhao et al., 1996**).

In mice, fibrous links connecting the stereocilia appear before birth and undergo a rapid evolution within a few developmental days (**Figure 8**). At E17.5, towards the base of the cochlea, where hair bundles already have a certain degree of organisation, a fairly important number of links are present, called lateral links. At this age, kinocilial and slanted apical links are clearly visible but the rest of the links situated below are more difficult to make out. As of postnatal day 2 (P2) however, from top to bottom of the hair bundle, three types of links can be described: the tip links (previously the slanted apical links), the shaft connectors and the ankle links (**Figure 8**) (**Goodyear et al., 2005**). Tip links play a direct role in the MET process, as it has previously been mentioned, and in hair bundle development, while shaft connectors and ankle links only play a role in hair bundle development. Despite them only being a transient structure in the developing hair bundle in the mouse cochlea, i.e. they exist from P2 to P9, ankle links play an essential role in hair bundle cohesion and shaping, as I will further discuss in the Results chapter of my manuscript.

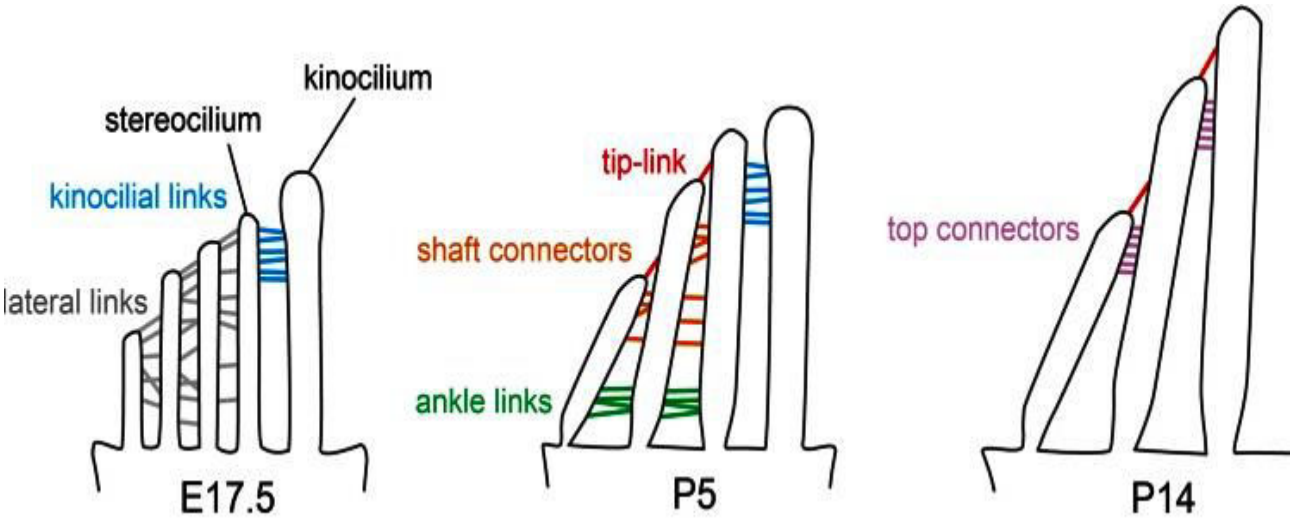

Figure 8. The different interstereociliary links during hair bundle development (adapted from Michalski and Petit, 2015)

In P2 OHCs and IHCs, tip links and ankle links are clearly present, while shaft connectors, distinct from tip links and ankle links, can be seen sporadically. From P2 to P9, although it increases in length, and stereocilia move slightly apart from one another, the hair bundle doesn't dramatically change in appearance. As of P9 however, ankle links start to disappear, and another type of link, the horizontal top connectors, that join the apical regions of adjacent stereocilia within OHC hair bundles, start to appear. By the onset of hearing at P12, ankle links are no longer present, and horizontal top connectors are continuing to develop and are seen more frequently than at P9. It is only at P14 that horizontal top connectors finally reach their mature appearance. Furthermore, from P19 onwards, OHCs have highly organised horizontal top connectors that exist both between the stereocilia within the same row and between the stereocilia of adjacent rows (**Goodyear et al., 2005**).

A

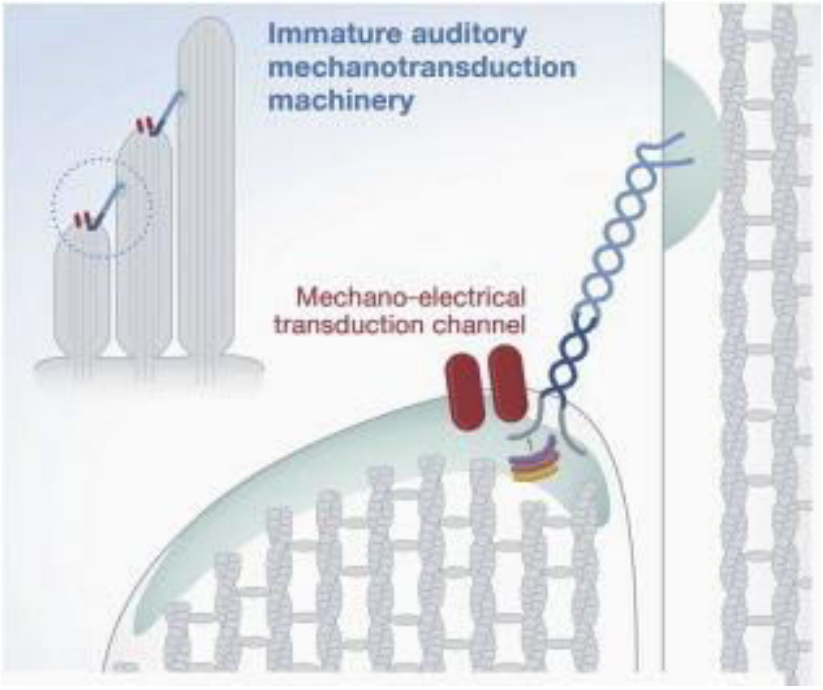

B

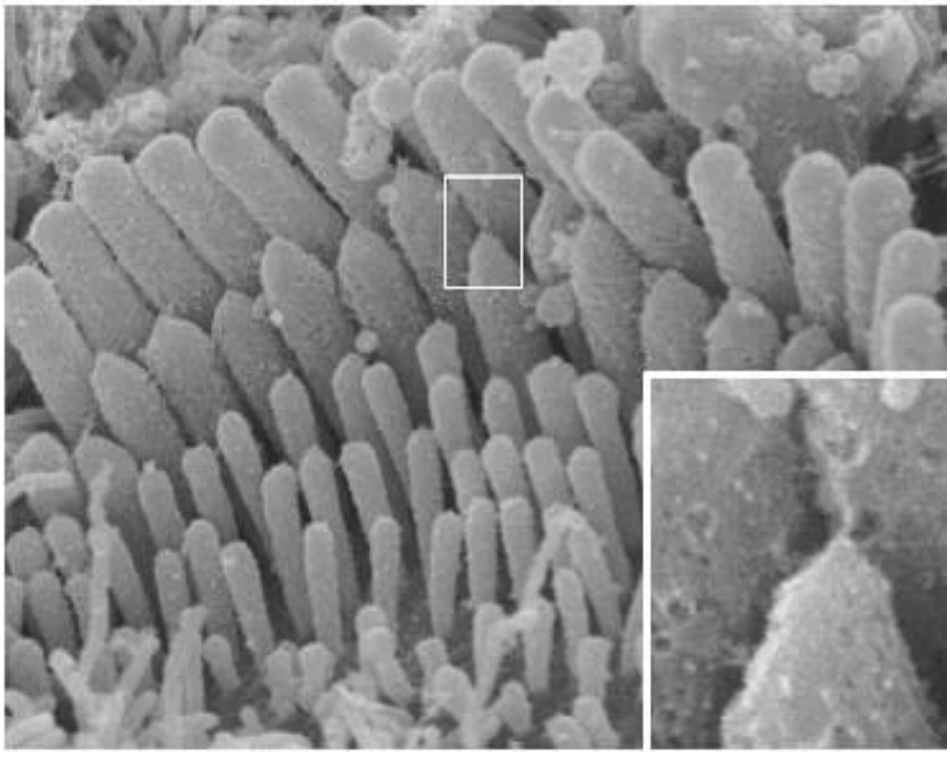

Figure 9. (A) Schematic representation of the tip link
(B) Scanning electron micrograph of an IHC and a tip link
(adapted from Pepermans and Petit, 2015)

Top connectors are the most resilient type of lateral link in the hair bundle, as they are the only links to persist in presence of both BAPTA and subtilisin, and ankle links are the weakest links because in presence of either BAPTA or subtilisin, they are disrupted (**Jacobs and Hudspeth, 1990; Assad et al., 1991; Goodyear and Richardson, 1999; Goodyear et al., 2003**)

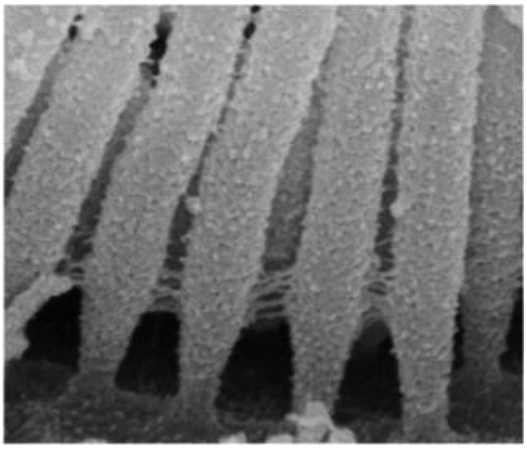

Figure 10. Scanning electron micrograph of the ankle links (image courtesy of Vincent Michel)

I.3.C.2. The MET channel

The first step of the MET process takes place in the hair bundle, and the first important biophysical properties of this process were characterised by A.J. Hudspeth, D.P. Corey and R. Jacobs in the late 70's (**Hudspeth and Corey, 1977; Hudspeth and Jacobs, 1979**). Using the *Rana Catesbeiana* bullfrog as a working model, Hudspeth and his collaborators were able to simultaneously control hair bundle movement as well as measure hair cell receptor potential. Through their experiments, they showed that the hair cell is depolarised following a displacement of its hair bundle in the excitatory direction, i.e.

towards the tallest stereocilia, and is hyperpolarised when the hair bundle is displaced in the inhibitory direction. They also showed that the hair cell's response to small displacements (up to 0.4 μm) is linear, but then starts to saturate as the displacement gets bigger. Finally, by isolating the kinocilium, they showed that the stereocilia, and not the kinocilium, were well and truly the structure where mechano-electrical transduction occured.

Several hypotheses were put forward to explain hair cell depolarisation but the most plausible one was that an ionic channel was located somewhere along the stereocilia or at the junction between stereocilia and the hair cell apex. To prove the veracity of this hypothesis, extracellular potentials were measured at different positions of mechanically stimulated hair bundles. These potentials were consistently larger near the top of the hair bundle than anywhere else around the hair bundle, suggesting that the transduction apparatus was situated toward the apical end of the stereocilia (**Figure 11**) (**Hudspeth, 1982**).

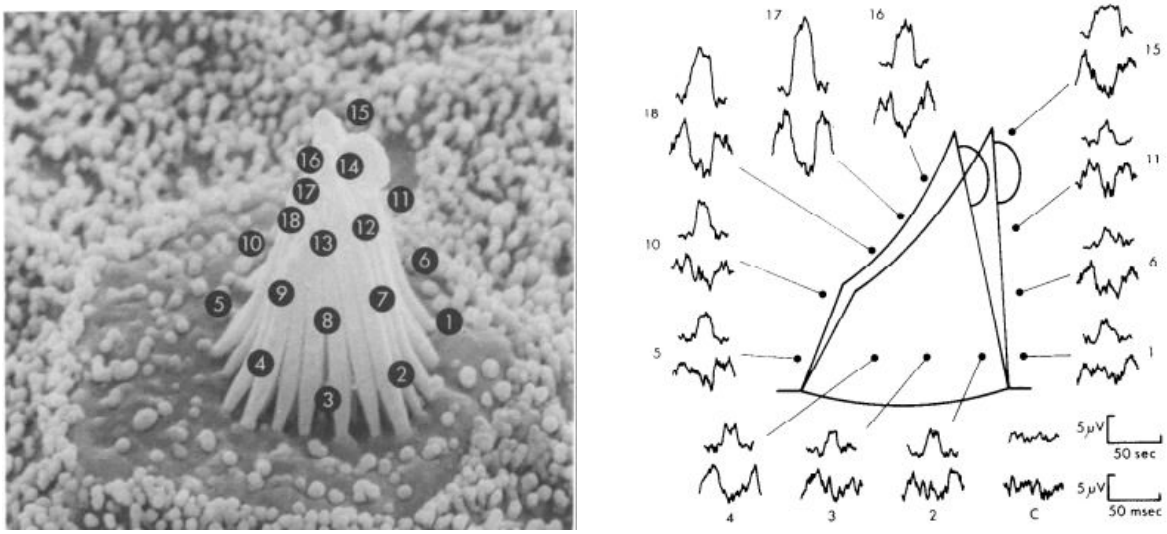

Figure 11. Localisation of mechano-electrical transduction channel by extracellular potential measurements
(adapted from Hudspeth, 1982)

On the back of these initial results, which type of mechanism activated the transduction apparatus was investigated. Three types of mechanisms were considered possible: (i) an enzymatic mechanism, (ii) a mechanism involving secondary messengers and (iii) a direct mechanical coupling of the MET channel to stereocilia. The first two mechanisms were rapidly discarded for kinetic reasons, i.e. the MET channel opening time is too fast to be compatible with processes involving enzymatic regulation or secondary messengers (**Corey and Hudspeth, 1983**). Mechanical coupling of the MET channel to stereocilia was thus considered to be the most consistent way of viewing the MET process. This hypothesis consisted in assuming that through a direct elastic link, the *gating spring* (which would later turn out to be the tip link), displacement of the stereocilia would directly influence the energy difference between open and closed states of the MET channel, as does the change of potential for voltage-activated channels (**Figure 12**) (**Corey and Hudspeth, 1983; Howard and Hudspeth, 1987**).

Further evidence supporting the gating spring theory was given in the late 1980's by Howard and Hudspeth. By measuring hair bundle stiffness, they observed an instantaneous relaxing of the hair bundle upon mechanical stimulation. This mechanism is called the *gating compliance* (**Howard and Hudspeth, 1988**) and can be described in the following way: a positive deflection of the hair bundle increases tension in the gating spring, and while the channel remains closed, only the length of the spring increases. However, because the spring is directly coupled with the MET channel, once the channel opens, the length of the spring instantly decreases leading to a general relaxing of the hair bundle. In addition, Howard and Hudspeth showed that in presence of gentamycine, a MET channel blocker, there is no relaxing of the hair bundle, providing further evidence in favour of the gating spring and gating compliance theories (**Howard and Hudspeth, 1988**).

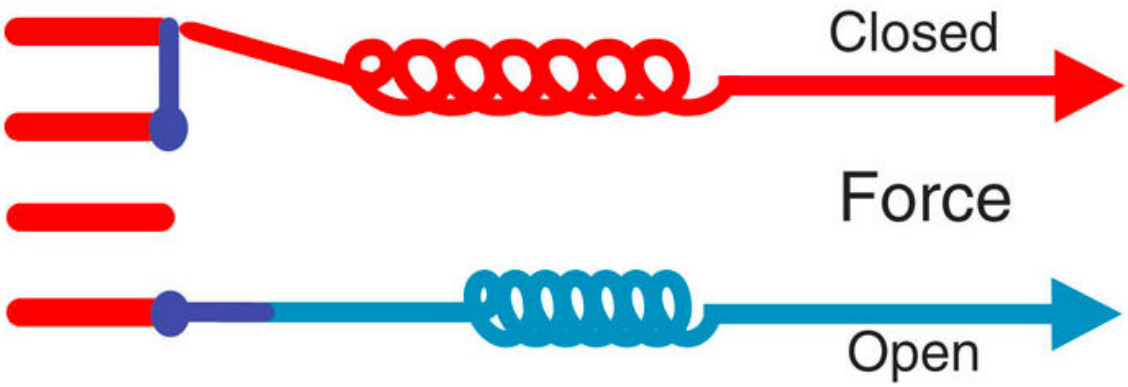

Figure 12. Schematic representation of the *gating spring* model (adapted from Peng et al., 2011)

Because MET channels are highly permeable to calcium, calcium-entry monitoring systems were used to locate the MET channel to the tip of the stereocilia (**Lumpkin and Hudspeth, 1995**), and determine the number of channels per stereocilium. A study led by Denk and colleagues in 1995, using two-photon imaging of calcium influx into single stereocilia of bullfrog hair bundles showed that calcium signals occurred in all three rows of stereocilia, during bundle stimulation. The conclusion of the study was to suggest that the MET channels were located both at the upper and lower end of the tip link (**Denk et al., 1995**). There were, however, certain limitations in this work. In order to visualise individual stereocilia, the localisation experiments were done at the base of the hair bundle, but without the adequate temporal resolution to determine the origin of calcium entry, the results of the study were later proven to be inaccurate. It was only in 2009, that Beurg and colleagues managed to show that, in fact, the MET channels are only located at the tip of the smallest and middle, and not the tallest, row of stereocilia (**Figure 14**) (**Beurg et al., 2009**). In their study, they overcame the problem related to spatial resolution, by using rat cochlear

inner hair cells, where the step in height between rows of large-diameter stereocilia allowed individual stereocilia to be imaged at the apical end of the bundle. To circumvent the temporal resolution problem, they used a high-speed camera coupled to a swept-field confocal system. In this way, they were able to visualise calcium signals predominantly in the small- and middle-row stereocilia. This meant that the MET channels could only be located at the lower end of the tip link (**Figure 15**). Furthermore, because the number of functional stereocilia was proportional to the amplitude of MET currents, it was suggested that there were about two channels per stereocilium (**Beurg et al., 2009**).

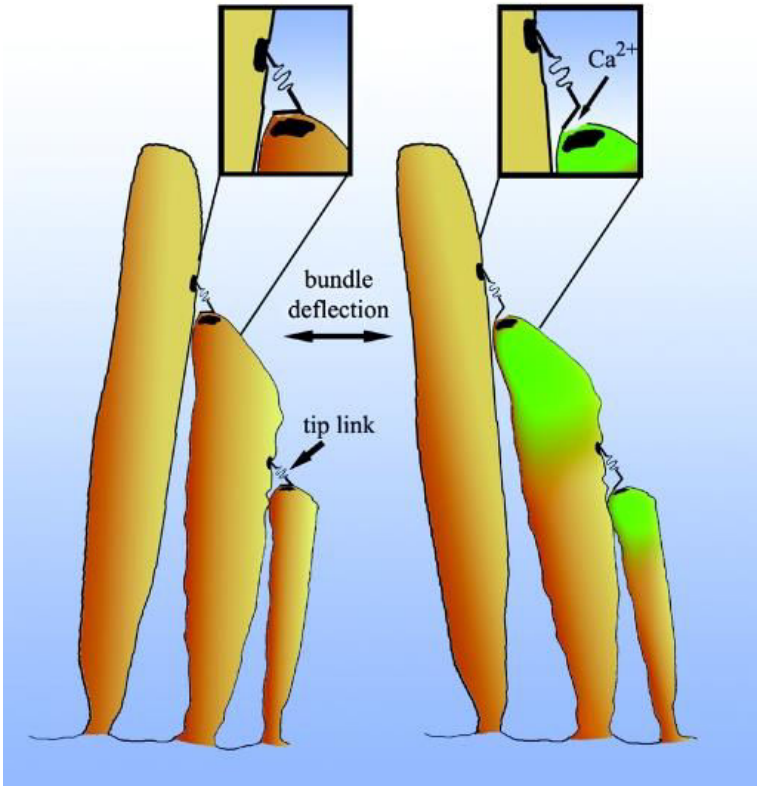

Figure 13. Calcium entry through the mechano-electrical transduction channel after hair bundle deflection
(adapted from Furness et al. 2010)

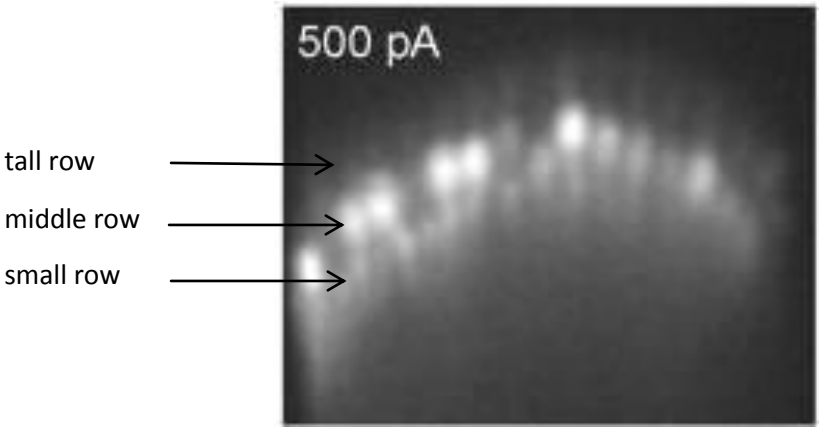

Figure 14. Calcium entry into the small- and middle-row stereocilia of the hair bundle (adapted from Beurg et al., 2009)

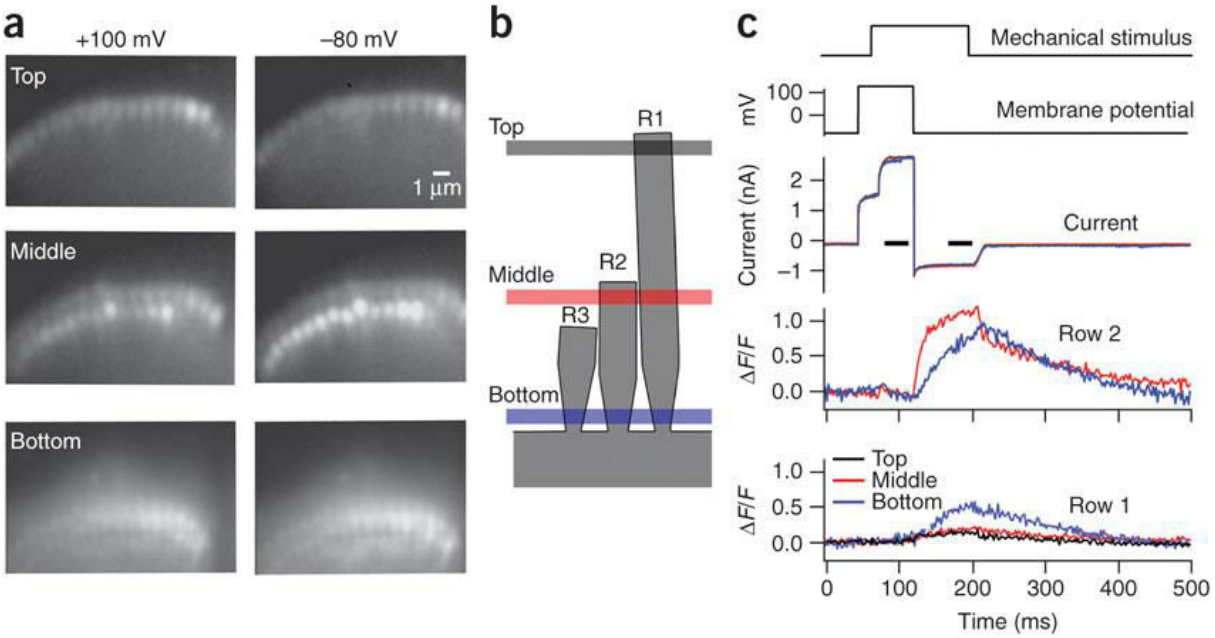

Figure 15. Localisation of mechano-electrical transduction channel by high-speed calcium imaging (adapted from Beurg et al., 2009)

I.3.C.3. Biophysical properties of the MET channel

The MET channel is a non-selective, cationic and voltage-independent channel, with a pore diameter of approximately 0.7 nm (**Corey and Hudspeth, 1979; Hudspeth and Jacobs, 1979; Ohmori, 1985; Crawford et al., 1991**). The relative permeability to certain cations, with respect to Na^+, are as follows: Li^+, 1.14 ; Na^+, 1 ; K^+, 0.96 ; Rb^+, 0.92 ; Cs^+, 0.82 ; Ca^{2+}, 3.8 ; Sr^{2+}, 2.3 ; Ba^{2+}, 2.2 ; Mg^{2+}, 2 (**Ohmori, 1985**) These initial findings, illustrated a preference of the MET channel for Ca^{2+} ions, although the MET current is carried predominantly by K^+ ions. However, these results were based on the assumption that the cations did not interact with the channel's pore. Yet, interaction at the pore level can in fact happen, as is seen with the fact that Ca^{2+} is a MET channel blocker. The channel can also be blocked by several other chemical components. Amilorides specifically and reversibly block the MET channel, in a dose- and voltage-dependent manner, with a half-blocking concentration of 50 mM (**Jorgensen and Ohmori, 1988**). Aminoglycosides, such as gentamicin and dihydrostreptomycin, are also capable of reversibly blocking the MET channel in a voltage-dependent manner, with a half-blocking concentration in the range of 2 to 95 μM (**Kroese et al., 1989**).

The conductance of the MET channel is also sensitive to extracellular concentration of Ca^{2+} ions (**Crawford et al., 1991**). When Ca^{2+} extracellular concentration varies from 2.8 mM to 0.05 mM, MET currents increase. When Ca^{2+} concentration is brought back to the 2.8 mM concentration, MET currents return to their original value as well. However, if the extracellular concentration of Ca^{2+} is brought down to the 1 μM range, MET currents totally disappear, and this effect is irreversible. Crawford and colleagues suggested that the decrease in the concentration of extracellular Ca^{2+} down to 1 μM caused the disruption of

the tip links, which in turn prevented MET currents from occurring (**Crawford et al., 1991**). This hypothesis was later confirmed by a study done on the hair bundles from the saccule of adult bullfrogs (**Assad et al., 1991**). When hair bundles were treated with a calcium chelator, BAPTA, MET currents were abolished, tip links were disrupted, voltage-dependent movement was eliminated and a positive displacement of the hair bundle could be observed. These results strongly pointed to the tip link conveying tension to the MET channels (**Assad et al., 1991**).

Furthermore, by locally perfusing hair bundles with a solution of 1 μM Ca^{2+}, and thus destroying almost all the MET channels in a hair bundle, Crawford and colleagues were able to determine single-channel currents (Figure 16), as well as estimate the conductance of the MET channel to approximately 100 pS (**Crawford et al., 1991**). Although MET channel conductance estimates can vary significantly from one species to another (single-channel conductance in mammals can reach 300 pS for example), it is important to note that these values are far greater than those of other more classical ionic channels, such as Ca^{2+} channels, K^+ channels, and Na^+ channels, which are in the 10-20 pS range.

The sensitivity of the MET channel can be determined by studying its current/displacement curve (also called I(X) curve). Through a series of experiments in the 70's and 80's, the relationship between inward transducer currents and bundle displacement, i.e. the I(X) curve, was shown to be an asymmetrical sigmoid (**Hudspeth and Corey, 1977; Crawford et al., 1989**). This led to the first biophysical model representing the function of the MET channel. The channel was considered to have one open state and two closed states:

$$C_1 < - - > C_2 < - - > O$$

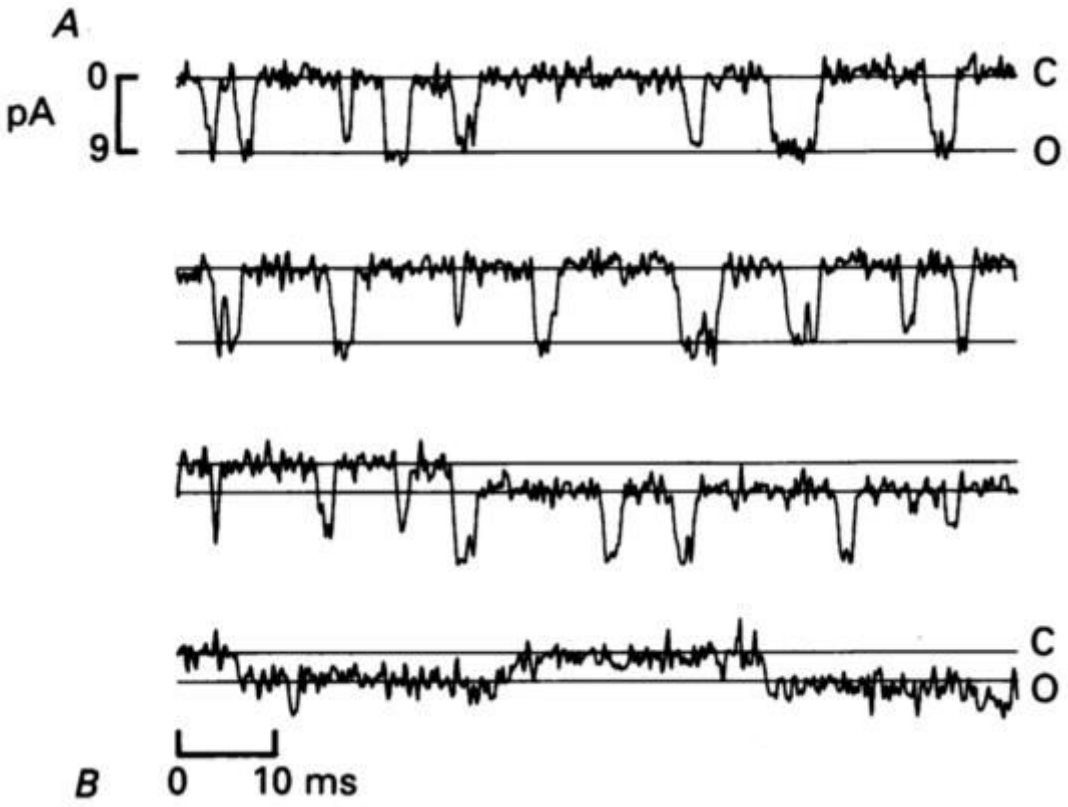

Figure 16. Examples of single-channel current recordings in turtle hair cells (adapted from Crawford et al., 1991)

Furthermore, the effects of extracellular calcium concentration on the I(X) curve were also investigated. When the extracellular concentration of Ca^{2+} is lowered, the I(X) curve is shifted leftward (towards the smallest displacements). This observed shift corresponds to an increase in the number of MET channels that are open at the resting state of the hair bundle (**Corey and Hudspeth, 1983**). This can easily be explained by the fact that Ca^{2+} is a blocker of the MET channel, so when its extracellular concentration is decreased, there are less blocked channels, and hence a bigger number of open channels. In return, when extracellular calcium concentration is increased, there is a decrease in MET current amplitude (**Corey and Hudspeth, 1983; Crawford et al., 1991; Lumpkin et al., 1997**).

I.3.C.4. Adaptation

In an inner ear hair cell, a deflection of the hair bundle in the positive direction elicits a MET current. A decline in the aforementioned current can then be observed despite the sustained stimulus, and this decline is referred to as adaptation (**Figure 17**). In other words, adaptation can be defined as the decay of a sensory response to a sustained stimulus, and it has been observed in all vertebrate species studied to date: bullfrog (**Eatock et al., 1987**), turtle (**Crawford et al., 1989**), mouse (**Russell et al., 1989; Kros et al., 1992**) and rat (**Kennedy et al., 2003**). This has allowed for an extensive description of the phenomenon.

Adaptation occurs over several distinct time frames from microseconds to tens of seconds, and it is commonly accepted that there are 2 major processes involved: the fast adaptation process (which operates on a millisecond or submillisecond time scale) and the slow adaptation process (acting over tens of milliseconds) (**Wu et al., 1999; Vollrath and Eatock, 2003**). Despite the extensive description, and several studies tackling the question, the underlying mechanisms of adaptation remain, to date, unclear and debated. There is however one generally accepted view, which is that adaptive mechanisms are calcium-dependent (although it should be mentioned that a recent study has challenged this view in mammalian cochlear hair cells: (**Peng et al., 2013**)). In 1989, Assad and colleagues showed that when the cell membrane was depolarised to +80 mV (a membrane potential close to the Ca^{2+} equilibrium), Ca^{2+} influx into the cell body was drastically reduced, and adaptation was abolished (**Assad et al., 1989**). Furthermore, it was shown that adaptation necessarily involves a change in the I(X) curve, since the MET current, at a given displacement, declines.

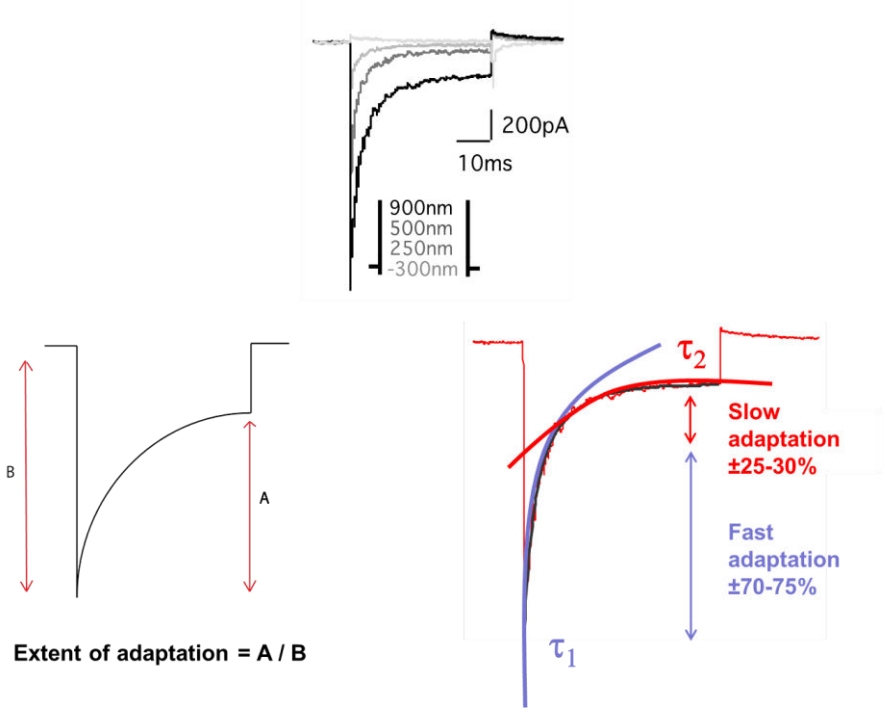

Figure 17. Mechano-electrical transduction current amplitude and characteristic parameters of adaptation

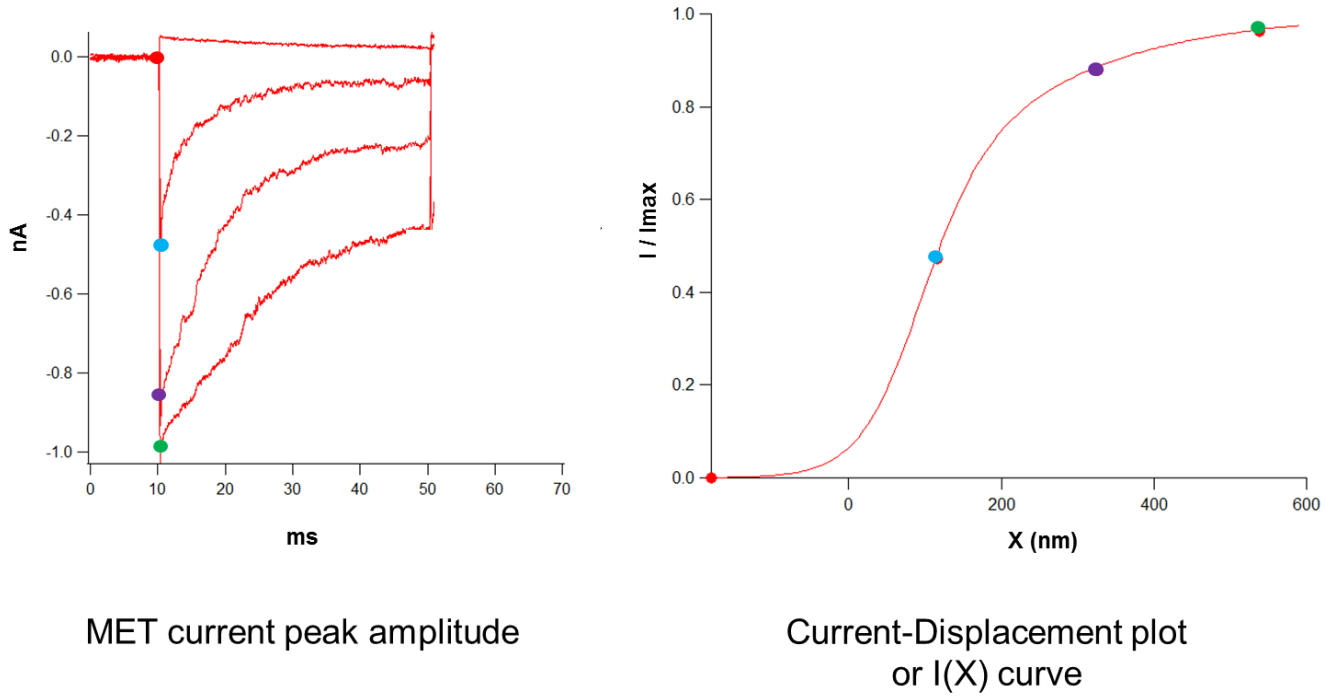

MET current peak amplitude

Current-Displacement plot
or I(X) curve

Figure 18. The current-displacement (I(X)) curve

The I(X) curve shifts towards the larger displacements, without a change in shape or decrease in maximum current. This is called the *adaptive shift* (**Figure 19**) (**Eatock et al., 1987**). In actual fact, the position of the I(X) curve on the displacement axis is sensitive to the extracellular Ca^{2+} concentration and intracellular Ca^{2+} buffering (**Hacohen et al., 1989; Ricci and Fettiplace, 1998; Ricci et al., 1998**). Changes in stereociliary Ca^{2+} concentration reset the range of bundle displacements over which the MET channel is activated. Elevating the Ca^{2+} influx, as it occurs during sustained channel opening, shifts the I(X) curve towards larger displacements, causing desensitisation. Reducing Ca^{2+} influx however, as is the case when channels are closed for a prolonged period or when extracellular Ca^{2+} concentration is lowered, shifts the I(X) curve towards smaller displacements. The site(s) at which binding of Ca^{2+} triggers adaptation are specific for this ion, and other alkaline earth cations do not substitute for Ca^{2+} (**Hacohen et al., 1989**), even though some, such as Sr^{2+}, permeate the channel with comparable ease (**Ohmori, 1985**).

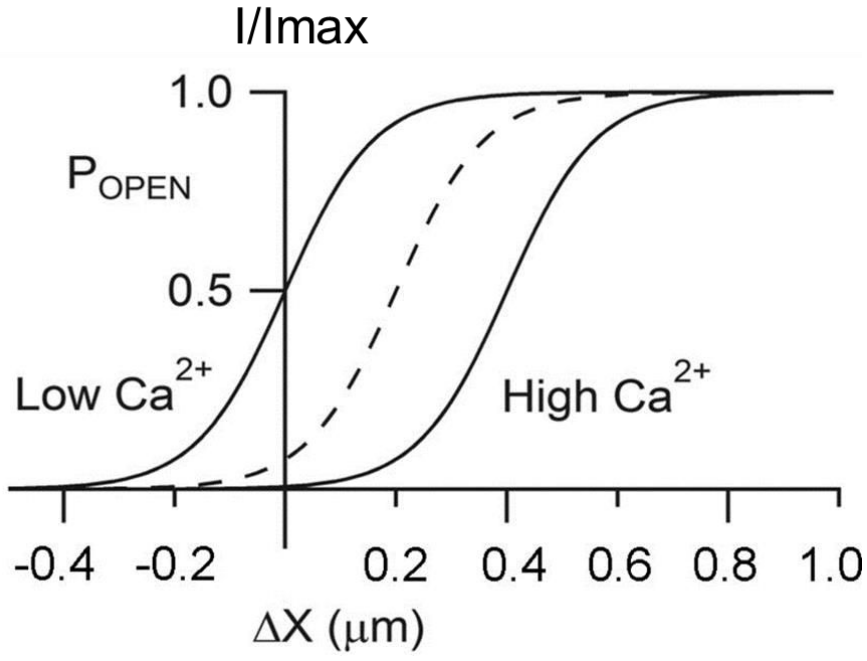

Figure 19. Illustration of the calcium-dependent adaptative shift (adapted from Fettiplace & Kim, 2014)

When it comes to molecular mechanisms, a change in the upper attachment point of the tip link has been used to explain slow adaptation. During a positive bundle deflection, the upper end of the tip link slips down the side of the stereocilium to reduce the tension in the elastic element (**Howard and Hudspeth, 1987**). Furthermore, it has been suggested that the resting tension in the tip link is maintained by an isoform of myosin. Previous studies have implicated myosin 1c in the process (**Holt et al., 2002; Gillespie and Cyr, 2004**), but it has also been shown that myosin1c is localised to both upper and lower ends of the tip links in frog vestibular hair cells (**Garcia et al., 1998**), and all along the stereocilia of cochlear hair cells (**Schneider et al., 2006**). This diffuse labeling contrasts sharply with that for three other myosins examined: myosin 3a and myosin 15a are both confined to the stereociliary tips (**Schneider et al., 2006**), whereas myosin 7a clusters in a complex with sans and harmonin-b at the upper end of the tip link (Grati and Kachar, 2011). Functional evidence for the role of myosin 7a in cochlear hair cells comes from the observation that several mutations of this motor protein affect adaptation of the MET current (**Kros et al., 2002**). Myosin 7a climbing up the actin filaments in the stereocilium may also be responsible for maintaining the resting tip link tension in mammalian OHCs (Grati and Kachar, 2011). Furthermore, how do myosins, located at the upper end of the tip link, get access to calcium entering through the MET channel, now believed to be located at the lower end of the tip link (Beurg et al., 2009)? How then are the myosins regulated and what determines the sliding of the attachment point with an increase in tension? Which specific myosin isoform(s) are implicated in adaptation, as well as their mode of action, is still up for debate.

Fast adaptation has a time constant inferior to 5 ms in bullfrogs and mouse vestibular hair cells (**Vollrath and Eatock, 2003**), in auditory hair cells of turtle (**Crawford et al., 1989;**

Ricci and Fettiplace, 1997) and rat (**Kennedy et al., 2003; Ricci, 2005**). Therefore, ATPase-mediated mechanisms, which are behind myosin activity, are incompatible with the speed of the fast component of adaptation. The millisecond time constant of fast adaptation is more consistent with adaptation occurring at a site very close to the MET channel (**Crawford et al., 1989; Ricci and Fettiplace, 1998; Wu et al., 1999**). One hypothesis along those lines is that, by binding to the MET channel pore, Ca^{2+} induces a change in the force sensitivity of the pore, making it harder to open (**Cheung and Corey, 2006**).

II. Usher syndrome

II.1. Clinical aspects of Usher syndrome

Initially the small number of hair cells in the inner ear (a few thousands) hampered the progression of understanding the molecular components and mechanisms underlying hearing. In the early 1990s, human genetics, the efficiency of which is independent from the number of hair cells, emerged as the best approach to identify molecules involved in MET. By using genetic approaches, scientists were able to, first, identify several causative genes responsible for hearing loss in patients, and second, engineer mouse models that mimicked the human pathologies. Through this approach, approximately 90 deafness genes were identified and more than 120 deafness loci characterised (Hereditary Hearing Loss Homepage, www.hereditaryhearingloss.org).

Syndromic deafness is defined as deafness accompanied by one or several other symptoms. Among the 400+ syndromes involving deafness (**Toriello et al. 2004**), Usher syndrome is one the most incapacitating, as it combines congenital hearing loss with progressive loss of vision. The latest data reveals a prevalence of 1/16 000 to 1/50 000, depending on the geographic region, among patients who are both deaf and blind. In the late 1970's, Davenport and collaborators (**Davenport et al., 1978**) classified the syndrome into three subtypes: Usher type 1 (USH1), Usher type 2 (USH2), Usher type 3 (USH3). USH1 is the most severe form of the syndrome, and is characterised by severe to profound congenital sensorineural deafness, constant vestibular dysfunction and a pre-pubertal onset of visual impairment by retinitis pigmentosa. Retinitis pigmentosa is characterised by the death of cells in the retina called cones and rods. Rods, which are responsible for peripheral

and night vision, die first, and then cones, which are responsible for color perception and central vision, degenerate. The result of retinitis pigmentosa is hence, tunnel vision, night blindness and eventually total loss of vision. USH2 is defined by a moderate to severe congenital hearing loss, an absence of vestibular dysfunction and a post-pubertal onset of retinitis pigmentosa. USH3 is the least severe form of Usher syndrome, and is characterised by progressive hearing loss, retinitis pigmentosa diagnosed between the second and forth decade of life, and only the occasional presence of vestibular dysfunction (**Petit, 2001**). Up to now, 10 causative genes of Usher syndrome have been identified: 6 causing USH1, 3 causing USH2 and 1 causing USH3.

II.2. Molecular aspects of Usher syndrome

II.2.A. Usher syndrome type 1

The 6 identified causative genes for USH1 have been shown to interact with one another and play an essential role in one or several of the following aspects: hair bundle morphogenesis, MET transduction and stereocilia length regulation. Here we briefly describe the 6 USH1 genes:

- ***USH1B (MYO7A)*:** this was the first deafness gene to be identified (**Weil et al., 1995**). In humans MYO7A is responsible for USH1B, and the murine orthologue (*Myo7a*) was found to be the causative gene in *shaker-1* mice (**Gibson et al., 1995**). *Myo7a* codes for myosin VIIa, an unconventional myosin consisting of a motor domain, a neck region and a cargo-binding tail. The motor domain, which has an unusually high affinity for ADP, is responsible for actin- and ATP-binding. The neck consists of five

IQ-motifs (isoleucine and glutamine), that are expected to bind calmodulin, a calcium-binding protein. The tail region is responsible for binding to interaction partners and could also be responsible for inducing dimerization (**Sakai et al., 2011**). In the inner ear, myo7a plays several roles, as it is implicated in intracellular transport, endocytosis, cell-cell adhesion, and in hair cell adaptation. Furthermore, myo7a is essential for stereocilia differentiation and organisation (**Self et al., 1998; Boëda et al., 2002; Kros et al., 2002; Wolfrum et al. 2003**)

- ***USH1C (HARMONIN)*****:** this gene encodes the scaffold protein harmonin (Hmn), a component of the USH interactome. In the inner ear, there are three different isoforms of harmonin: Hmn-a, -b and –c. Through their PDZ-domains (Post-synaptic density protein - Drosophila disc large tumor suppressor – Zonula occludens-1), these proteins interact with the C-terminal PDZ-binding motif (PBM) of most of the other USH proteins. Furthermore, Hmn-b was shown to be located at the upper tip link density in mature auditory hair cells, further confirming harmonin as an essential element for stereocilia formation and hair bundle function (**Bitner-Glindzicz et al., 2000; Verpy et al., 2000; Boëda et al., 2002; Grillet et al., 2009; Michalski et al., 2009**).

- ***USH1D (CDH23)*****:** this gene codes for cadherin-23, an unconventional member of the cadherin superfamily. The murine orthologue (*Cdh23*) was found to underlie the abnormal phenotype in *Waltzer (v)* mice (**Bolz et al., 2001a; Bork et al., 2001; Di Palma et al., 2001**). Cdh23 comprises an extracellular domain of 27 extracellular cadherin (EC) repeats, a single transmembrane domain and a cytoplasmic domain

with a type I C-terminal PBM. In the immature hair bundle it is found all along the stereocilia, where it forms part of the transient lateral links during development. It also forms the stereocilia-associated part of the kinocilial links (**Michel et al., 2005; Goodyear et al., 2010**), and is the upper-most component of the two that make up the tip link (**Siemens et al., 2004**).

- ***USH1F (PCDH15)*****:** this gene codes for protocadherin-15, also an unconventional member of the cadherin superfamily, and the murine orthologue of the gene (*Pcdh15*) has been identified as the causative gene in *Ames Waltzer (av)* mice. Pcdh15 consists of an extracellular domain of 11 EC repeats, a single transmembrane domain and a cytoplasmic domain with a C-terminal PBM. Three transmembrane splice isoforms can be distinguished based on the C-terminal exon: CD1 (exon 35), CD2 (exon 38) and CD3 (exon 39). A forth secreted isoform (SI) lacking the transmembrane domain also exists. Pcdh15 makes up the lower part of the tip link while cdh23 makes up the upper part. Furthermore, it has recently been shown that the CD2 isoform of pcdh15 is the only pcdh15 isoform to persist in mature auditory hair cells, at the tip link (**Ahmed et al., 2001; Alagramam et al., 2001a, 2001b; Pepermans et al., 2014**).

- ***USH1G (SANS)*****:** this gene codes for sans (Scaffold protein containing ANkyrin-repeats and a SAM domain), a small scaffold protein which consists of 4 ankyrin repeats, a central domain, a SAM domain and a C-terminal type I PBM. In the stereocilia, sans has been localised both at the upper and at the lower part of the MET machinery at different time points in maturation (**Caberlotto et al., 2011b; Grati and Kachar, 2011**)

but it has also been shown in the synaptic region, at the cuticular plate and in the adhesion region. Sans is essential to stereocilia formation and in the absence of this protein there is a loss of short- and middle-row stereocilia (**Caberlotto et al., 2011b**). The murine orthologue *Sans* is responsible for the phenotype in Jackson shaker mice (*js*).

- ***USH1J (CIB2)*****:** this gene codes for a calcium and integrin binding protein. The USH1J locus was first shown to be responsible for DFNB48, which is a genetic form of isolated deafness (**Ahmad et al., 2005**). Later on, however, mutations in this gene, resulting in USH1J, were identified (**Riazuddin et al., 2012**). Cib2 contains three EF-hand domains that change conformation upon binding of Ca^{2+} and presumably mediate calcium signalling (**Gentry et al., 2005; Blazejczyk et al., 2009**). It is present all along the hair bundle, in the cuticular plate and is also present in supporting cells. Furthermore, cib2 interacts with whirlin and myosin 7a at the tips of the stereocilia in cochlear hair cells of mice.

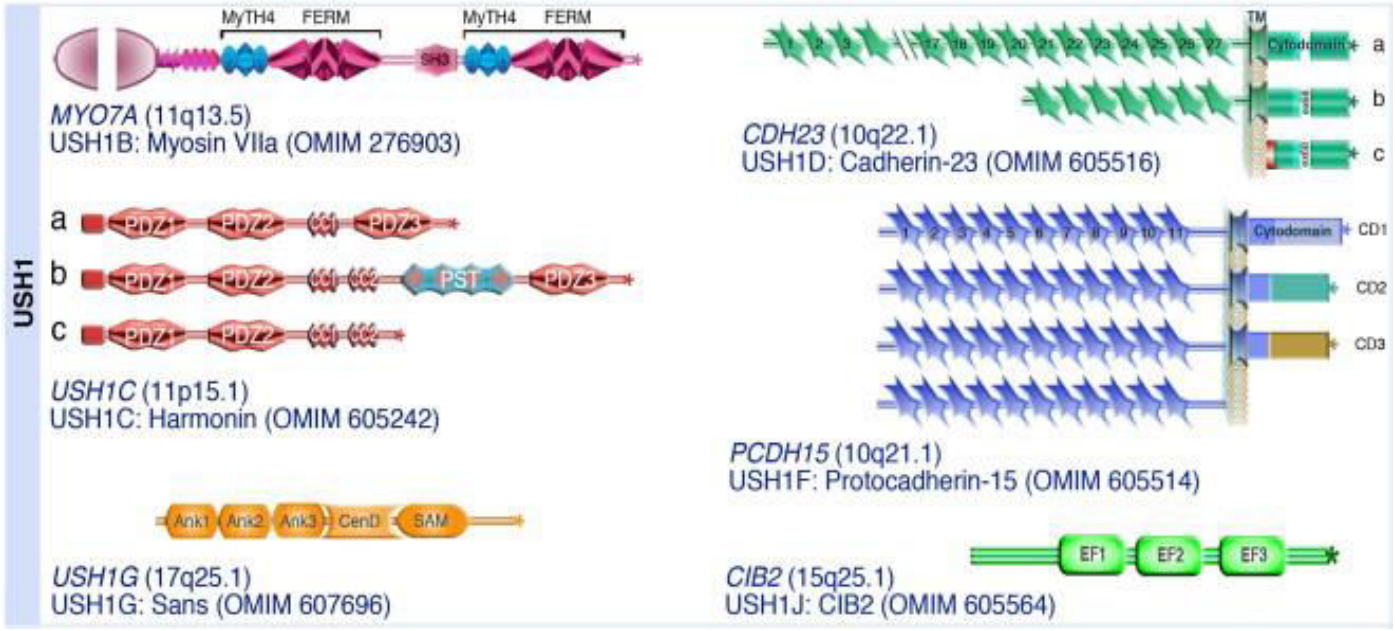

Figure 20. USH1 proteins
(adapted from El Amraoui & Petit, 2014)

Although the role of cib2 in cochlear hair cells remains unclear, as I will show in the Results chapter, all the other known USH1 proteins interact together directly or indirectly, and form the MET complex (**Figure 21**).

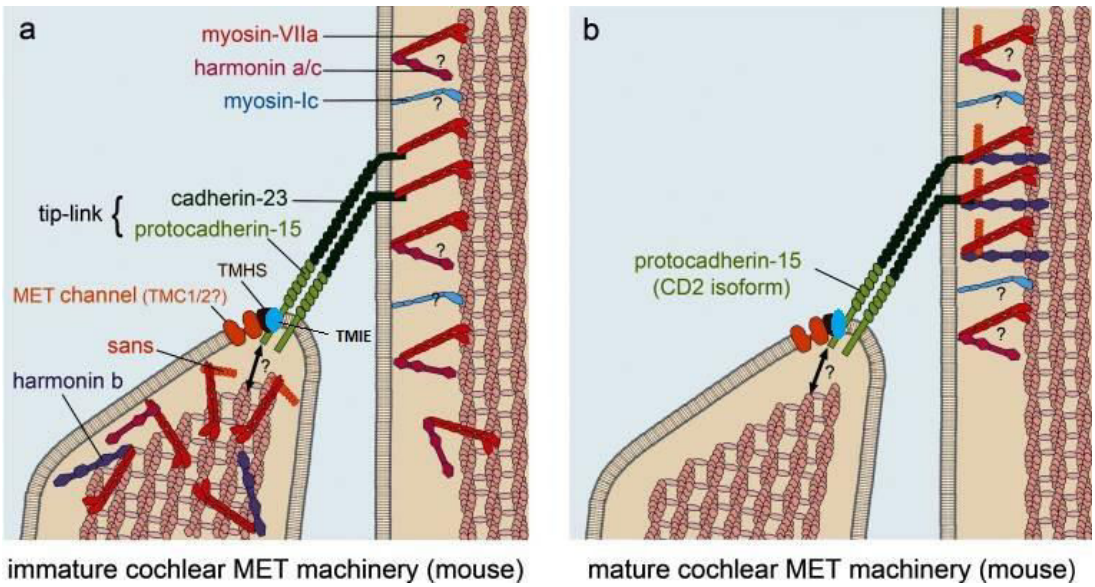

Figure 21. USH1 proteins interacting and forming the MET complex
(adapted from Michalski & Petit, 2015)

II.2.B. Usher syndrome type 2

As it has been mentioned previously, 3 causative genes for USH2 have, to date, been identified. Together with the protein encoded by the modifier gene *Pdzd7*, the three proteins encoded by the USH2 genes, whirlin, usherin and adgrv1, form the *ankle link* complex (**Adato et al., 2005; Michalski et al., 2007; Chen et al., 2014; Zou et al., 2014**). The ankle links are a subset of filamentous lateral links connecting stereocilia at the base, and the ankle link complex has been reported as being essential to hair bundle shaping, rigidity as well as IHC thickness (**Zou et al., 2015**). In the next section, I will go further into detail about the ankle link complex and its components but here I give a brief description of the three genes responsible for USH2:

- ***USH2A (USHERIN)*:** this gene encodes usherin, which was first described as a basement membrane protein, before being described as a transmembrane protein of the inner ear, implicated in the formation of the ankle link complex. In the human ear and retina, there exists two isoforms of usherin: usherin a-isoform and usherin b-isoform. The a-isoform is an extracellular matrix protein (**Pearsall et al., 2002**) whereas the b-isoform is a transmembrane protein with a relatively short cytoplasmic domain and a C-terminal type I PBM. The extracellular domain of the b-isoform consists of one laminin G domain, one laminin N-terminal domain, 10 laminin EGF-like domains, 2 laminin G-like domains and 36 fibronectin type III domains, all of which are common to adhesion proteins (**Weston et al., 2000**) . Usherin has been localised at the ankle link region of the hair bundle and in the synaptic region **(Adato et al., 2005; van Wijk et al., 2006**).

- ***USH2C (ADGRV1):*** this gene encodes adgrv1 (adhesion G protein-coupled receptor v1), a protein responsible for reflex seizures prior to its identification as an USH protein. It was formally referred to as mass1, vlgr1 or gpr98. Several isoforms have been identified, but the b-isoform is responsible for USH. This isoform consists of an N-terminal extracellular domain, a 7-transmembrane receptor domain formed by 3 intracellular and 3 extracellular loops, a relatively short cytoplasmic domain with a C-terminal class I PBM. The extracellular domain consists of 35 Calx-beta domains (calcium binding domains), 6 EAR (epilepsy associated repeats) and a laminin globular domain. Just before the 7-transmembrane domain, a GPCR proteolytic site (GPS) can be found. This is a signature domain of family B G-protein coupled receptors (**McMillan et al., 2002**). The b-isoform of adgrv1 is located at the ankle link region of the hair bundle as well as at the synaptic region (**McGee et al., 2006**).

- ***USH2D (WHIRLIN)***: this gene codes for whirlin, a scaffold protein that interacts with usherin, adgrv1 through their PBMs. Two isoforms of the protein exist and mutations in WHIRLIN can cause either USH2 or non-syndromic deafness (DFNB). Only the long isoform, containing an N-terminal harmonin homology domain, 2 type I PDZ domains followed by a second harmonin homology domain (**Florent Delhommel, unpublished results**), a proline-rich region, a third type I PDZ domain and a C-terminal type II PBM, is expressed in the retina. In the inner ear however, both long and short isoforms (the short isoform only contains the C-terminal proline-rich region, the third PDZ domain and the PBM) are expressed.

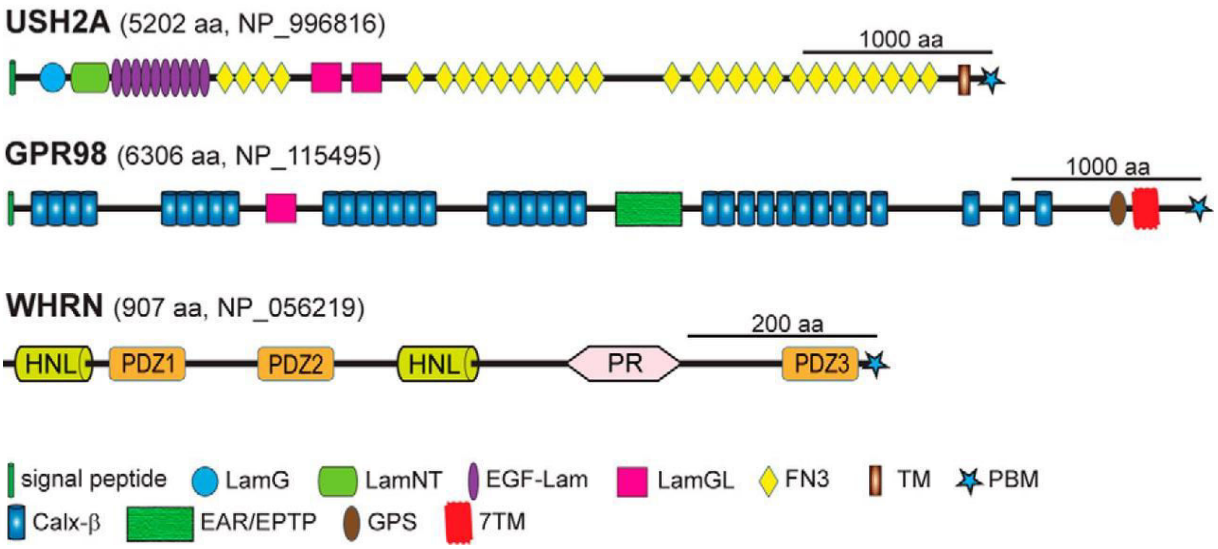

Figure 22. Schematic representation of USH2 proteins
PDZ: (PSD95/Dlg1/ZO-1) domain, PR: proline-rich regions, HNL: harmonin-N like domain (adapted from Chen et al., 2014)

II.2.C. Usher syndrome type 3

Up to date, there is only one gene that has been identified as responsible for USH3. This gene is *CLRN1* and leads to USH3A. The protein encoded by this gene is a four-transmembrane domain protein that is found in hair cell and photoreceptor cell synapses.

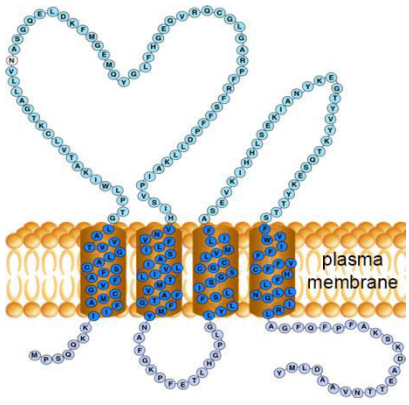

Figure 23. Schematic represention of the USH3 protein clarin

II.3. Usher syndrome type 2 and the ankle link (AL) complex

As mentioned previously, to ensure normal mechano-electrical transduction, an essential step in sound perception, auditory hair cell hair bundle cohesion is essential. During development, the stereocilia of hair bundles differentiate from microvilli and grow differentially to reach their final lengths, thicknesses and rigidity. Throughout this process, several types of lateral links between the stereocilia develop, helping to maintain hair bundle cohesion (**Goodyear et al., 2005**). One set of links, which has been reported as essential to proper hair bundle cohesion and rigidity, is the ankle links, located at the base of the hair bundle. Up until now, it has been generally accepted that two transmembrane proteins coded by USH2 genes, adgrv1 and usherin, make up the ankle links, *per se* (**Adato et al., 2005; McGee et al., 2006; Michalski et al., 2007**). Through their interaction with a third protein, also coded by an USH2 gene, whirlin, and pdzd7, a protein coded by modifier gene *Pdzd7*, these proteins form what is called, the ankle link complex (**Chen et al., 2014; Zou et al., 2014**). In this section I will give detailed information about the function of each of the four proteins which make up the ankle link complex, as well as detailed explanations of how they interact together.

II.3.A Whirlin

The first gene to be discovered that formed part of, what was to be later called, the USH2 complex, was the gene encoding whirlin (*WHRN)*. The murine ortholog of *WHRN*, was first mapped to chromosome 4 in mice in 1963 (**Lane, 1963**). In that study, mice presenting with an autosomal recessive mutation (whirler (*wi*)) in the *Whrn* gene were reported to display deafness, rapid circling and head-tossing. It was only in 2002, however, that the

human orthologue of *Whrn*, *DFNB31*, first reported to be responsible for an autosomal recessive form of hearing loss, was identified in a Palestinian consanguineous family from Jordan (**Mustapha et al., 2002**). Later that year, a study showed that whirlin was implicated in the process of IHC and OHC stereocilia elongation and maintenance in mice (**Holme et al., 2002**). Stereocilia of cochlear hair cells in whirler mutant mice were reported to have abnormal lengths and shapes. In 35-day old (P35) *wi/wi* mutant IHCs, stereocilia were approximately half the length of the equivalent stereocilia in *+/wi* control mice (**Figure** 24), all along the tonotopic axis of the cochlea (**Figure** 25). The difference in stereocilia length could be observed as early as embryonic day 18.5 (E18.5). While mutant mice stereocilia were reported to elongate at a normal rate until P1, between P1 and P4 they prematurely stopped elongating. Their length then decreased, before disappearing completely. Furthermore, *wi/wi* mutant OHCs were closer to normal in length but were arranged in a rounded, "U" shape rather than the normal "W" or "V" shape.

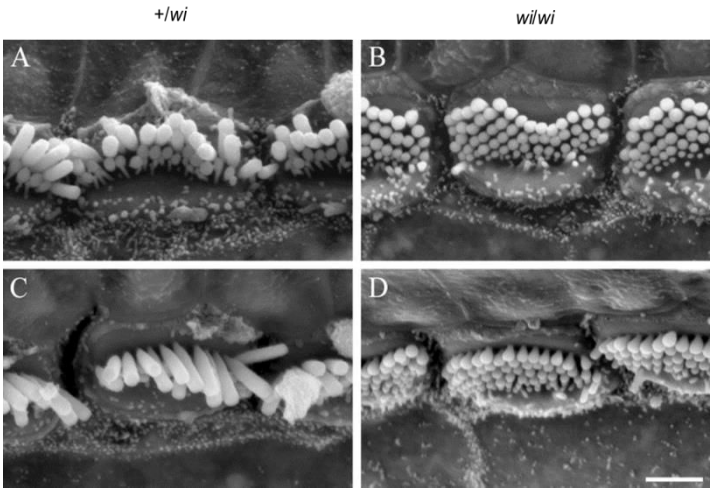

Figure 24. Scanning electron micrographs of P35 +/wi and wi/wi IHCs (adapted from Holme et al., 2002)

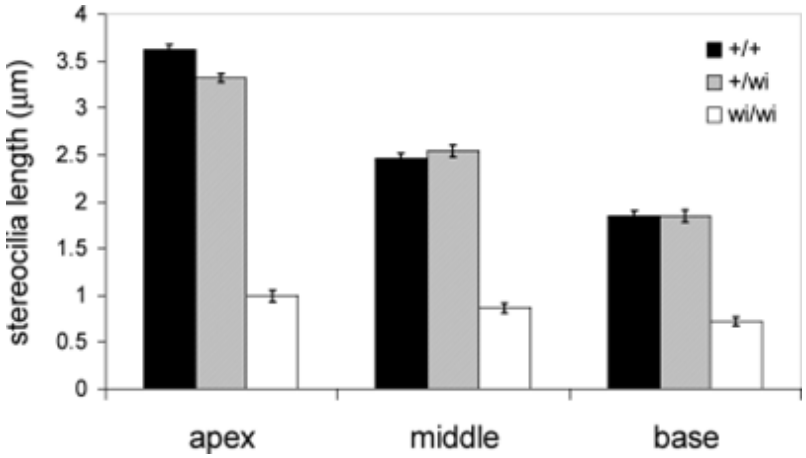

Figure 25. IHC stereocilia length along the tonotopic axis (adapted from Holme et al., 2002)

Whirlin has two reported isoforms: a short C-terminal isoform, and a long isoform, and it is a PDZ domain-containing protein (**Mburu et al., 2003**). As previously mentioned, the long isoform contains three PDZ domains while the short isoform only contains one PDZ domain. In mouse inner ear hair cells, PDZ domains have been shown to mediate the assembly of proteins into functional complexes (**Sheng and Sala, 2001**). These complexes, in at least some cases, are thought to provide a link between transmembrane proteins and the actin cytoskeleton (**Fanning and Anderson, 1999**). Because mutations in *whrn* lead to shortened stereocilia in whirler mutant mice, it was hypothesised that whirlin mediated the organisation of other proteins to form a complex required for stereocilia elongation, such as espin and myosin 15a. Using an antibody raised against its short isoform, whirlin was initially reported to be located at the tip of cochlear hair bundle stereocilia (**Kikkawa et al., 2005**). In the same study, myosin 15a was shown to play a major role in the stabilisation of whirlin expression in the stereocilia. The interaction between these two proteins was shown to occur via the PDZ domain of whirlin and the carboxy-terminal PDZ-ligand of myosin 15a (**Belyantseva et al., 2005**). It was only in 2006 that the interaction of whirlin with the USH2 proteins usherin and vlgr1 was reported. Whirlin was shown to colocalise with usherin and

adgrv1 in photoreceptor cells (synaptic regions, connecting cilium and outer limiting membrane) and auditory hair cells (synapse, stereocilia) (**van Wijk et al., 2006; Michalski et al., 2007**). In 2007, a study, on human patients, revealed that mutations in exons 1 to 6, which are specific for the long isoform of whirlin, were responsible for a new form of USH2, named USH2D (**Ebermann et al., 2007**). This was the first time a clear causal relation between *whrn* and USH2 was established. Indeed, mutations in the C-terminal half of whirlin (common to both long and short isoforms) were only previously reported in non-syndromic deafness (DFNB31). These observations were later confirmed in mice. Indeed, it was shown that mutations near the N-terminus of whirlin lead to retinal and inner ear defects, reproducing the clinical features of the human USH2 disease (**Yang et al., 2010**). In the same study, it was also shown that only the long, and not the short, isoform of whirlin was expressed in the retina, while both long and short isoforms were expressed in the inner ear. The N-terminal PDZ domains of the long isoform of whirlin mediate the formation of the ankle link complex in the inner ear, and a multi-protein complex located in the periciliary membrane complex, in the retina.

The precise distribution, as well as the functional role, of the different whirlin isoforms was only very recently confirmed (**Mathur et al., 2015**). While the long isoform of whirlin is important for the USH2 protein complexes in hair cell stereociliary bases and photoreceptors, both the long and short isoforms participate in stereociliary elongation in hair cell stereociliary tips. Mutations in the whirlin N-terminal region led to retinal degeneration and moderate to severe hearing loss, while a mutation in the C-terminal region eliminated all normal whirlin isoforms and generated a truncated N-terminal whirlin protein fragment, which was partially functional in the retina, thus preventing retinal degeneration (**Mathur et al., 2015**).

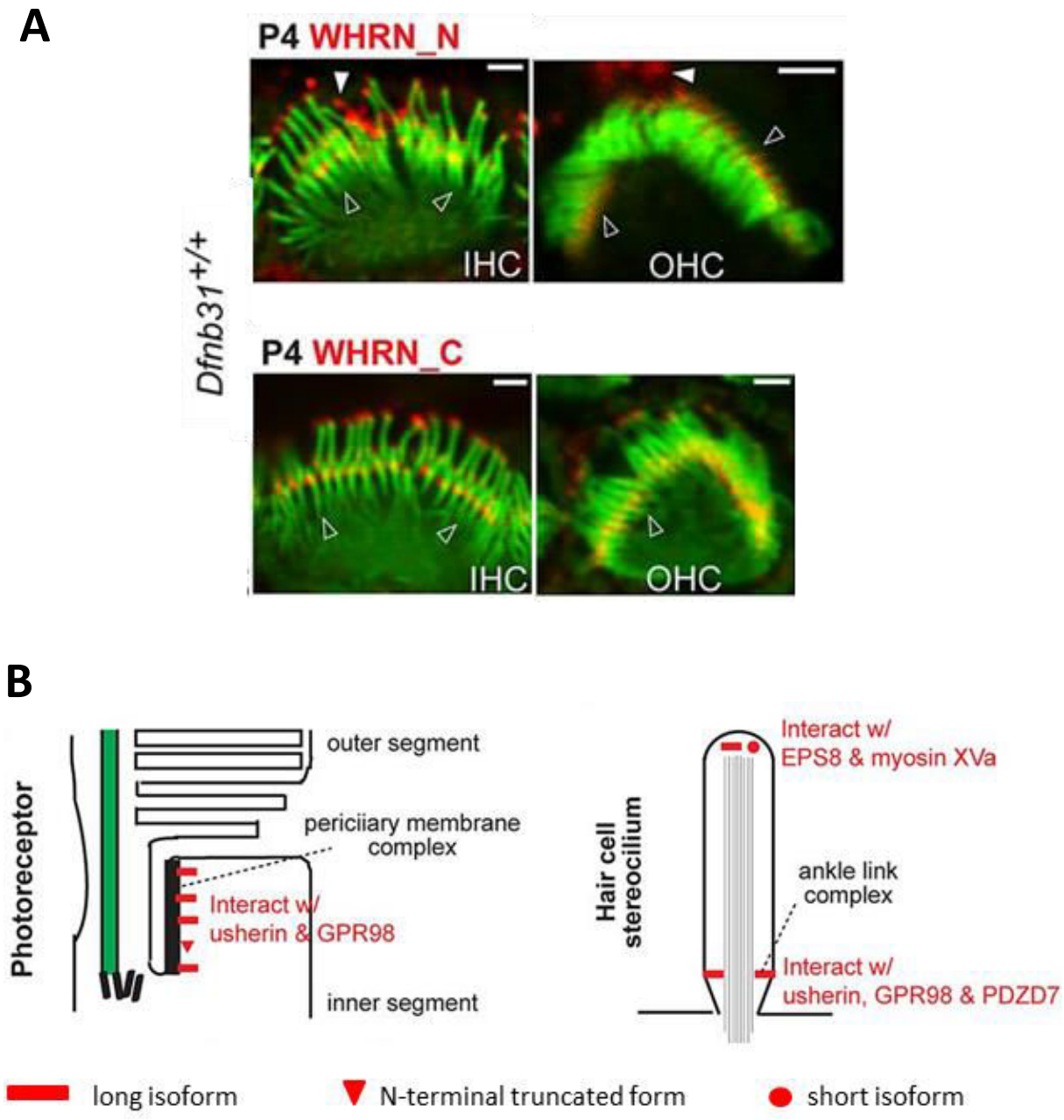

Figure 26. (A) Whirlin distribution in wild-type mouse IHCs and OHCs at P4
(B) Schematic representation of the distribution of whirlin in photoreceptors and inner ear hair cells
(adapted from Mathur et al., 2015)

The different studies on whirlin are a very good example of how different isoforms can play very distinct functional roles within cochlear hair cells and photoreceptor cells. The work I have done during my PhD, and that I will detail in the Results chapter, suggests that this could also be the case for usherin.

II.3.B Usherin

During the mid-90's, through gene mapping, the *USH2A* gene was localised on human chromosome 1q41 (**Kimberling et al., 1995**). It was only a few years later however that the genomic structure of the gene was determined. At the time, the *USH2A* gene was reported to be encoded by 21 exons, and to code for a protein with a predicted molecular weight of 171.5 kDa, containing laminin epidermal growth factor and fibronectin type III domains (**Weston et al., 2000**). These domains are observed in other protein components of the basal lamina and extracellular matrixes, and a study in 2002, described usherin as a basement membrane protein. Usherin was found in all of the capillary and structural basement membranes of the human retina and inner ear (**Bhattacharya et al., 2002; Pearsall et al., 2002**). Usherin was also found in other tissues not affected in USH2A (testis, spleen for example). This usherin distribution in humans was later found to be consistent with the distribution seen in mice, and conservation of usherin was also seen at the nucleotide and amino acid level when comparing the mouse and human gene sequences (**Pearsall et al., 2002**).

It was only in 2004, that the full length structure of usherin was determined. USH2A is the most common form of Usher syndrome. However, when van Wijk and collaborators undertook mutation analysis by DNA sequencing of exons 1 to 21, only ~63% of the expected USH2A mutations were revealed. This led them to search for, and identify 51 new exons, at the 3' end of the *USH2A* gene (**van Wijk et al., 2004**). The long usherin isoform (usherin b-isoform) contains two laminin G and 28 fibronectin type III repeats, a transmembrane domain and a C-terminal PDZ-binding motif (PBM) domain, in addition to the aforementioned functional domains. Several pathogenic mutations were found in these novel exons, implicating the long isoform of usherin in both hearing and vision (**van Wijk et al., 2004**).

Drawing on these results, the role of usherin b-isoform in the inner ear was assessed. Through immunofluorescent staining experiments, it was shown that usherin b-isoform first appears all along the stereocilia in OHCs (embryonic day 18, E18), and then at the base of the stereocilia in IHCs (E20). From P0 to P10, usherin persists at the base of both OHCs and IHCs, but as of P10, usherin starts to disappear from IHCs, then later from OHCs. Similar experiments were conducted in the vestibule, and usherin stainings were still observed at the base of the stereocilia at P15, an age at which usherin is no longer detected in the hair bundle of auditory hair cells. Therefore, the presence of usherin b-isoform is transient in the auditory hair cells, whereas it persists in mature vestibular hair cells. Furthermore, usherin was also detected in the soma of hair cells and supporting cells and the immunofluorescent staining was more intense in the apical region of the hair cells, corresponding to the junctions with adjacent supporting cells.

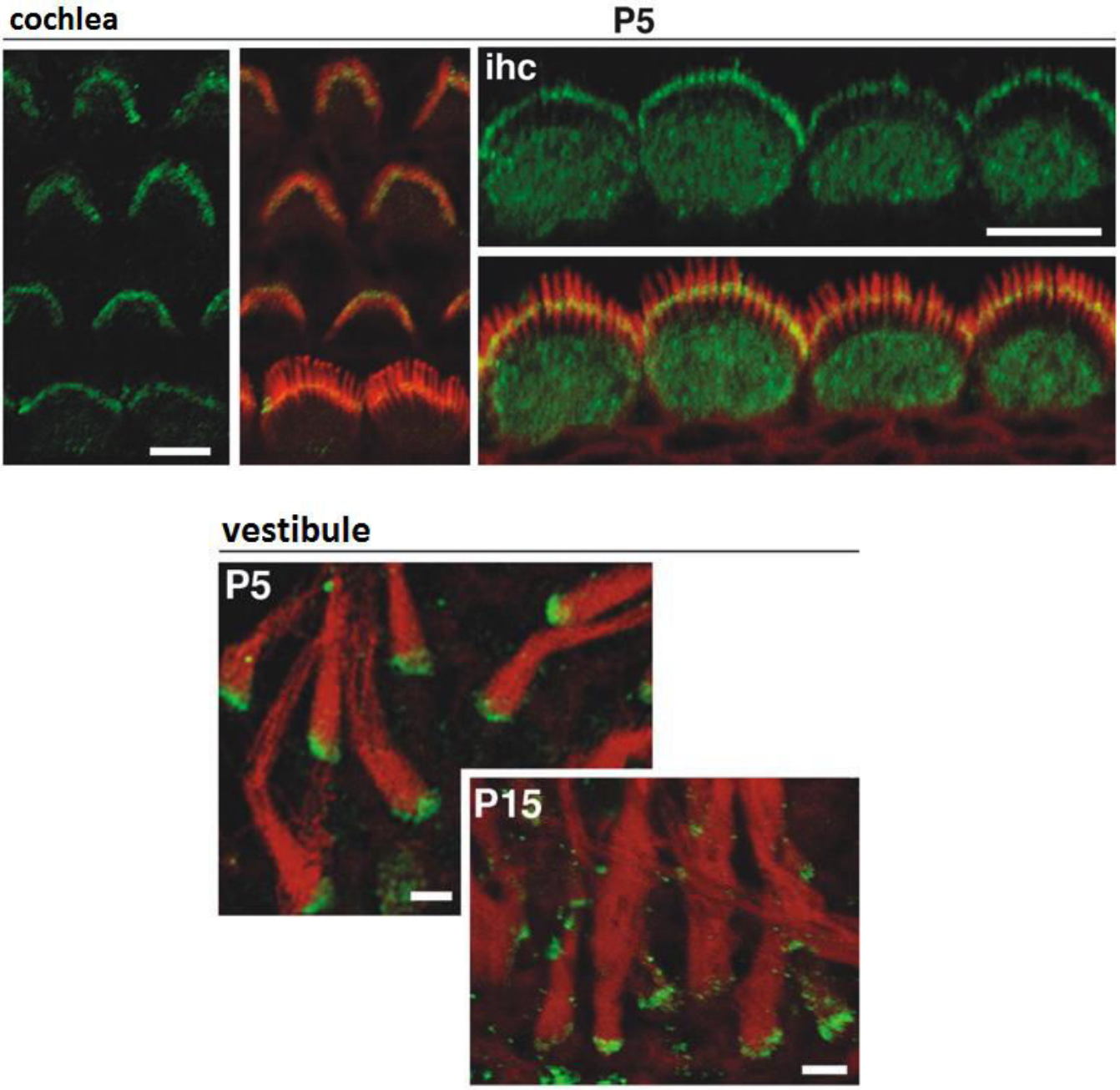

Figure 27. Usherin distribution in murine cochlear and vestibular hair cells (adapted from Adato et al., 2005)

A 2005 study on the development and properties of murine cochlear hair cell stereociliary links showed that immature-looking ankle links first appear at the base of the stereocilia around P0. At P2, they are more distinct and are detected in the hair bundles of OHCs and IHCs. They persist until approximately P9, when they start to disappear first from

IHC. In contrast, the ankle links persist in the mature vestibular hair cells (**Goodyear et al., 2005**). The described spatio-temporal profile was very similar to that observed for usherin. Hence, put together, the data from both studies, strongly suggested that usherin was a component of the ankle links.

In addition, it was shown by co-immunoprecipitation and *in vitro* binding assays, that the usherin cytodomain could bind to whirlin and harmonin, two PDZ domain-containing proteins, defective in Usher syndrome type I, and capable of anchoring usherin to the F-actin core of stereocilia. Usherin interaction with other USH2 proteins will further be discussed in the Results chapter.

II.3.C Adgrv1

The gene responsible for USH2C was actually first described in relation to monogenic audiogenic seizures. A naturally occurring mutation in the *mass1* (monogenic audiogenic seizure-susceptible) gene, was reported to be the cause behind audiogenic seizures in *Frings* mice (**Skradski et al., 1998**). The human orthologous gene to the murine mass1 gene was first described in a study in 2000. *FEB4*, as it was named at the time, was mapped to chromosome 5q14 and reported to be linked to febrile seizures (**Nakayama et al., 2000**). The same year, a novel G protein-coupled receptor was reported, and because of its length, it was referred to as *very large G protein-coupled receptor.* This gene was also mapped to chromosome 5q14, and the protein it encoded was described as having a role in calcium sensing, or binding of its physiological ligand through Ca^{2+}-mediated interactions (**Nikkila et al., 2000**).

Though Nikkila and colleagues did not know it at the time, *VLGR1* was the same gene as FEB4. In 2002, a study on *VLGR1* revealed that in humans 3 isoforms existed: *VLGR1a, VLGR1b and VLGR1c.* With a length of 6307 amino acids, *VLGR1b* was described as the largest known cell surface protein and was suggested to play a role in calcium-mediated protein-protein interaction. *In situ* hybridisation showed that *VLGR1* was predominantly expressed in the central nervous system during development but also in the eye lens, suggesting a role in vision (**McMillan et al., 2002**). It was only in 2004, that *VLGR1* was reported to play a role in hearing. Genetic testing identified four isoform-specific VLGR1 mutations from three families with USH2C, thus implicating *VlGR1* in Usher syndrome type 2. The *VLGR1* gene was considered a likely candidate because of its protein motif structure and expressed-sequence-tag representation from both cochlear and retinal subtracted libraries (**Weston et al., 2004**). The study concluded that the ligand(s) for the VLGR1 protein were unknown, but on the basis of its potential extracellular and intracellular protein-protein interaction domains and its wide mRNA expression profile, VLGR1 could serve diverse cellular and signalling processes. The first functional analysis of the consequences of mutations in the gene responsible for USH2C, were undertaken in 2005 by Johnson and colleagues, on BUB/BnJ mice. In these mice, the $Mass1^{frings}$ mutation is shown to be responsible for the observed early onset hearing impairment. Furthermore, the study shows that during postnatal cochlear development in the BUB/BnJ mice, stereocilia bundles develop abnormally and remain immature and splayed into adulthood, which corresponds to the early onset of the hearing impairment (**Johnson et al., 2005**).

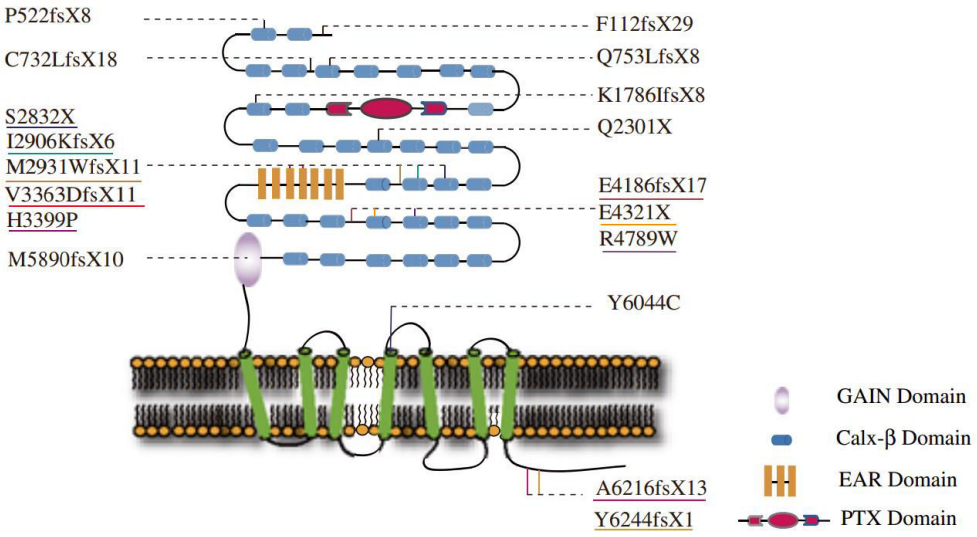

Figure 28. Domain architecture and disease-related mutations of Vlgr1 protein (adapted from Sun et al., 2013)

Several other studies on *Vlgr1* in mice helped to understand the role of the transmembrane isoform in the inner ear (**McGee et al., 2006; Michalski et al., 2007; Yagi et al., 2007**). These studies showed that ankle links failed to form in the cochleas of mice carrying a mutation in *Vlgr1*, and that the hair bundles were disorganised just after birth. Whole-cell patch clamp recordings indicated that mechano-transduction was impaired in cochlear OHCs, but not in IHCs nor VHCs, in early postnatal mutant mice. Furthermore, auditory brainstem response (ABR) recordings and distortion product measurements indicated that these mice were severely deaf by the third week of life. In addition, Michalski and colleagues showed that usherin, vezatin and whirlin are co-localized with vlgr1 at the stereocilia base in developing cochlear hair cells and are absent in Vlgr1 mutant mice, that lack the ankle links. It was hence suggested that these proteins are involved in a molecular complex associated with the ankle links, and scaffolded by whirlin, which has since then been referred to as the ankle link complex (**Michalski et al., 2007**).

Put together, all these results lead to conclude that vlgr1, now known as adgrv1, is essential for the formation of the ankle link complex and the normal development of cochlear hair bundles.

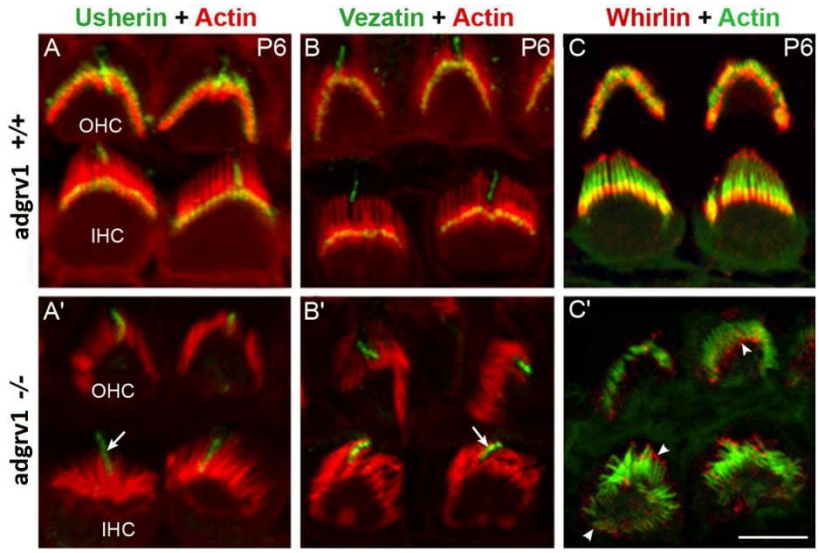

Figure 29. USH2 protein distribution in *Adgrv1*$^{+/+}$ and *Adgrv1*$^{-/-}$ mice (adapted from Michalski et al., 2007)

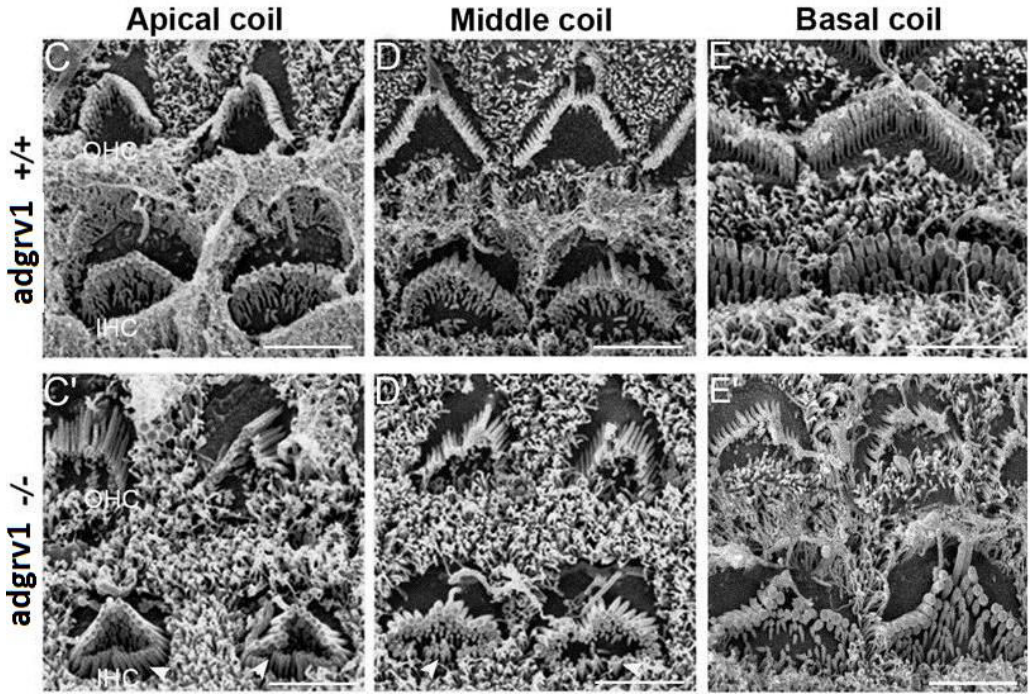

Figure 30. Scanning electron micrographs of *Adgrv1*$^{+/-}$ and *Adgrv1*$^{-/-}$ cochlear hair bundles (adapted from Michalski et al., 2007)

II.3.D Pdzd7

USH2A, *ADGRV1*, and *WHRN* are three known causative genes of USH2, but a 4th gene, a modifier gene called *PDZD7*, is also implicated in the mutli-protein USH2 complex. In humans, four known isoforms of PDZD7, the protein encoded by the *PDZD7* gene (PDZD7-A, PDZD7-B, PDZD7-C, and PDZD7-D) exist, of which only two (PDZD7-A and PDZD7-B) have PDZ domains. The existence of this gene, and the presence of the corresponding protein in the inner ear in humans, was revealed for the first time in 2009 (**Schneider et al., 2009**). In a study published a year later, patients known to have mutations in Usher genes were also shown to have mutations in *PDZD7* that modified the "normal" USH phenotype. In a set of sisters, for example, each with a homozygous mutation in the gene encoding usherin, a mutation in PDZD7 was also present in the sister with the more severe retinitis pigmentosa, and with the earlier disease onset. In addition, heterozygous PDZD7 mutations were also found in patients with truncating mutations in *USH2A*, and *ADGRV1* (**Ebermann et al., 2010**).

Figure 31. Longest alternatively spliced isoform of PDZD7
PDZ: (PSD95/Dlg1/ZO-1) domain, PR: proline-rich region, HNL: harmonin-N like domain (adapted from Chen et al., 2014)

Based on the results from these previous studies, and the fact that PDZD7 is a paralog of the scaffolding proteins harmonin and whirlin, which are implicated in Usher type 1 and type 2 syndromes, the direct interaction between PDZD7, USHERIN, ADGRV1 and WHIRLIN was investigated. Using mouse models, initial evidence for this interaction was provided in a

2012 study, where pdzd7 was first shown to localise to the ankle link region in murine and rat cochlear hair cells, just like the other USH2 proteins (Fig. XX). The study also showed that the cytosolic domains of usherin and adgrv1 could bind to both whirlin and pdzd7, in LLC-PK1 cells (**Grati et al., 2012**).

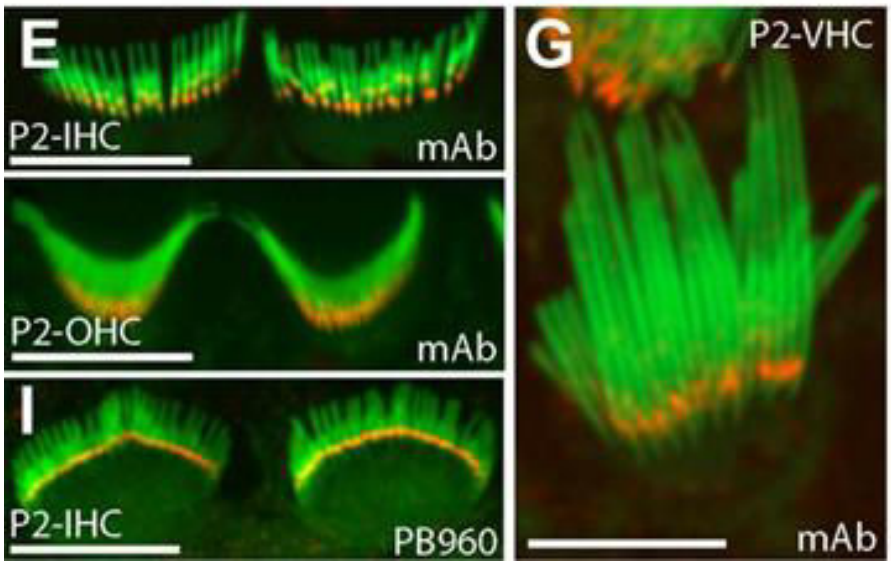

Figure 32. Pdzd7 distribution in P2 rat cochlear and vestibular hair cells (adapted from Grati et al., 2012)

The next step to understanding the role of pdzd7 within the ankle link complex was to generate a *Pdzd7* knockout mouse and study the functional consequences caused by the absence of pdzd7. This work was done in 2014 by Zou and colleagues, who showed that the *Pdzd7* knockout mouse had congenital profound deafness, normal vestibular function, and normal visual function. In the inner ear, the absence of pdzd7 lead to disorganised hair bundles, and reduced mechano-electrical transduction currents and sensitivity in cochlear outer hair cells. Furthermore, through its direct interactions with the three USH2 proteins, pdzd7 was shown to play an essential role in the correct localisation of the USH2 multi-

protein complex to the ankle link region of developing cochlear hair cells (**Zou et al., 2014**). In another study, using FLAG pull-down assays, it was shown that all three PDZ domains of both pdzd7 and whirlin were capable of binding to one another, but that only the heterodimerisation of whirlin PDZ1 and pdzd7 PDZ2 domains was necessary for the interaction with usherin and adgrv1. Therefore, it is imperative that both whirlin and pdzd7 be present and interact with each other for the USH2 complex to be formed in cochlear hair cells (Chen et al., 2014). Furthermore, the study showed that *in vitro* whirlin preferentially binds to usherin, rather than to adgrv1, whereas pdzd7 preferentially binds to adgrv1, rather than to usherin. These observations lead to the suggestion that in the inner ear, a short term, and dynamic USH2 quaternary protein complex may exist *in vivo*.

In photoreceptors however, because the three USH2 proteins largely remain unchanged at the periciliary membrane complex in *Pdzd7* knockout mice, it seems as though pdzd7 is not as essential to the USH2 protein complex as it is in cochlear hair cells (**Zou et al., 2014**).

III. Non-Usher MET complex components

Although extensive work has been done to determine the biophysical, and biochemical properties of the mechano-electrical transduction process in the inner ear, the molecular nature of the MET channel remains a mystery. To date, the best candidates are two non-USH proteins, from the transmembrane channel-like family: TMC1 and TMC2.

The *TMC1* gene is linked to inherited forms of deafness (**Kurima et al., 2002**), and codes for the six-transmembrane domain protein, TMC1, which together with TMC2, have been proposed to encode subunits of the MET channel. Indeed, cochlear hair cells from double knock-out mice for *Tmc1* and *Tmc2* display no MET currents (**Kawashima et al., 2011; Kim and Fettiplace, 2013**). A debate still exists however over whether TMC1 and TMC2 are pore-forming subunits of the MET channel (**Pan et al., 2013**), or whether they are in fact accessory subunits that play a role in targeting the MET channel to the stereocilia tips (**Kim et al., 2013**).

Tetraspan membrane protein of hair cell stereocilia (*TMHS*) is another non-USH gene, responsible for an autosomal recessive form of deafness, that is part of the MET machinery. It encodes a four-transmembrane domain protein that is located at the lower tip-link insertion point. TMHS binds to protocadherin-15 in vitro, and in $Tmhs^{-/-}$ mice, the amplitude of the MET currents is very small. This phenotype is partially rescued by the overexpression of protocadherin-15, illustrating that decrease in MET currents in $Tmhs^{-/-}$ mice was mostly due to the defective recruitment of this protein. This would suggest that TMHS is not a component of the MET channel itself, but rather an essential component of the MET

machinery, playing the role of connecting protocadherin-15 to the MET channel (**Xiong et al., 2012**).

The third non-USH protein known, to date, to be implicated in the MET complex is the transmembrane inner ear (TMIE) protein. Using pull-down experiments, it was shown that TMIE forms a ternary complex with the tip-link component protocadherin-15 and its binding partner TMHS, but does not interact directly with either TMC1 or TMC2. Mice presenting with a *Tmie*-null mutation had no MET currents, and mutations in *Tmie,* that have been linked to inherited forms of deafness in humans, disrupted interactions between TMIE and tip links, suggesting that TMIE functionally couples the tip link to the MET channel (**Zhao et al., 2014**).

MATERIALS & METHODS

Animal experiments were carried out according to the European Community Council Directive 2010/63/UE under the authorizations n°2012-028 and n°2012-038 of the Institut Pasteur ethics committee for animal experimentation.

Immunofluorescence studies

Whole cochleas of P6 mice were dissected in phosphate-buffered saline (PBS) and fixed in 4% paraformaldehyde (PFA) for thirty minutes at room temperature, washed in PBS and blocked in 20% normal goat serum/0.01% Triton-X100/PBS for one hour. For whirlin immunolabelling, samples were immersed in ice-cold methanol (100%) for thirty seconds, after PFA treatment. The samples were incubated with the appropriate primary antibodies overnight at 4°C.

A newly generated anti-usherin polyclonal antibody (Proteogenix) was raised against the transmembrane domain of the protein (aa 5064-5193, NCBI RefSeq: NP_067383.3; 1:50) and its specificity was verified by immunofluorescence experiments using *Ush2a*$^{\Delta TM/\Delta TM}$ mice. Affinity-purified rabbit polyclonal antibodies against the C-terminal region of adgrv1 (aa 6149-6297, NCBI RefSeq: NP_473394.3; 1:500), the N-terminal region of whirlin (aa 2-506NCBI RefSeq: NP_001008791; 1:50), and the N-terminal region of pdzd7 (aa 2-175, NCBI RefSeq: NP_001182194.1; 1:100) were also used.

The samples were then rinsed in PBS and incubated with the Atto-488-conjugated goat anti-rabbit IgG (1:500, Sigma 18772) secondary antibody for one hour at room temperature. The samples were mounted on microscopic slides using FluorSave^{TM} Reagent (Calbiochem) and analysed using a LSM700 microscope (Zeiss). Atto-565 phalloidin (1:600, Sigma 94072) was used to label F-actin.

RT-PCR and transcripts analysis

For RT-PCR analysis of *Ush2a* transcripts, total RNA was extracted from the dissected organ of Corti of *Ush2a*$^{+/\Delta TM}$ and *Ush2a*$^{\Delta TM /\Delta TM}$ P7 and P15 mice with the NucleoSpin® RNA II kit (Macherey-Nagel). RNA was reverse-transcribed using oligo(dT) primers and the Superscript II enzyme (Invitrogen). Reverse transcription negative controls, containing all RT-PCR reagents except the reverse transcriptase, were performed. The sequences of the PCR primers used to characterize the *Ush2a* transcripts (NCBI: AF151717.1 and NM_021408) were as following:

- Ush2a-E19F1 5'- TGTCTCCTGGGAGAAGCCAGCAG

  Ush2a-E20R1 5'-TAAGGTTTGTCCTGATCCCAAAGCAC
- Ush2a-E19F2 5'- GGTACAAGATCAGCATGGTTTCTGAAC

  Ush2a-E20R2 5'-GGAACCATTCGCTTTCCCTATCTGATC

As a positive control, PCR for the ubiquitously expressed *Hprt* gene was performed with the forward primer 5'-GCTGGTGAAAAGGACCTCT and the reverse primer 5'-CACAGGACTAGAACACCTGC.

Scanning electron microscopy

Mouse inner ears were processed with the osmium tetroxide/thiocarbohydrazide technique as previously described (**Furness et al., 2008; Kamiya et al., 2014**). Samples were analysed by field emission scanning electron microscopy operated at 5 kV (Jeol JSM6700F).

Electrophysiological recordings

Electrophysiological recordings from cochlear explants were performed on P7 *Ush2a*$^{+/\Delta TM}$ and *Ush2a*$^{\Delta TM/\Delta TM}$ mice, injected and non-injected *Ush1g*$^{+/-}$ and *Ush1g*$^{-/-}$ mice, *Cib2*$^{+/-}$ and *Cib2*$^{-/-}$ mice, and *Pcdh15*$^{+/\Delta ex37}$ and *Pcdh15*$^{\Delta ex37/\Delta ex37}$ mice. The cochlear coils were excised, placed under two nylon meshes, and observed under a 40× water-immersion objective (Olympus). Extracellular and dissecting solutions were identical and were composed of 143 mM NaCl, 6 mM KCl, 1.3 mM $CaCl_2$, 0.7 mM NaH_2PO_4, 2 mM Na-pyruvate, 10 mM glucose, and 10 mM HEPES, pH 7.4, 305 mOsm/kg. Intracellular solution contained 130 mM KCl, 10 mM NaCl, 3.5 mM $MgCl_2$, 1 mM EGTA, 5 mM K_2ATP, 0.5 mM GTP, and 5 mM HEPES, pH 7.3, 290 mOsm/kg.

Hair cells were whole-cell voltage clamped at -80 mV, and at room temperature (20-25°C), using an EPC-9 patch-clamp amplifier and the Patchmaster software (HEKA, Lambrecht, Germany). No correction was made for liquid junction potentials. Borosilicate patch pipettes (1-2.5 MΩ) were approached parallel to the hair cell rows through a hole in the reticular lamina. During this approach, extracellular solution was abundantly perfused to avoid contact between EGTA and the MET apparatus, which is sensitive to calcium chelators. Patch-clamped OHCs and IHCs were located at a distance of ∼30–40% the total length of the uncoiled cochlea from the apex. Series resistance was always < 10 MΩ and was compensated to 70%. Data were sampled at 100 kHz and filtered at 10 kHz (eight-pole Bessel). Stereocilia were mechanically stimulated with a glass probe fixed on a stack actuator (PA8/12; Piezosystem Jena, Jena, Germany). The tip diameter of the glass probe was 2-3 µm. The tilt of the probe relative to the cell apical surface was ∼30°. Voltage steps were preconditioned to avoid resonance of the actuator.

Data were analysed using the IgorPro software (WaveMetrics, Lake Oswego, OR). P_o-displacement curves were fitted with a second order Boltzmann function (**Kros et al., 2002; Michalski et al., 2009**).

***In vivo* recordings and data analysis**

Auditory brainstem responses (ABRs) and distortion product otoacoustic emissions (DPOAEs) were recorded as previously described (**Le Calvez et al., 1998**) in *Ush2a*$^{+/\Delta TM}$ and *Ush2a*$^{\Delta TM/\Delta TM}$ mice aged between 3 and 10 months, in 1-month old injected *Ush1g*$^{-/-}$ and *Ush1g*$^{+/-}$ mice, and in P16 *Cib2*$^{+/-}$ and *Cib2*$^{-/-}$ mice. ABR waves were recorded in response to pure tone bursts at frequencies of 10, 15, 20, 32 and 40 kHz. ABR signals were averaged following 100-200 pure tone stimulus presentations. ABR thresholds were determined as the lowest stimulus for which recognisable ABR waves could be observed. DPOAEs were collected with a miniature microphone positioned at the entry of the ear canal. Two primary pure-tone stimuli of frequencies f_1 and f_2, and equal intensities, were applied simultaneously, where f_2 was between 5 and 20 kHz and the f_2/f_1 ratio was kept constant at 1.2. The cubic difference tone at $2f_1 - f_2$, the most prominent distortion product tone produced by the mammalian ear, was measured for primary tone frequencies ranging from 30 to 75 dB SPL. Masking tuning curves (TCs) were recorded using a protocol previously described (**Kamiya et al., 2014**).

Statistical tests

Statistical significance was evaluated using unpaired, two-tailed t test with Welch's correction (Prism software), unless stated otherwise. Statistical significance was accepted at $p < 0.05$. Asterisks above brackets in data bar graphs indicate the level of statistical significance (*$p < 0.05$; **$p < 0.01$; and ***$p < 0.001$).

RESULTS

During my PhD, the focus of my work was to decipher the mechanisms which underlie the mechano-electrical transduction process in auditory sensory hair cells. To achieve my goals, I worked on mice bearing mutations in genes responsible for Usher syndrome, and mainly used an electrophysiological approach to understand the implications these mutations have on hearing in mice.

USHERIN PROJECT

My main project was centred on understanding the role of usherin, a gene responsible for Usher syndrome type 2, in the auditory hair cells, and more specifically, in hair bundle development and function during the early postnatal life of mice. Previous work on mice carrying mutations in the *Ush2a* gene (*Ush2a*$^{-/-}$ mice), focused mainly on the retina (**Liu et al., 2007**). The study did, however, report a moderate, non-progressive hearing loss at 4 months old, but failed to mention the onset of the said hearing impairment. Furthermore, as mentioned in the Introduction of this manuscript, two main isoforms of usherin have been reported (**Pearsall et al., 2002; van Wijk et al., 2004**). The disruption of exon 5 in the *Ush2a*$^{-/-}$ mice leads to the absence of production of both the short a-isoform and the long b-isoform of usherin. In fact, by disrupting any exon ranging from 1 to 20, none of the usherin isoforms should be produced. By using this approach, the specific role of each isoform, within the ankle link complex, is overlooked. To circumvent this problem, our lab embarked on a strategy to generate a mouse model in which exon 69, encoding the transmembrane domain of usherin, was disrupted (*Ush2a*$^{\Delta TM/\Delta TM}$ mice). In this way, all the extracellular links formed by usherin were abolished, enabling us to study the structural and functional consequences of the absence of the long b-isoform of usherin. Furthermore, during the course of my PhD, a second study focusing on the contribution of each USH2 protein to the ankle link complex was published (**Zou et al., 2015**). In this most recent study, the same *Ush2a*$^{-/-}$ mice previously used were backcrossed onto a different genetic background. This lead to a difference in phenotype: the *neo Ush2a*$^{-/-}$ mice displayed moderate-to-severe hearing loss at one month of age. Here again, however, the study failed to show data concerning the mechano-electrical transduction function during early postnatal stages.

It is within this context that I conducted my research project, the results of which I shall present now.

Introduction

Usher syndrome (USH), an autosomal recessive genetic disease, is the most common cause of inherited deafness and blindness. There are three USH clinical subtypes: USH1, USH2, and USH3. USH1, the most severe form, is characterised by severe to profound congenital deafness, constant vestibular dysfunction and pre-pubertal onset of retinitis pigmentosa. USH2, the most prevalent form, involves moderate to severe hearing loss, an onset of retinitis pigmentosa in early adolescence, and normal vestibular function. Although comparable in severity, USH3 is distinguished from USH2 by the progressiveness of the hearing impairment and the occasional presence of vestibular dysfunction (**Petit, 2001**). Hearing defects in USH patients result from the dysfunction of the cochlear hair cells: inner hair cells (IHCs), which are the genuine auditory sensory cells, forming synaptic connections with the primary auditory neurons, and outer hair cells (OHCs), which mechanically amplify sound stimuli to the IHCs. Thanks to their hair bundle, composed of actin-filled stereocilia, interconnected by different types of fibrous links, both IHCs and OHCs convert cochlear vibration waves into electrical signals in a process called mechano-electrical transduction. Most reported mouse models for USH1 and USH2 faithfully reproduce the hearing defects of USH patients (Weil et al., 1995, 2003; Bitner-Glindzicz et al., 2000; Verpy et al., 2000; Ahmed et al., 2001; Bolz et al., 2001b; Bork et al., 2001; Weston et al., 2004; Ebermann et al., 2007). This, however, is not the case for USH2A. In the first knockout mouse model of USH2A, in which exon 5 was deleted (*Ush2a*$^{-/-}$ mice) (**Liu et al., 2007**), late-onset degeneration of the retina due to photoreceptor loss and moderate non-progressive hearing impairment as of 4 months old were reported (**Liu et al., 2007**). When backcrossed on a different genetic

background however, these mice showed a 60 dB SPL increase in auditory thresholds as early as 1 month-old (**Zou et al., 2015**).

USH2A encodes at least two usherin isoforms: a 180 kDa widely expressed short N-terminal extracellular a-isoform (**Pearsall et al., 2002**) and a transmembrane long b-isoform preferentially expressed in the retina and cochlea (**van Wijk et al., 2004**). The long b-isoform is made of an extracellular region containing 33 fibronectin type III repeats as well as laminin, lamG-like, lamNT and laminin-EGF domains, a transmembrane domain, and a short intracellular region containing a C-terminal PDZ-binding motif. Because the *Ush2a*$^{-/-}$ mice were not designed to study the specific role of the usherin long b-isoform, we generated a mouse model in which exon 69 of the *Ush2a* gene, that codes for the transmembrane domain of usherin, was targeted for deletion. This strategy was aimed at disrupting all extracellular links in which usherin could be involved, while leaving the short a-isoform intact. Our study sheds new light on the role of the long b-isoform of usherin, challenges the view that hearing loss is exclusively non-progressive in mice lacking usherin, and highlights the need for genetic testing in all USH2 patients to establish a strong genotype/phenotype correlation.

Results

The usherin long b-isoform is absent in Ush2a$^{\Delta TM/\Delta TM}$ mice

We specifically inactivated the long transmembrane usherin b-isoform by deleting exon 69, which encodes the transmembrane domain of usherin. The resulting *Ush2a*$^{\Delta TM/\Delta TM}$ mice were first analysed by immunohistochemistry to verify the absence of the transmembrane usherin b-isoform in the cochlear hair cells. This protein is associated with the ankle links, transient lateral links located at the base of the stereocilia that play a critical role in the development of the hair bundle (**Goodyear et al., 2005; McGee et al., 2006; Michalski et al., 2007**). Using a polyclonal antibody directed against the C-terminal end of usherin, an intense labelling was detected in the ankle link region, at the base of the hair bundles of IHCs and OHCs of P6 *Ush2a*$^{+/\Delta TM}$ mice, which were used as controls, but not in *Ush2a*$^{\Delta TM/\Delta TM}$ mice, indicating that the long usherin b-isoform was not produced in homozygous mutant mice (**Figure** 33**A**).

We next investigated whether the transcript encoding the short a-isoform of usherin could be detected in *Ush2a*$^{\Delta TM/\Delta TM}$ mice, by using reverse transcription-polymerase chain reaction (RT-PCR) experiments. Both transcripts encoding the short and the mutated long isoforms were found to be present in the organ of Corti of both *Ush2a*$^{+/\Delta TM}$ and *Ush2a*$^{\Delta TM/\Delta TM}$ mice (**Figure** 33**B**). Because there are no mutations in the first 21 exons of *Ush2a*, the presence of the short transcript in *Ush2a*$^{\Delta TM/\Delta TM}$ mice indicates that the corresponding protein is produced in these mice. All our attempts to generate specific antibodies directed against the N-terminal region of usherin were unsuccessful.

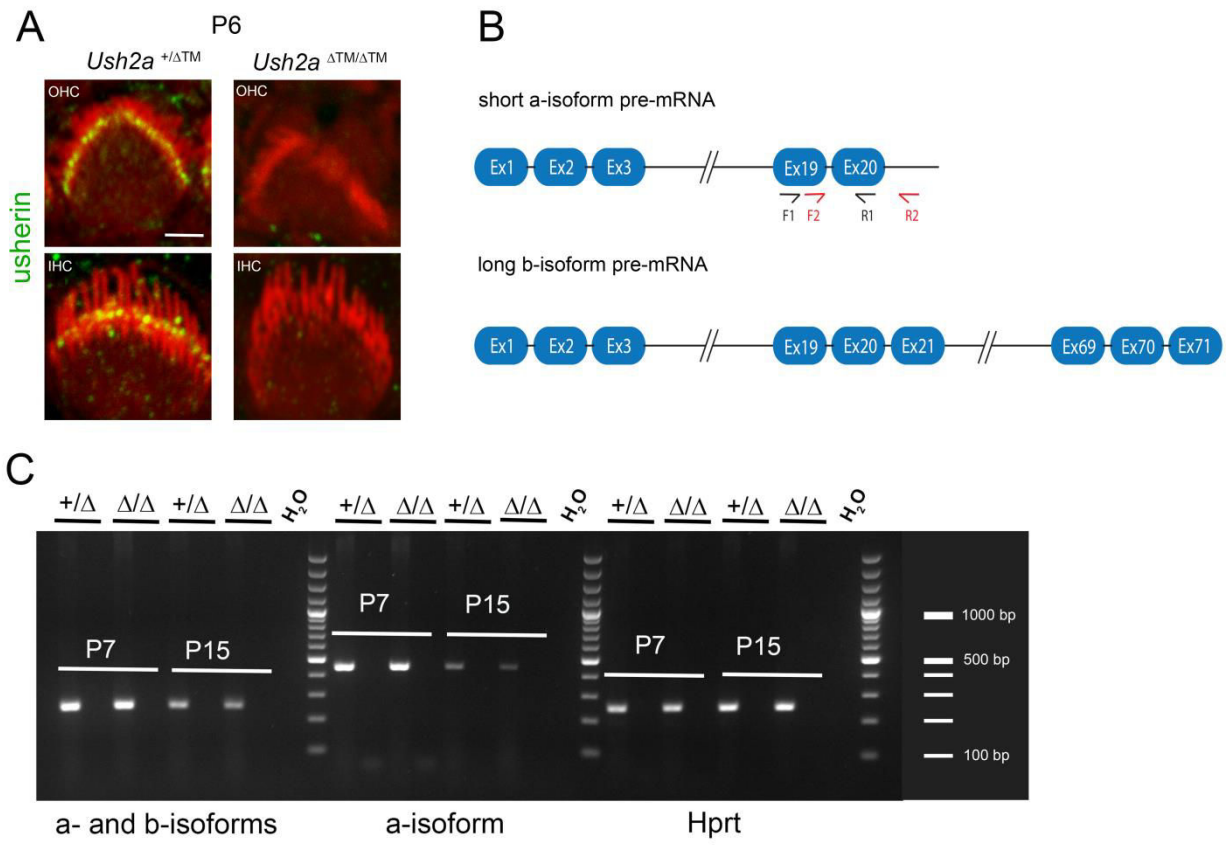

Figure 33. *Ush2a*$^{\Delta TM/\Delta TM}$ mice are defective for the usherin long b-isoform

(A) Hair bundle distribution of usherin in cochlear hair cells of Ush2a$^{+/\Delta TM}$ *and Ush2a*$^{\Delta TM/\Delta TM}$ *P6 mice. Scale bar, 1 µm. (B) Schematic representation of the unspliced transcripts coding for the short and long isoforms of usherin. Boxes show exons and lines show introns. F1/R1 and F2/R2 respectively indicate primer pairs used for RT-PCR amplification of both a- and b-isoforms, and a-isoform only. (C) Both usherin a-isoform and usherin b-isoform transcripts were present in the cochlea of Ush2a*$^{+/\Delta TM}$ *(+/Δ) and Ush2a*$^{\Delta TM/\Delta TM}$ *(Δ/Δ) mice on P7 and P15. The a-isoform transcript was more abundant on P7 than on P15. The ubiquitously expressed Hprt transcript was present both on P7 and P15.*

Ush2a$^{\Delta TM/\Delta TM}$ mice have normal mechano-electrical transduction currents on P7

To assess the role of the usherin long b-isoform in the hair cell mechano-electrical transduction process, we recorded mechano-electrical transduction currents in both IHCs and OHCs of *Ush2a*$^{\Delta TM/\Delta TM}$ mice and *Ush2a*$^{+/\Delta TM}$ mice. In P7 *Ush2a*$^{\Delta TM/\Delta TM}$ mice, both IHCs and OHCs exhibited normal mechano-electrical transduction currents in response to displacements of the hair bundle in the direction of the tallest stereocilia (Figure 34). For IHCs, the averaged peak amplitudes of the mechano-electrical currents were 610 ±27 pA in *Ush2a*$^{+/\Delta TM}$ mice (n = 7), and 605 ± 55 pA (n = 14) in *Ush2a*$^{\Delta TM/\Delta TM}$ mice (Figure 34**A**, p = 0.94). For OHCs, the averaged peak amplitudes were 1221 ± 102 pA in *Ush2a*$^{+/\Delta TM}$ mice (n = 12), and 1144 ± 83 pA in *Ush2a*$^{\Delta TM/\Delta TM}$ mice (n = 16) (Figure 34**B**, p = 0.55). The displacement-current (I(X)) curves showed no significant difference between *Ush2a*$^{\Delta TM/\Delta TM}$ mice and *Ush2a*$^{+/\Delta TM}$ mice, for both IHCs (p = 0.69) and OHCs (p = 0.83) (Figure 34). Characteristic parameters such as the extent of adaptation and the fast adaptation time constant were also indistinguishable (data not shown). These results suggest that the absence of the long usherin b-isoform in homozygous mutant mice does not affect the mechano-electrical transduction process during the first postnatal week.

Ush2a$^{\Delta TM/\Delta TM}$ mice display late onset progressive hearing loss

To assess the hearing function of *Ush2a*$^{\Delta TM/\Delta TM}$ mice, we recorded their auditory-evoked brainstem responses (ABRs). ABRs monitor the electrical activity of the primary auditory neurons, and successive relays of the central auditory pathway, in response to brief sound stimuli (**Møller and Jannetta, 1983**). In 2- to 3-month-old *Ush2a*$^{\Delta TM/\Delta TM}$ mice, hearing thresholds were normal for low frequencies (5-15 kHz) (p = 0.054) and were slightly, but significantly, increased for mid-high frequencies (20-32 kHz) (p = 0.023).

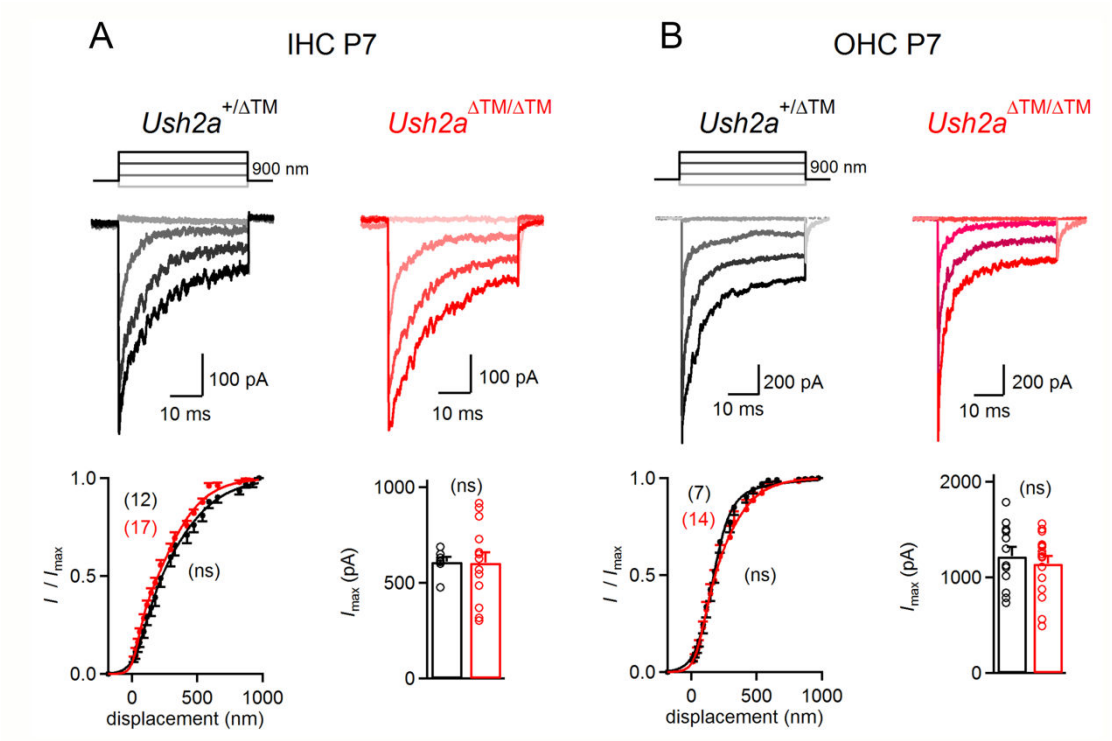

Figure 34. Mechano-electrical transduction current recordings, by mechanical stimulation of the hair bundle in the excitatory direction

(A – B) Examples of mechano-electrical transduction current recordings in IHCs (A) and OHCs (B) of Ush2a$^{+/\Delta TM}$ (black) and Ush2a$^{\Delta TM/\Delta TM}$ (red) P7 mice. Different displacement steps in the excitatory direction and one 300 nm step in the opposite direction (shown above) were applied. Corresponding averaged peak amplitudes of mechano-electrical currents, and I(X) curves were plotted.

In 4-month old *Ush2a*$^{\Delta TM/\Delta TM}$ mice, variable ABR threshold profiles were observed but the average increase in hearing thresholds was 14 ± 8 dB SPL (p = 0.089) for low frequencies and 15 ± 5 dB SPL (p = 0.11) for mid-high frequencies as compared to *Ush2a*$^{+/\Delta TM}$ littermates. In 5- to 8-month-old *Ush2a*$^{\Delta TM/\Delta TM}$ mice, hearing loss was well established in all individuals, illustrated by an increase of 33 ± 15 dB SPL ($p < 10^{-4}$) for low frequencies, and 33 ± 6 dB SPL ($p < 10^{-4}$) for mid-high frequencies. In 9- to 10-month-old *Ush2a*$^{\Delta TM/\Delta TM}$ mice, the increase was 44 ± 13 dB SPL (p = 0.009) for low frequencies, and 46 ± 11 dB SPL (p = 0.007) for mid-high frequencies (**Figure 35A**). These results suggest that *Ush2a*$^{\Delta TM/\Delta TM}$ mice undergo a progressive hearing loss from 3 months of age onward.

Both OHC and IHC dysfunction contribute to the hearing loss in *Ush2a*$^{\Delta TM/\Delta TM}$ mice

Because they probe both the mechano-electrical transduction and the amplification functions of OHCs, distortion product otoacoustic emissions (DPOAEs) provide a non-invasive way to detect local defects in these cells (**Trautwein et al., 1996**). To reveal the potential existence of such defects, as well as tonotopic and/or age-related progressiveness of the auditory impairment in *Ush2a*$^{\Delta TM/\Delta TM}$ mice, we measured DPOAEs and determined for which frequency of the probe tones they were no longer detectable, here termed the DPOAE cut-off frequency (**Figure 35B**). In the 2- to 3-month old age group, the average DPOAE cut-off frequency, 19 ± 1 kHz (n = 6) in *Ush2a*$^{\Delta TM/\Delta TM}$ mice and 20 kHz (n = 6) in *Ush2a*$^{+/\Delta TM}$ mice (p = 0.19, for both comparisons), reached the recording limits of our equipment. In 5- to 8-month-old mice, the average DPOAE cut-off frequency remained constant for *Ush2a*$^{+/\Delta TM}$ mice, 19.5 ± 0.5 kHz (n = 12), but decreased to 11.5 ± 1 kHz for *Ush2a*$^{\Delta TM/\Delta TM}$ mice (n = 16) ($p < 10^{-4}$) .

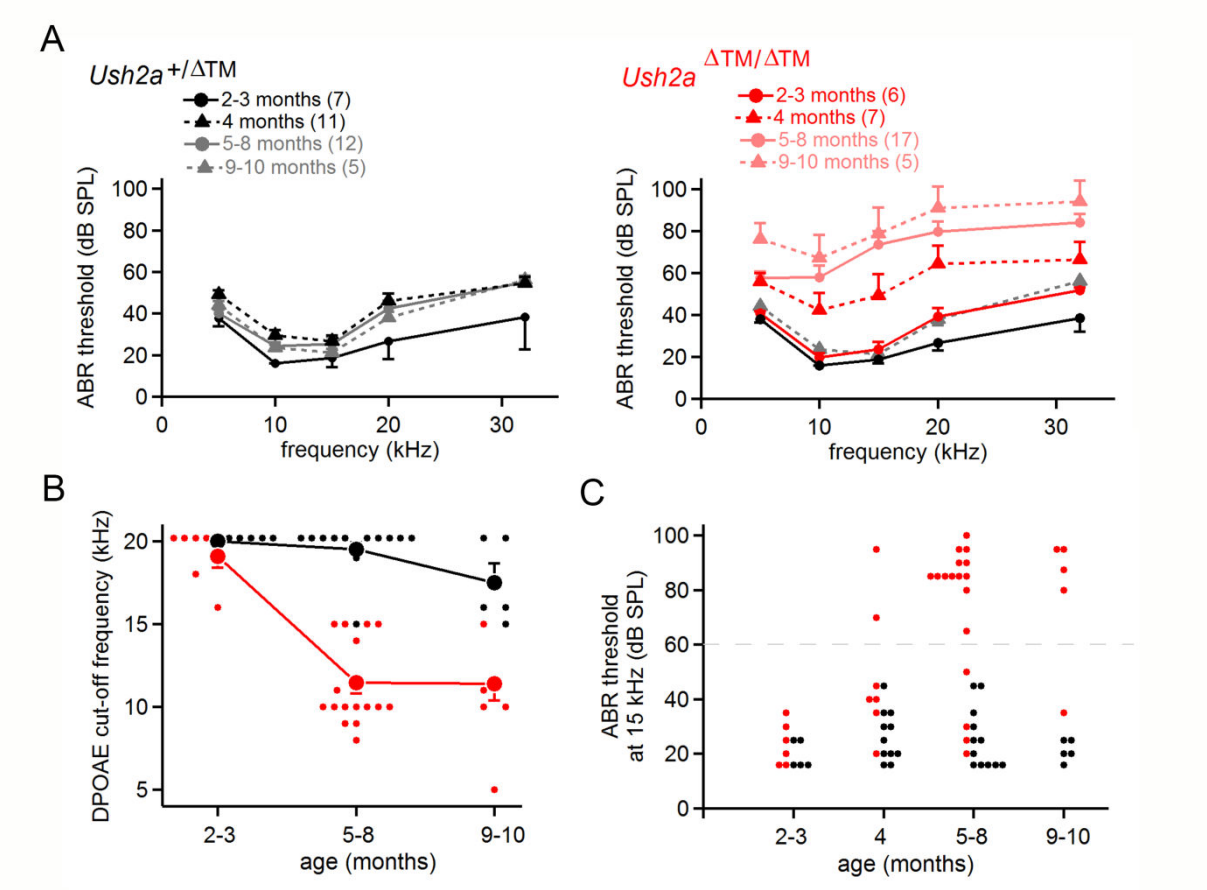

Figure 35. Hearing impairment at low and mid-high sound frequencies in *Ush2a*$^{\Delta TM/\Delta TM}$ mice

(A) ABR thresholds recorded in Ush2a$^{+/\Delta TM}$ *and Ush2a*$^{\Delta TM/\Delta TM}$ *mice from 2 to 10 months old. (B) DPOAE cut-off frequency plotted as a function of age in Ush2a*$^{+/\Delta TM}$ *and Ush2a*$^{\Delta TM/\Delta TM}$ *mice. Averages are shown as big dots, whereas individual values are shown as small dots. (C) ABR thresholds in Ush2a*$^{+/\Delta TM}$ *and Ush2a*$^{\Delta TM/\Delta TM}$ *mice at 15 kHz. Individual recordings are shown to illustrate mice with hearing loss under and over 60 dB (grey dotted line). Hearing losses over the 60 dB mark usually implicate IHC defects.*

In the 9- to 10-month-old mice, the average DPOAE cut-off frequency decreased slightly to 17.5 ± 1 kHz (n = 5) for control mice, but remained stable at 11.5 ± 1 kHz (n = 5) for *Ush2a*$^{\Delta TM/\Delta TM}$ mice (p = 0.002). These results indicate that OHC dysfunction contributes to the abnormal auditory phenotype of *Ush2a*$^{\Delta TM/\Delta TM}$ mice.

OHCs, when defective, may account for a 60 dB maximal increase in ABR thresholds (**Lopez-Poveda and Johannesen, 2012; Kamiya et al., 2014**). More severe hearing losses usually involve a dysfunction of the IHCs as well. This does not, however, exclude a possible contribution of IHCs for ABR threshold increases less than 60 dB. In *Ush2a*$^{+/\Delta TM}$ mice, auditory threshold elevation with a 15 kHz probe tone was always inferior to 60 dB, regardless of age (**Figure 35C**). In *Ush2a*$^{\Delta TM/\Delta TM}$ mice, however, only the 2-3-month-old group had hearing thresholds inferior to 60 dB, while the older animals showed variability in their auditory threshold elevations. In the 4-month-old group, 2 out of 7 *Ush2a*$^{\Delta TM/\Delta TM}$ mice had hearing loss superior to 60 dB (p = 0.13, Fischer's exact test). In the 5- to 8-month-old group, this fraction rose to 13 out of 17 mice (p = $6 \cdot 10^{-5}$, Fischer's exact test), and in the 9- to 10-month old group, it affected 4 out of 5 mice (p = 0.047, Fischer's exact test) (**Figure 35C**). In conclusion, both IHC and OHC dysfunction can reasonably be assumed to contribute to hearing loss in *Ush2a*$^{\Delta TM/\Delta TM}$ mice, as of 3 months old.

Ush2a$^{\Delta TM/\Delta TM}$ mice display masking tuning curve shifts, from mid-high to low frequencies, as of 3 months old

We further assessed the auditory function in *Ush2a*$^{\Delta TM/\Delta TM}$ mice by using masking tuning curves, which probe cochlear frequency selectivity. Masking tuning curves depict the minimum intensity of a masking sound required to suppress the response produced by a probe tone near its detection threshold, as a function of masking sound frequency.

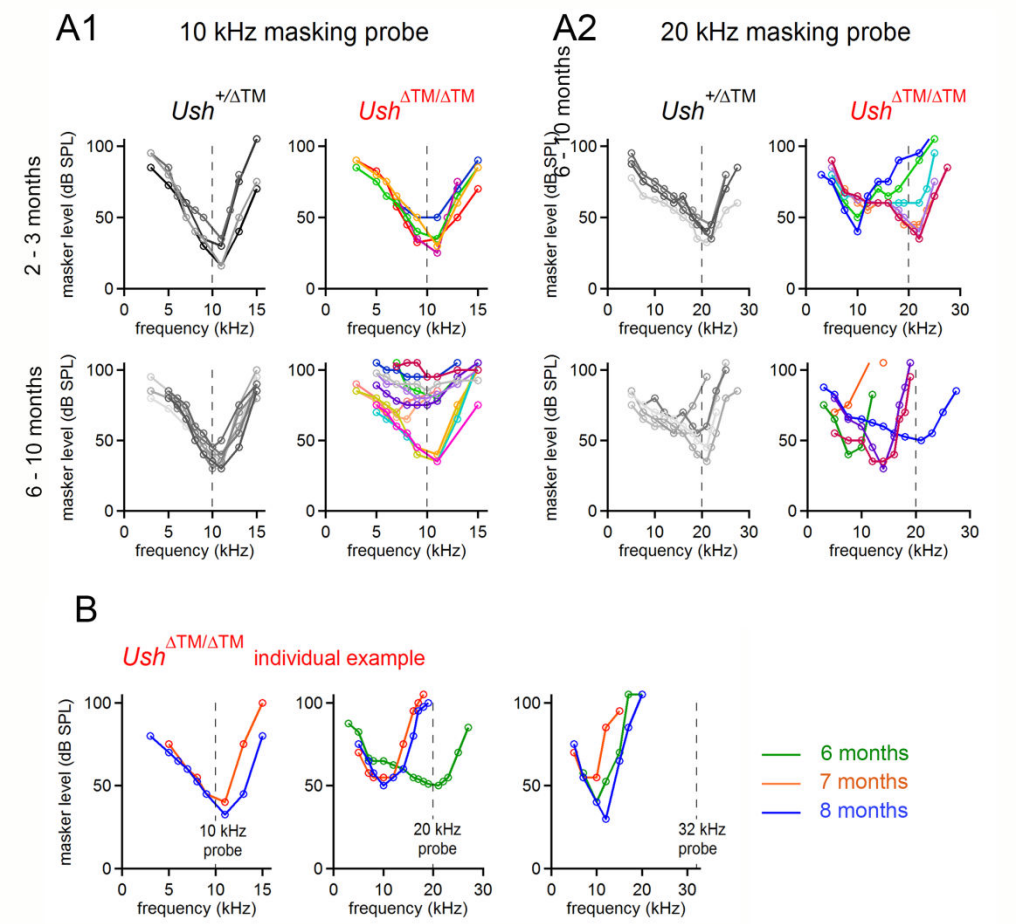

Figure 36. Abnormally efficient masking of mid-high frequency sounds by lower frequency sounds in *a subset of Ush2a*$^{\Delta TM/\Delta TM}$ mice

(*A) Masking tuning curves recorded in either 2- to 3-month or 6- to 10-month old Ush2a*$^{+/\Delta TM}$ *and Ush2a*$^{\Delta TM/\Delta TM}$ *mice, for a low frequency probe tone (A1) and a mid-high frequency probe tone (A2). The most efficient masker (dip of the V-shaped curve) was at or near the probe frequency and within 10 dB of the probe intensity for 2- to 3-month old mice (see Figure 35 for ABR thresholds curve). At 6- to 10 months of age, the most efficient masker was at or near the probe frequency but in 8 out of 12 Ush2a*$^{\Delta TM/\Delta TM}$ *mice the intensity of the masker needed to be elevated (A1). For a mid-high frequency probe tone (20 kHz), the efficient masking (the dip of the tuning curve) was shifted toward low-frequency sounds (10-15 kHz) in two out of six 2- to 3-month old Ush2a*$^{\Delta TM/\Delta TM}$ *mice, and in four out of five 6- to 10-month old Ush2a*$^{\Delta TM/\Delta TM}$ *mice. The masking tuning curve shift never occurred in Ush2a*$^{+/\Delta TM}$ *mice, regardless of age. (B) Evolution of masking tuning curves in the same Ush2a*$^{\Delta TM/\Delta TM}$ *mouse. For a low probe tone (10 kHz), the most efficient masker was at or near the probe frequency, independent of age. For mid-high probe tone (20 kHz), the most efficient masker was at or near the probe frequency at the age of 6 months but shifted towards 10 kHz at the age of 7 and 8 months. For a higher frequency probe tone (32 kHz), at the age of 6 months, a shift could already be observed.*

In a normally sensitive cochlea, the most effective masking sounds have frequencies very close to that of the probe tone. The dip that appears in the masking tuning curve indicates the place along the cochlea where the masker and probe sounds interact the most (**Kamiya et al., 2014**). In *Ush2a*$^{\Delta TM/\Delta TM}$ mice, we used 10 kHz, 20 kHz and in some cases, 32 kHz probe tones, representative of low and mid-high frequencies, at different ages. With a 10 kHz probe tone, masking tuning curve dips in 2- to 3-month and 6- to 10-month-old *Ush2a*$^{\Delta TM/\Delta TM}$ mice were close to the frequency of the probe tone tested, just as in *Ush2a*$^{+/\Delta TM}$ mice at the same age (**Figure** 36**A**). In the 6- to 10-month old *Ush2a*$^{\Delta TM/\Delta TM}$ mice however, the intensity of the masking sound needed to be elevated by approximately 40 dB SPL in order to mask the probe tone (**Figure** 36**A1**), a result compatible with the ABR threshold elevations observed in these mice from the age of 5 months onward (**Figure 35A**). When using a 20 kHz probe tone, however, we observed an abnormal shift of the masking tuning curve dip towards low frequencies in some (2 out of 6 mice), but not all, 2- to 3-month old *Ush2a*$^{\Delta TM/\Delta TM}$ mice, suggesting that the age onset of the shift varied from one mouse to the other. In 6- to 10-month old *Ush2a*$^{\Delta TM/\Delta TM}$ mice, the shift was more frequently observed (4 out 5 mice). In control mice, no such shift away from the probe tone was ever observed (n = 5) (**Figure** 36**A2**). We also followed the individual evolution of masking tuning curves in a few mice, and thereby, further illustrated the progressive nature of the shift in masking tuning curves in *Ush2a*$^{\Delta TM/\Delta TM}$ mice (see example in **Figure** 36**B**).

Ankle links persist despite the absence of the usherin long b-isoform

To try and explain the late onset of functional defects observed in *Ush2a*$^{\Delta TM/\Delta TM}$ mice, we searched for morphological defects of the IHC and OHC hair bundles. Because *Ush2a* expression is correlated with the presence of ankle links between P2 and P12 (**Goodyear et al., 2005**), we analysed the hair bundles in P5 *Ush2a*$^{\Delta TM/\Delta TM}$ mice by scanning electron microscopy (SEM) imaging. The IHC and OHC hair bundles all had three rows of stereocilia of graded length (**Figure 37A1**), and the average wedge angle of both the OHC V-shaped and IHC U-shaped hair bundles was normal (**Figure 37A2**). We did however observe a few supernumerary microvilli in the centre of IHC and OHC hair bundles (**Figure 37A1**), and the tallest row of stereocilia was on average 13% shorter for IHCs (n = 63) and 20% shorter for OHCs (n = 60) than in *Ush2a*$^{+/\Delta TM}$ mice (n = 29, and n = 55, respectively; $p < 10^{-4}$ for both comparisons) (**Figure 37A2**). Furthermore, and quite unexpectedly, basal lateral links resembling ankle links could be observed in the hair bundles of *Ush2a*$^{\Delta TM/\Delta TM}$ OHCs on P4, despite the absence of the usherin long b-isoform (**Figure 37B**).

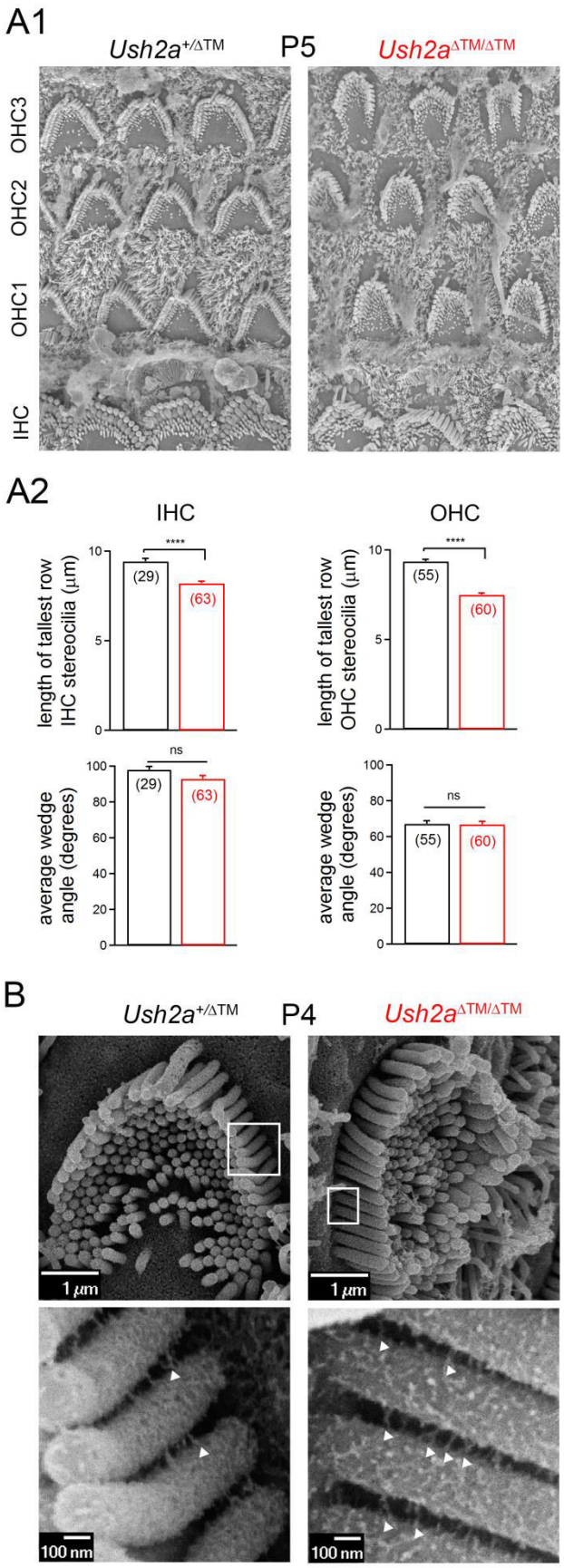

Figure 37. Scanning electron micrographs (SEM) of cochlear hair bundles in *Ush2a*$^{\Delta TM/\Delta TM}$ and *Ush2a*$^{\Delta TM/\Delta TM}$ P5 mice

(A1) IHC and OHC hair bundles show mild defects in the Ush2a$^{\Delta TM/\Delta TM}$ *mouse. Supernumerary microvilli can be observed in the centre of the U- and V-shaped hair bundles. Some hair bundles also display sometimes shorter, sometimes longer "branches". (A2) Average length of tallest-row stereocilia, and average wedge angle, for IHCs and OHCs in Ush2a*$^{\Delta TM/\Delta TM}$ *and Ush2a*$^{\Delta TM/\Delta TM}$ *mice. (B) Scanning electron micrographs (SEM) of P4 Ush2a*$^{+/\Delta TM}$ *and Ush2a*$^{\Delta TM/\Delta TM}$ *OHCs. Insets: enlarged views of stereocilia bases. Fibrous links resembling ankle links can be observed in both Ush2a*$^{+/\Delta TM}$ *and Ush2a*$^{\Delta TM/\Delta TM}$ *OHC hair bundles.*

The distribution of whirlin, but not adgrv1 and pdzd7, in the hair bundle, is affected by the absence of the usherin long b-isoform

It has previously been shown that the ankle link molecular complex is made of adgrv1, usherin, and whirlin, the proteins encoded by the three *USH2A* genes, as well as pdzd7, encoded by an *USH2* modifier gene (**Adato et al., 2005; Michalski et al., 2007; Grati et al., 2012; Chen et al., 2014; Zou et al., 2015**). In mice lacking adgrv1 (*Adgrv1*$^{-/-}$), the ankle link complex is disrupted, as shown by the concomitant absence of usherin, whirlin (**Michalski et al., 2007**) and pdzd7 (**Zou et al., 2014**). In whirler mice that lack a functional whirlin, usherin could not be detected in the ankle link region (**Michalski et al., 2007**). In *Ush2a*$^{\Delta TM/\Delta TM}$ mice, the distribution of both adgrv1 and pdzd7 was unaffected (**Figure 38**). Whirlin, however, could not be detected at the base, but was still present at the tips of the stereocilia (**Figure 38**). This result is consistent with a recent report suggesting that whirlin has a higher affinity for usherin than for adgrv1, while pdzd7 has a higher affinity for adgrv1 than for usherin (**Chen et al., 2014**).

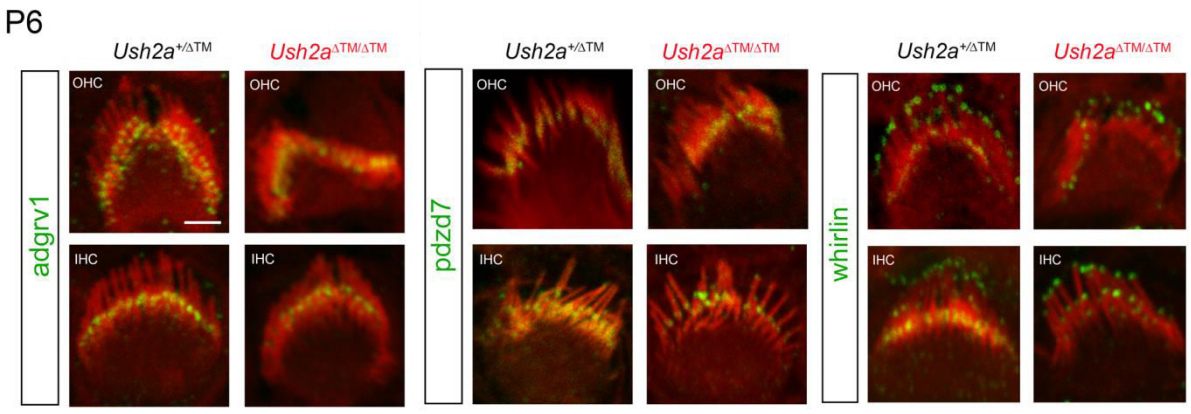

Figure 38. Hair bundle distribution of adgrv1, pdzd7 and whirlin in the cochlear hair bundles of *Ush2a*$^{+/\Delta TM}$ and *Ush2a*$^{\Delta TM/\Delta TM}$ P6 mice

SANS RESCUE PROJECT

Another project I participated in, focused on using virally mediated gene therapy in a bid to restore hearing and vestibular functions in mice lacking the scaffold protein sans (*Ush1g*$^{-/-}$ mice), considered as a model for Usher syndrome type 1 (**Weil et al., 2003**).

In humans, mild to severe deafness can be treated by hearing aids, and for severe to profound deafness a cochlear implant can be considered, for some but not all patients. In addition, vestibular disorders are a significant cause of balance dysfunction, and can lead to dizziness and falling (**Agrawal et al., 2009**). Currently, several clinical approaches exist to treat these disorders, but they are still far from being ideal. Vertigo can be relieved by pharmacological treatments (**Brandt, 2000; Strupp et al., 2011**), or vestibular compensation and rehabilitation (**Balaban et al., 2012; Deveze et al., 2014**). However, whatever the approach, the restoration of audition and/or vestibular function is always incomplete, especially in noisy environments. Thus, alternatives are being investigated. Pharmacologic, stem cell or gene therapies **(Meyer et al., 2013; Géléoc & Holt, 2014**) are some of the avenues being explored.

For hereditary deafness, various studies have used virally mediated gene therapy with promising results in hearing restoration (**Akil et al., 2012**). For example, virally mediated gene therapy has been used to restore hearing in deaf mice lacking transmembrane channel-like gene 1 (T*mc1*) (**Askew et al., 2015**). Tmc1, the protein encoded by the *Tmc1* gene, is reported to make part of the mechano-electrical transduction channel located at the tips of the small- and middle-row stereocilia of auditory sensory cell hair bundles, and in vestibular hair cells. Virally mediated gene therapy was efficient to restore mechano-electrical transduction in IHCs, but only partially restored hearing in treated *Tmc1* knockout mice. Another study showed that injection of exogenous whirlin, by means of virally mediated

gene therapy, in deaf whirler mice, was capable of restoring whirlin expression and distribution, and the characteristic morphology of auditory hair cells (**Chien et al., 2015**). Whirlin gene therapy also increased IHC survival, but was not sufficient to restore hearing.

It is in this context that Alice Emptoz, a PhD student in our laboratory undertook the study of virally mediated gene therapy on *Ush1g*$^{-/-}$ mice. *Ush1g*$^{-/-}$ mice, generated in our laboratory, suffer from profound deafness and severe vestibular dysfunction characterised by circling behaviour and head tossing. Sans, the protein encoded by *Ush1g*, is a small scaffold protein which consists of 4 ankyrin repeats, a central domain, a SAM domain and a C-terminal type I PDZ binding motif. It is an essential component of the molecular complex present at the lower insertion point of the tip-link and plays a critical role in hair bundle cohesion (**Weil et al., 2003; Lefevre et al., 2008; Caberlotto et al., 2011b; Grati and Kachar, 2011**). Adeno-associated viruses (AAV) were chosen as the preferred gene transfer system to try and restore hearing and vestibular function in *Ush1g*$^{-/-}$ mice. AAVs are derived from a replication-deficient non-pathogenic parvovirus, have a lower immunogenicity than many other vector systems, and are capable of infecting non-dividing cells with a long-term transgene expression. For this reason, they have emerged as one of the most promising gene transfer systems to date. My contribution to the study was to measure mechano-electrical transduction currents in auditory hair cells of injected mice.

Results

Injected *Ush1g*$^{-/-}$ mice have normal mechano-electrical transduction currents on P7

The left ear of *Ush1g*$^{-/-}$ mice was injected with AAVs containing the *Ush1g* gene, in a bid to restore hearing and vestibular function. Andrea Lelli (a post-doctoral fellow participating on the project) and I recorded mechano-electrical transduction currents in cochlear hair cells of injected *Ush1g*$^{-/-}$ and non-injected *Ush1g*$^{-/-}$ mice. As previously reported (**Caberlotto et al., 2011b**), in non-injected *Ush1g*$^{-/-}$ mice currents were very small (**Figure 39**). In P7 injected *Ush1g*$^{-/-}$ IHCs and OHCs, displacements of the hair bundle in the positive direction elicited mechano-electrical currents close to that of positive control *Ush1g*$^{+/-}$ mice (injected or non-injected) (**Figure 39 & Figure 40**). Furthermore, the displacement-current (I(X)) curve in IHCs showed no significant difference between injected *Ush1g*$^{-/-}$ and injected *Ush1g*$^{+/-}$ mice (**Figure 39**). The averaged peak amplitudes of the mechano-electrical currents are reported in the following tables:

IHCs:

	Injected	Non-injected
Ush1g$^{-/-}$	424 ± 69 pA	111 ± 30 pA
Ush1g$^{+/-}$	763 ± 126 pA	-

OHCs:

	Injected	Non-injected
Ush1g$^{-/-}$	641 ± 35 pA	47 ± 6 pA
Ush1g$^{+/-}$	721 ± 98 pA	694 ± 87 pA

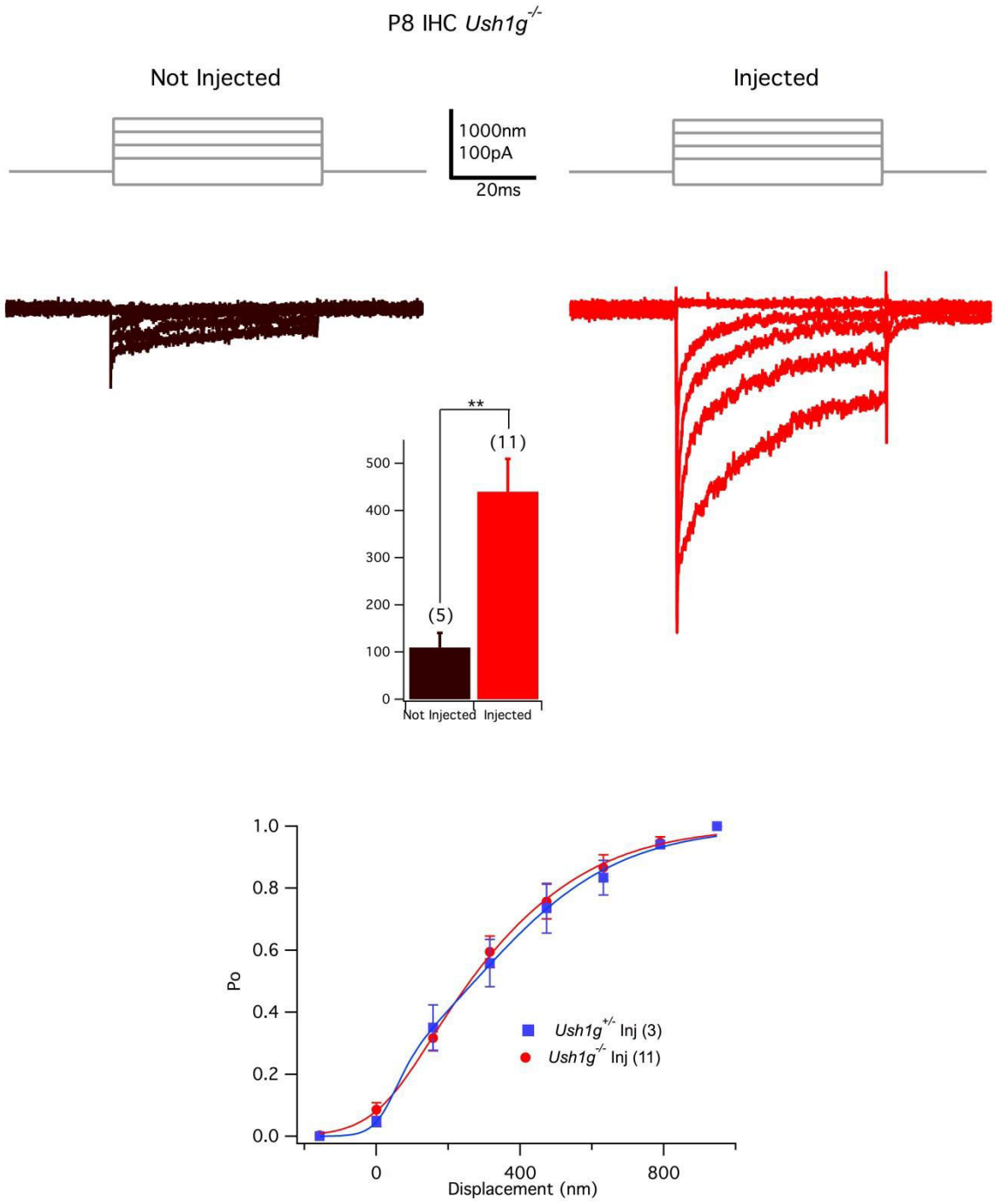

Figure 39. Mechano-electrical transduction currents and I(X) curves in injected and non-injected *Ush1g*$^{+/-}$ and *Ush1g*$^{-/-}$ IHCs

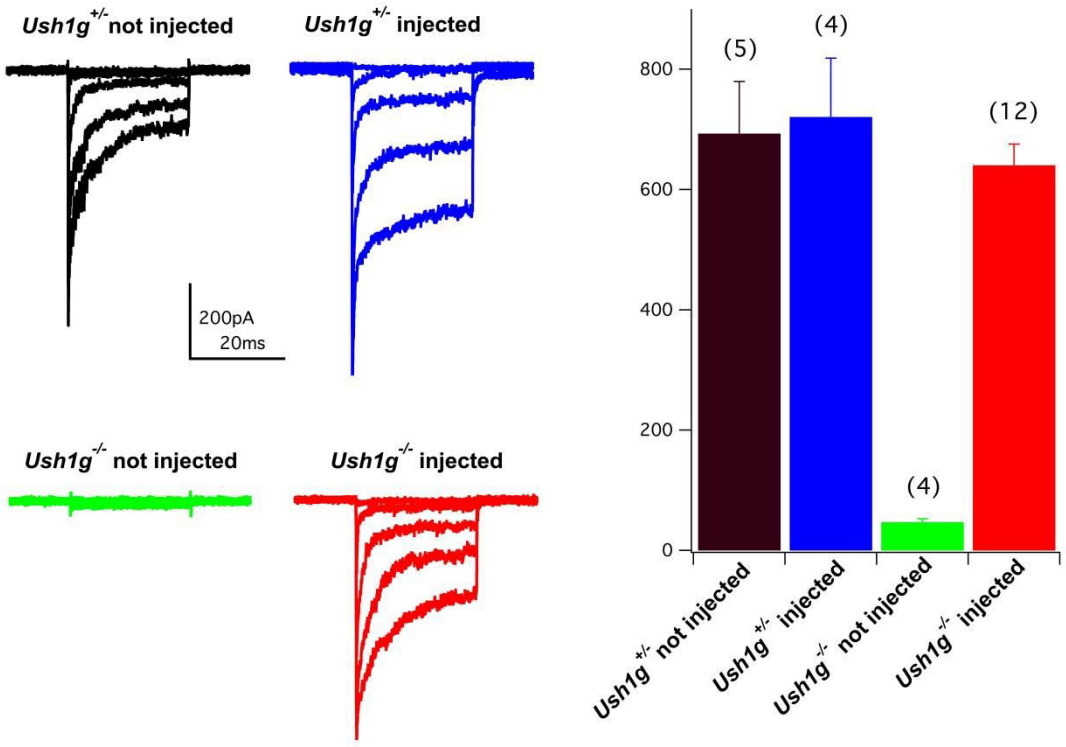

Figure 40. Mechano-electrical transduction currents and I(X) curves in injected and non-injected *Ush1g*$^{+/-}$ and *Ush1g*$^{-/-}$ OHCs

Injected *Ush1g*$^{-/-}$ mice partially recover auditory function, mainly for low frequencies

One-month old injected *Ush1g*$^{-/-}$ mice and *Ush1g*$^{+/-}$ mice were subjected to auditory brainstem response tests, to determine whether they had recovered any auditory function. Because only the left ear was injected in *Ush1g*$^{-/-}$ mice, the right ear from the same mouse served as a negative control. A partial restoration of hearing, 10 to 15 dB SPL for frequencies ranging from 5-20 kHz, was recorded in the left ear, when compared to the right ear of injected *Ush1g*$^{-/-}$ mice (**Figure 41**). For high frequencies (30 to 40 kHz) however, there was no restoration of auditory function. These results are consistent with the fact that there was a high transduction rate of the AAVs in the apical and middle turns of the cochlea, but a low transduction rate in the basal turn (figure not shown).

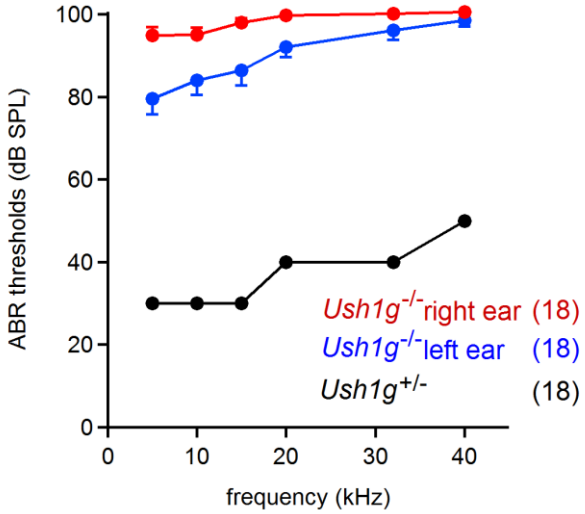

Figure 41. Auditory brainstem response recordings in 1-month old injected *Ush1g*$^{-/-}$ and *Ush1g*$^{+/-}$ mice

Although the rate of transduction of the AAVs was high in IHCs towards the apex of the cochlea (90% of apical and 70% of middle-turn hair cells were transduced), the transduction rate was low in OHCs. Furthermore, when MET currents were recorded, individual hair cells were selected according to whether they had been transduced or not, whereas auditory brainstem response recordings give a broader view of the auditory function of the cochlea. This could be the reason why a discrepancy is observed between *ex vivo* recordings on P7, where MET currents are close to normal, and *in vivo* recordings around 1 month of age, where hearing function is only partially restored.

Alice Emptoz, the main investigator on this project, also tested vestibular function in the same injected *Ush1g*$^{-/-}$ mice. Surprisingly, despite single unilateral injection of the left ear with the AAV, treated *Ush1g*$^{-/-}$ mice displayed normal balance function, as compared to wild type mice. Thus the injection of *Ush1g*-containing AAVs led to complete recovery of the vestibular function in *Ush1g*$^{-/-}$ mice. Taken together, these results indicate that although improvements, such as an earlier injection time for example, need to be made, virally mediated gene therapy is a promising solution to help restore auditory and vestibular function in *Ush1g*$^{-/-}$ mice.

CIB2 PROJECT

CIB2 is the latest causative gene for Usher syndrome 1 (USH1J) to have been reported (**Riazuddin et al., 2012**). It codes for CIB2, a member of the calcium- and integrin-binding protein family that contains three predicted EF-hand domains that change conformation upon binding of calcium, and previous work on zebrafish, drosophila and rats have shown that cib2 plays a role in mediating intracellular calcium signalling (**Blazejczyk et al., 2009; Riazuddin et al., 2012**). In the mammalian cochlea, intracellular calcium levels play a critical role in various phenomena such as mechano-electrical transduction, adaptation, frequency tuning and outer hair cell electromotility. A tight control of calcium concentrations within the stereocilia is essential to proper hair cell function. To investigate the role of cib2 in the inner ear, morpho-functional analyses were carried out in *Cib2*$^{-/-}$ mice.

Results

Cib2$^{-/-}$ mice are profoundly deaf

Auditory function was assessed first by auditory brainstem response recordings and DPOAE measurements. In *Cib2*$^{-/-}$ mice, ABR thresholds in response to tone bursts were markedly increased throughout the 5-40 kHz frequency range from P15 onwards, while no DPOAEs could be recorded (figure not shown). Interestingly, while these mice were profoundly deaf, no balance defects were observed irrespective of the analysed stages, from P20 to P90.

Absent MET current responses in cochlear hair cells of *Cib2*$^{-/-}$ mice

Considering the profound deafness and absent vestibular dysfunction, we studied the MET currents in cochlear outer hair cells (OHCs), and the utricular hair cells (UHCs) of P7 *Cib2*$^{-/-}$ mice. I mechanically stimulated hair bundles, and found that in *Cib2*$^{-/-}$ OHCs, displacements of the hair bundle in the positive direction did not elicit any MET currents ($p < 10^{-4}$) (**Figure 42**), consistent with the previously observed profound deafness and absence of DPOAEs. When MET currents were measured in UHCs however, I found that the averaged peak amplitude of the MET currents was unaltered ($p = 0.39$, Welsh's t-test), when compared to the averaged peak amplitudes of control UHCs (**Figure 43**). *Cib2*$^{-/-}$ UHCs displayed robust MET current responses, with averaged peak amplitudes of 328 ± 60 pA ($n = 5$), versus 320 ± 32 pA in control UHCs ($n = 5$).

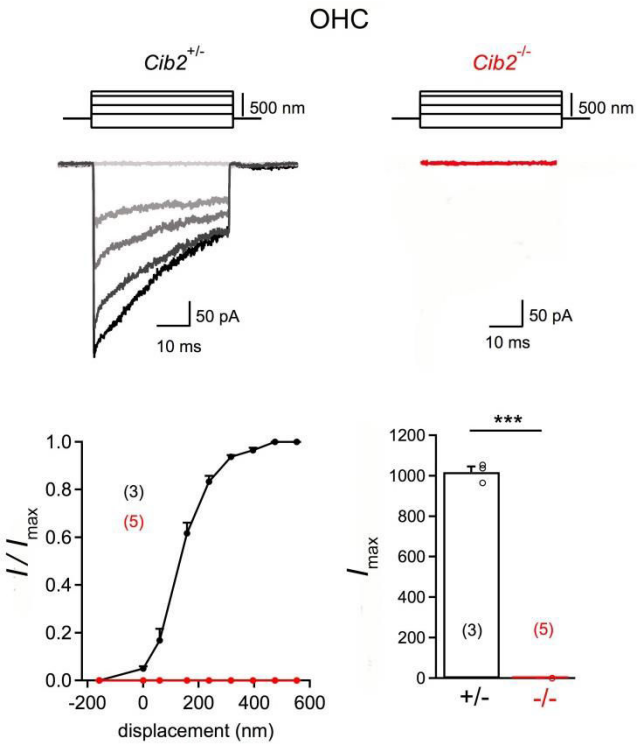

Figure 42. Mechano-electrical transduction current recordings, by mechanical stimulation of OHC hair bundles in the excitatory direction

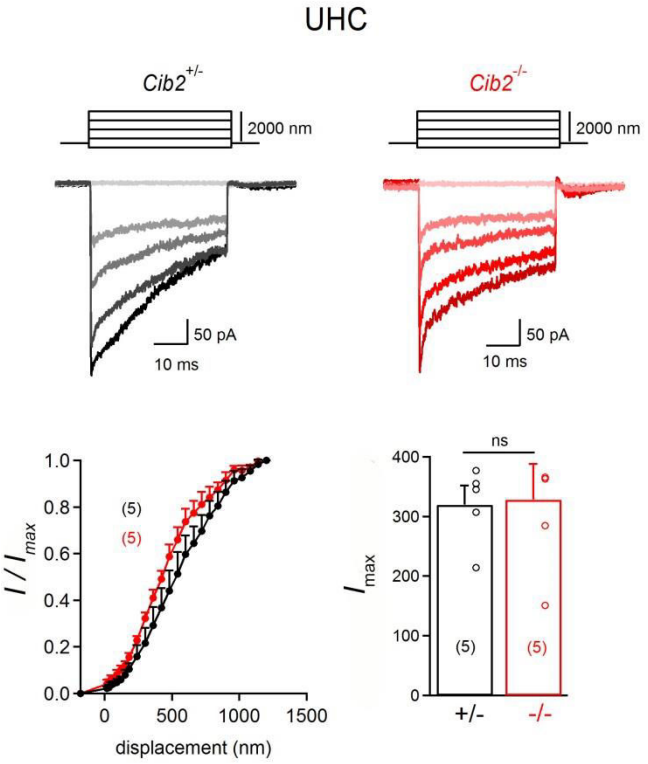

Figure 43. Mechano-electrical transduction current recordings, by mechanical stimulation of UHC hair bundles in the excitatory direction

The sensitivity of the MET response, measured by determining the maximum slope of the current-displacement curve, was similar to that in controls for *Cib2*$^{-/-}$ UHCs. Furthermore, characteristic parameters of adaptation, such as the extent of adaptation, and fast and slow adaptation time constants, displayed no significant alteration in the UHCs of *Cib2*$^{-/-}$ mice when compared to control mice (data not shown).

Cochlear, but not vestibular, hair bundles of *Cib2*$^{-/-}$ mice have abnormally shaped architecture

We investigated possible hair bundle defects underlying the deafness of *Cib2*$^{-/-}$ mice by analysing scanning electron micrographs at pre- and post-hearing stages. Up to P6, *Cib2*$^{-/-}$ cochlear and vestibular hair bundles displayed a normal morphology. As of P7, IHC hair bundles displayed slight morphological defects, and OHC hair bundles appeared more rounded than normal. Furthermore, a detachment from the kinocilium of the stereocilia in some OHC hair bundles could be observed (**Figure 44**). On P18, OHC hair bundles were clearly split in 2 through the middle, slight defects persisted in IHC hair bundles (**Figure 44**), and vestibular hair bundles did not display any visible defects (data not shown).

The lack of visible morphological defects in UHCs is consistent with the mechano-electrical transduction recordings on P7. However, the discrepancy between the total absence of MET currents and only the slight morphological defects in OHCS was puzzling. In other mouse models for USH1, when no MET current could be recorded, cochlear hair bundles displayed far more severe morphological defects.

In light of these results, several questions can be raised: why do mechano-electrical transduction currents persist in vestibular hair cells and not cochlear hair cells? Are there any functionally redundant isoforms of *Cib2* that persist in UHCs and not OHCs? Is our mouse model truly representative of the human phenotype? If so, how does that affect the classification of *CIB2* as a gene responsible for Usher syndrome type 1? Further experiments are still needed to try and resolve these questions.

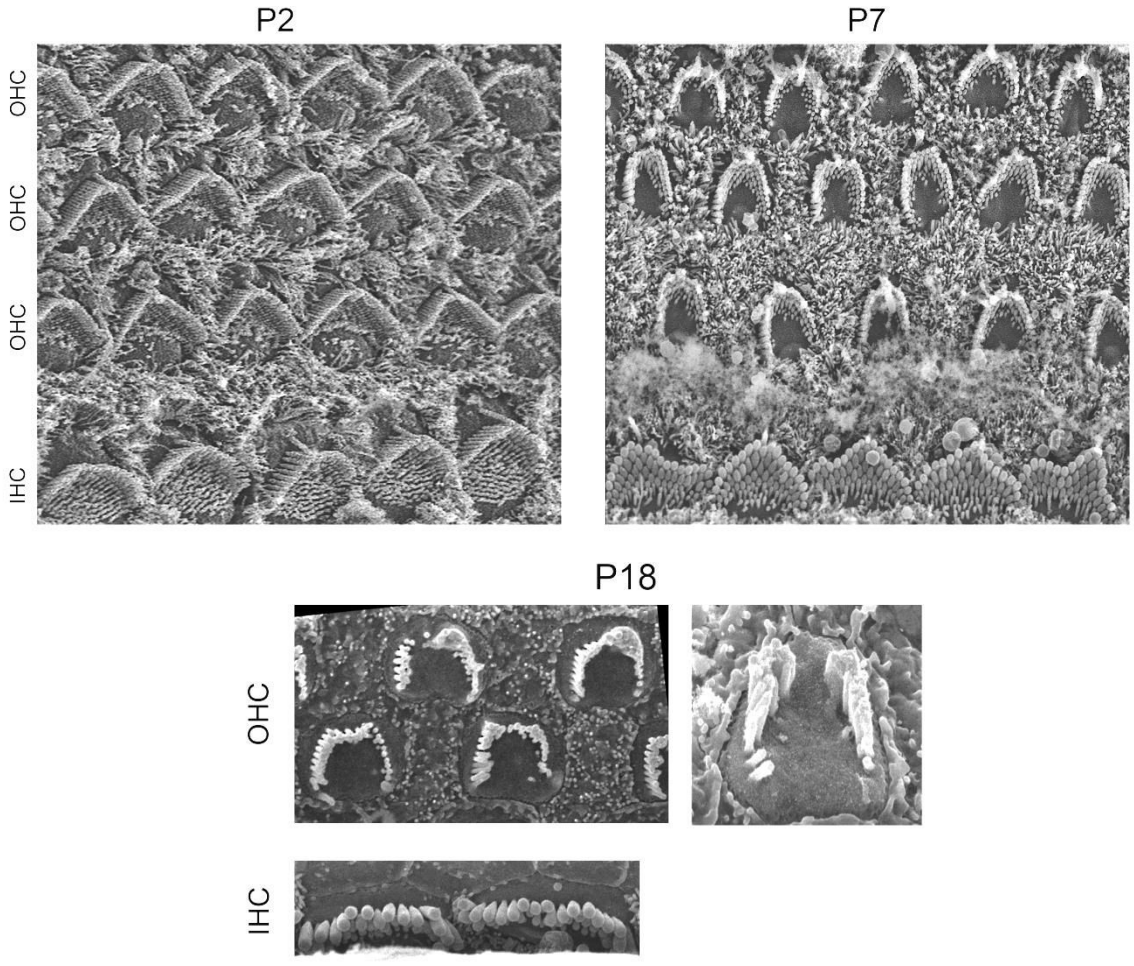

Figure 44. Scanning electron micrographs of P2, P7, and P18 *Cib2*$^{-/-}$ cochlear hair bundles (images courtesy of Vincent Michel)

PROTOCADHERIN-15 PROJECT

The tip-link is a key component of the auditory mechano-electrical transduction machinery. During development in mice, it becomes clearly distinguishable from the other links as of P5, as an oblique link connecting the tip of the short- and middle-row stereocilia to the side of the adjacent taller stereocilia (**Kachar et al., 2000; Goodyear et al., 2005; Furness et al., 2008**). Sound-induced motion of the hair bundle affects the tension in the tip-link, and this tension in turn gates the mechano-electrical transduction channel(s), located at the apex of short- and middle-row stereocilia (**Beurg et al., 2009**). In transmission electron micrographs of stereocilia, there are electron dense areas at the upper and at the lower insertion points of the tip-link (**Furness and Hackney, 1985**). These densities presumably contain the proteins of the mechano-electrical transduction machinery that connect the tip-link to the actin cytoskeleton. Conditional knockout mice (mice in which a gene is deleted only after the period of hair bundle development) which have lost the tip-link, show regression of the short- and middle-row stereocilia, indicating a connection between the tip-link and the F-actin polymerisation machinery located at the tips of these stereocilia (**Caberlotto et al., 2011a; Pepermans et al., 2014**). After the period of hair bundle morphogenesis, stereocilia actin cores are largely static, with a dynamic regulation at the tips to maintain a critical length. Short- and middle-row stereocilia, which have mechanically gated ion channels, show more variable actin turnover than the tallest stereocilia, which lack channels (**Narayanan et al., 2015**).

Protocadherin-15 (Pcdh15) and cadherin-23 (Cdh23), two non-conventional cadherins, have been identified as components of several types of links in the hair bundle, including the tip link. The tip-link is formed by homodimers of Pcdh15 and homodimers of Cdh23, connected together in a transdimer conformation (**Siemens et al., 2004; Ahmed et al., 2006;**

Kazmierczak et al., 2007). Pcdh15 forms the lower part of the tip-link, whereas Cdh23 forms the upper part.

Three different classes of Pcdh15 splice-transmembrane isoforms can be distinguished based on their C-terminal cytoplasmic sequence, encoded by the 3'-most coding exon: CD1, CD2 and CD3. They are predicted to encode type I transmembrane proteins with an extracellular region composed of 11 ectocadherin repeats, and different cytoplasmic regions, including at their very end, an isoform specific C-terminal PDZ binding motif (PBM). Absence of Pcdh15 or Cdh23 leads to Usher syndrome type I. The precise contribution of each Pcdh15 isoform in the stereocilia links is however, still poorly understood. Pcdh15-CD2 is essential for the formation of kinocialiary links (**Webb et al., 2011**) and previous work in our laboratory has shown that in mature murine auditory hair cells, Pcdh15-CD2 is the only Pcdh15 isoform essential for tip-link formation (**Pepermans et al., 2014**).

Functional redundancy between Pcdh15 isoforms has been suggested as a hypothesis to explain the persistence of tip-links in the vestibular and immature auditory hair cells in mutant mice lacking any one of the isoforms. To try and validate or invalidate this hypothesis, Elise Pepermans and other members of our laboratory generated a new knockout mouse model lacking both Pcdh15-CD2 and Pcdh15-CD3, and a mouse model lacking all the Pcdh15 isoforms, and analysed the distribution of the different Pcdh15 isoforms in cochlear hair bundles. In this project, my role was to study mechano-electrical transduction currents in OHCs of mutant mice lacking both CD2 and CD3 isoforms.

Results

We took advantage of the presence of exon 37 in Pcdh15-CD2 and Pcdh15-CD3 transcripts to generate mutant mice lacking both Pcdh15-CD2 and Pcdh15-CD3 (while Pcdh15-CD1 is still produced) (*Pcdh15*$^{\Delta ex37/\Delta ex37}$ mice).

To analyse the functional consequence of the absence of Pcdh15-CD2 and Pcdh15-CD3, I recorded mechano-electrical transduction currents in OHCs of *Pcdh15*$^{\Delta ex37/\Delta ex37}$ mice on P7 (**Figure 46**). In OHCs, the average sensitivity of the mechano-electrical transduction currents to hair bundle displacement was slightly shifted towards the smaller displacements, while the averaged peak amplitude of the mechano-electrical transduction currents was reduced by 29%, when compared to heterozygous littermates (775 $\pm$ 46 pA, n = 10, versus 1043 $\pm$ 52 pA, n = 17; p = 0.001). Similar recordings were done in *Pcdh15*$^{\Delta ex37/\Delta ex37}$ IHCs, where it was determined that mechano-electrical transduction currents were reduced by 74% (251 $\pm$ 19 pA n = 15, versus 869 $\pm$ 51 pA for heterozygous littermates, n = 17; $p < 0.001$). These results confirm that the presence of Pcdh15-CD2 and/or Pcdh15-CD3 is required for normal mechano-electrical transduction function in immature auditory hair cells, and that Pcdh15-CD1 is only able to partially compensate for the combined absence of Pcdh15-CD2 and Pcdh15-CD3.

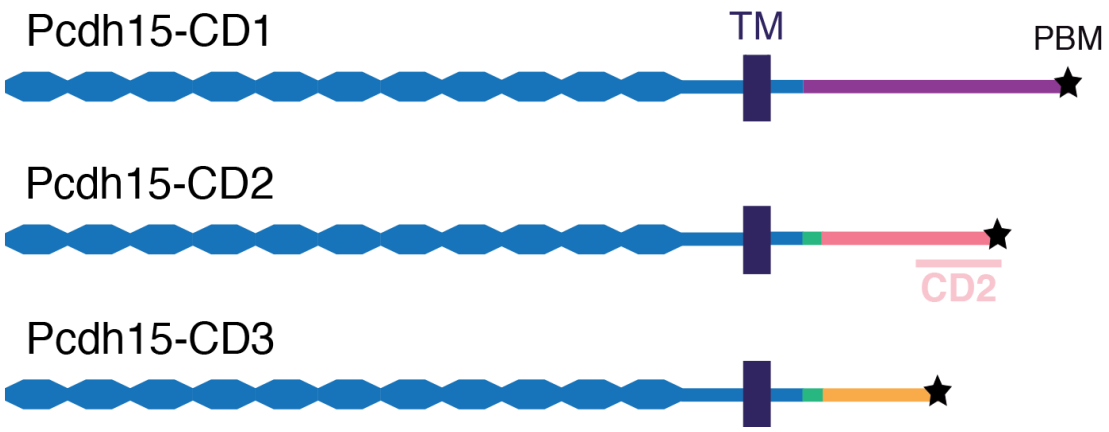

Figure 45. Schematic representation of pcdh15 isoforms

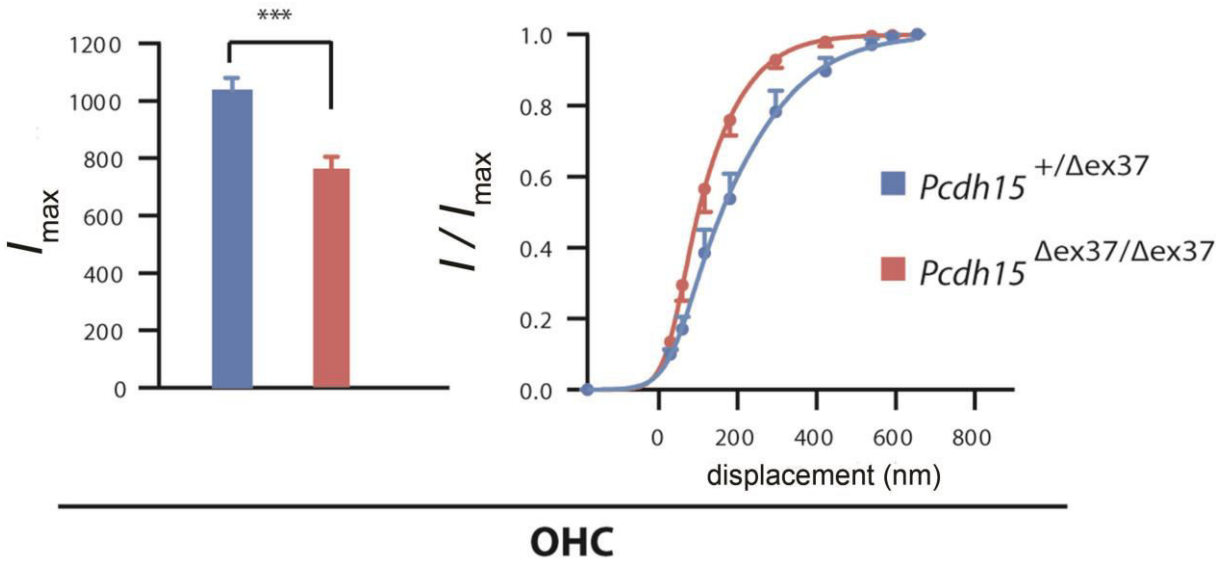

Figure 46. Averaged peak amplitudes of mechano-electrical transduction currents and I(X) curves in *Pcdh15*$^{+/\Delta ex37}$ and *Pcdh15*$^{\Delta ex37/\Delta ex37}$ OHCs

DISCUSSION

During my Phd, the general focus of my work has been on deciphering the specific role of certain proteins within the Usher interactome. The results from my main project have enabled a better understanding of the specific role of the usherin long b-isoform, while my contribution to other projects has allowed us to (i) suggest gene therapy as a viable way to restore vestibular function in mice lacking the USH1 protein sans, (ii) study the structural and functional consequences, in mice, of mutations in *Cib2*, another USH1 causative gene, and (iii) determine which isoforms of protocadherin-15 are essential for the formation of the tip link.

Regarding usherin, a new mouse mutant (*Ush2a*$^{\Delta TM/\Delta TM}$) was produced and analysed. In this model, the long usherin b-isoform, a component of the ankle link complex, was inactivated. Based on the congenital moderate to severe deafness reported in USH2A patients, early postnatal cochlear defects were expected in *Ush2a*$^{\Delta TM/\Delta TM}$ mice. Surprisingly though, OHC and IHC hair bundles only showed moderate morphological defects on P7, with no evidence of any functional impact on mechano-electrical transduction at this pre-hearing stage. Furthermore, basal lateral links similar to ankle links could be observed in the hair bundles of the homozygous mutant mice. This contrasts with previous studies which showed that the ankle links and/or basal lateral links looking like ankle links were no longer present in mice carrying mutations in *Adgrv1*, *Whrn*, and *Pdzd7*, and that the corresponding proteins were essential to the early postnatal development of the hair bundle. In *Adgrv1*$^{-/-}$ mice, OHC hair bundles are either U-shaped or rounded on P6, and IHC hair bundles display asymmetrical “branches” (**Michalski et al., 2007**). In whirler mutant mice, developing IHC hair bundles are markedly shorter than in control mice, while OHC hair bundles are U-

shaped and have irregular stereocilia heights, as of P4 (**Holme et al., 2002**). In *Pdzd7*$^{-/-}$ mice, during the first postnatal week, OHCs already have tilting and sometimes missing stereocilia, as well as mislocalised kinocilia, and at mature stages, these defects are even more severe (**Zou et al., 2014**). Together, the results obtained on *Ush2a*$^{\Delta TM/\Delta TM}$ mice suggest that the long b-isoform of usherin is not critical for the formation of ankle links and early development of the hair bundles, but could play a stabilising role within the ankle link complex.

Despite the absence of auditory defects in early life, *Ush2a*$^{\Delta TM/\Delta TM}$ mice suffer from a progressive form of hearing loss, which manifests itself as a slow elevation of hearing thresholds on ABRs between 3 and 10 months of age. A clear shift of DPOAE cut-off frequencies towards low-frequency regions was also observed as age increased, illustrating an age-dependent progressiveness of OHC dysfunction, hair cell death (dead regions) or a combination of both, along the tonotopic axis. The masking tuning curves further illustrated the dysfunction of OHCs, and the frequency selectivity defects affecting *Ush2a*$^{\Delta TM/\Delta TM}$ mice after 3 months of age. In a normal cochlea, hair cells from the apical and basal region respond to low and high frequency sound stimuli, respectively. The results in *Ush2a*$^{\Delta TM/\Delta TM}$ mice instead suggest that in the absence of the usherin long b-isoform, a mid-high frequency stimulation abnormally induces a response from low frequency-tuned hair cells.

Sound wave propagation along the tectorial membrane in *Ush2a*$^{\Delta TM/\Delta TM}$ mice?

Because there are frequency selectivity defects in *Ush2a*$^{\Delta TM/\Delta TM}$ mice, and that OHCs are more affected than IHCs, it is interesting to compare my results with what has recently been reported in *Nherf1*$^{-/-}$ mice (**Kamiya et al., 2014**). Nherf1 is a member of the nherf (Na^+/H^+ exchanger regulatory factor) protein family, and has been suggested to interact with

cdh23. Although present in IHCs and OHCs during embryonic stages, it disappears from IHCs at P0, but persists in OHCs until P10, when it starts to decline (**Kamiya et al., 2014**). It is a four PDZ domain-containing adaptor protein that interacts with ion channels and transporters, and plays a role in maintaining the ionic composition of the endolymph and perilymph, in the cochlea (**Kanjhan et al., 2006**). In the mouse cochlea, ABR and DPOAE thresholds in P20-P25 *Nherf1*$^{-/-}$ mice were normal for probe tone frequencies ranging from 5 to 15 kHz, but beyond 15 kHz, both ABR and DPOAE thresholds were significantly higher in *Nherf1*$^{-/-}$ mice than in control littermates, illustrating the major structural abnormalities of OHCs observed on scanning electron micrographs (**Kamiya et al., 2014**). When masking tuning curve tests were carried out in *Nherf1*$^{-/-}$ mice, for a 10 kHz probe tone, the masking tuning curves displayed a narrow dip near the frequency of the probe tone, similar to what we observed in 2- to 3-month old *Ush2a*$^{\Delta TM/\Delta TM}$ mice. For probe tone frequencies equal to or above 20 kHz, the most efficient masker was shifted towards low-frequency sounds in *Nherf1*$^{-/-}$ mice, not in control mice, similar to what we observed in 6-10 month old *Ush2a*$^{\Delta TM/\Delta TM}$ mice. Thus, in *Nherf1*$^{-/-}$ mice, the masking tuning curve dips could shift downward by up to two octaves with neural responses to 32 or 40 kHz probe tone bursts at 60 dB SPL being masked optimally by masker tones at 10-12 kHz. Because high-frequency vibrations could not have travelled along the basilar membrane, the observed masking tuning curve shift raised the question of how these vibrations could have reached the apical detection site. With both the Reissner membrane and the tectorial membrane having recently been described as being capable of supporting wave propagation along their longitudinal axis (**Ghaffari et al., 2007, 2011; Lamb and Chadwick, 2011; Reichenbach et al., 2012; Lee et al., 2015**), this might explain the masking tuning curve shifts observed in *Nherf1*$^{-/-}$ and *Ush2a*$^{\Delta TM/\Delta TM}$ mice.

As mentioned in the Introduction, the organ of Corti rests upon the basilar membrane and is covered by the tectorial membrane. IHC hair bundles are free-standing in the subtectorial space, whereas the tips of the tallest row of OHC stereocilia are embedded in the tectorial membrane. In *Ush2a*$^{\Delta TM/\Delta TM}$ OHC hair bundles, the slight morphological defects observed during the first postnatal week do not seem to have perturbed this embedding process: in 3-month and 8-month old *Ush2a*$^{\Delta TM/\Delta TM}$ mice, OHC tallest-row-stereocilia imprints could be observed on the lower surface of the tectorial membrane (**Figure 47**). The imprints however, displayed variable shapes (linear, misoriented, rounded) when compared to the normal "V"- or "W"-shaped imprints in *Ush2a*$^{+/\Delta TM}$ mice. It could be that, although mechanical coupling still exists between OHCs and the tectorial membrane in mice lacking the b-isoform of usherin, the slightly abnormal shape of certain hair bundle eases the mechanical constraints present at the stereocilia/tectorial membrane junction, and this facilitates wave propagation along the tectorial membrane.

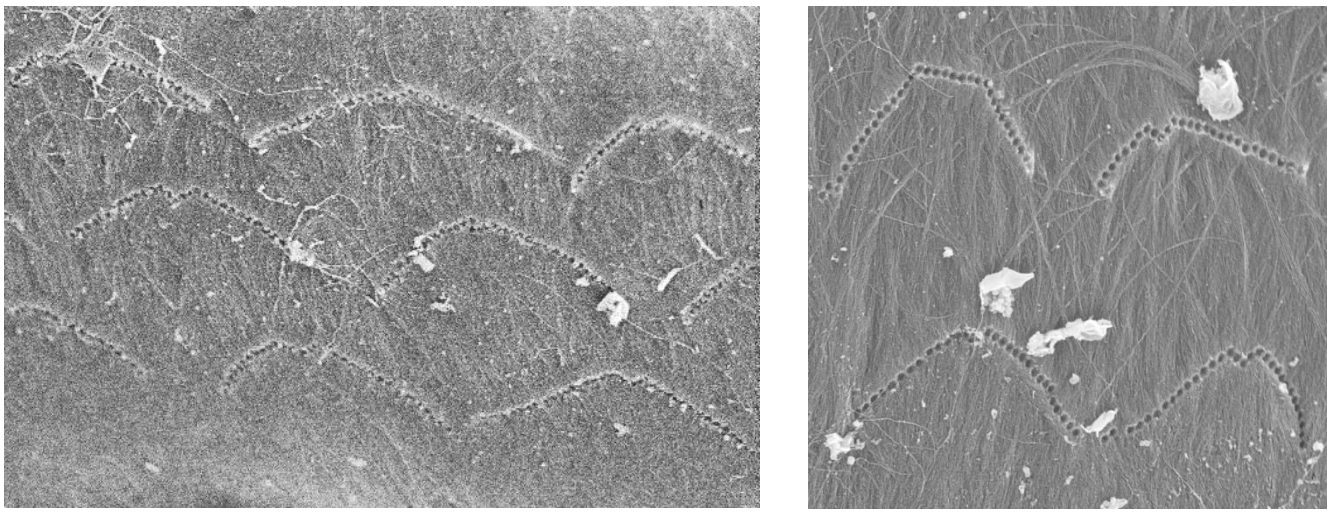

Figure 47. OHC stereocilia imprints on the lower surface of the tectorial membrane in 3-month (left) and 8-month (right) old *Ush2a*$^{\Delta TM/\Delta TM}$ mice

What causes the delay in onset of auditory defects in *Ush2a*$^{\Delta TM/\Delta TM}$ mice?

The delay in onset and progressiveness of the auditory defects in *Ush2a*$^{\Delta TM/\Delta TM}$ mice was not expected because *Ush2a*$^{-/-}$ mice (in which *Ush2a* exon 5 has been deleted) have non-progressive moderate to severe hearing loss as early as 1 month old (**Zou et al., 2015**). It has been reported that a functional polymorphism (G753A) in the coding sequence of cadherin-23 (Cdh23) can lead to age-related progressive hearing loss in certain strains of laboratory mice (**Noben-Trauth and Johnson, 2009**). We investigated whether this hearing-loss-susceptibility variant of Cdh23 (*Cdh23*^{ahl}) plays a part in the progressive nature of the auditory dysfunction in *Ush2a*$^{\Delta TM/\Delta TM}$ mice. The *Cdh23*^{ahl} allele was indeed present both in *Ush2a*$^{+/\Delta TM}$ and *Ush2a*$^{\Delta TM/\Delta TM}$ mice, but *Ush2a*$^{+/\Delta TM}$ mice have stable hearing thresholds until 9 months of age. The progressive nature of the hearing loss in *Ush2a*$^{\Delta TM/\Delta TM}$ mice is therefore unlikely to result from the presence of this *Cdh23*^{ah} allele. This observation is consistent with a previous report suggesting that the *Cdh23*^{ahl} allele is not sufficient to account for accelerated hearing loss, and that other genes could play a protective role (**Kane et al., 2012**).

The fact that in *Ush2a*$^{\Delta TM/\Delta TM}$ mice, adgrv1 and pdzd7 are still restricted to the ankle link region of the hair bundle, whereas in the *Ush2a*$^{-/-}$ mice, adgrv1 and pdzd7 are mislocalised all along the stereocilia (**Zou et al., 2015**), could provide a more plausible explanation for the difference between these two mutant lines. This would suggest that adgrv1 and pdzd7 fulfil their normal role in *Ush2a*$^{\Delta TM/\Delta TM}$ mice but not in *Ush2a*$^{-/-}$ mice. This, in turn, could explain the normal mechano-electrical transduction currents observed in *Ush2a*$^{\Delta TM/\Delta TM}$ P7 mice and the delay in the onset of auditory defects observed in the absence of the usherin long b-isoform. Alternatively, the short a-isoform of usherin, which is still

present in *Ush2a*$^{\Delta TM/\Delta TM}$ mice, could play a role at the ankle link level and/or in the signalling pathway involving the G protein-coupled receptor adgrv1 (**Hamann et al., 2015**) during the first postnatal week, allowing the hair bundle to function normally during the first months of life despite the absence of the long b-isoform. To investigate the potential role of the a-isoform in *Ush2a*$^{\Delta TM/\Delta TM}$ mice, we attempted to generate an antibody directed against the N-terminal domain of usherin. We were, however, unsuccessful in our endeavour, but further attemps should be undertaken, as such an antibody would provide useful information concerning the cochlear distribution of the a-isoform, which in turn could allow a better understanding of its function in *Ush2a*$^{\Delta TM/\Delta TM}$ mice.

Does usherin form a new type of basal lateral links, distinct from the ankle links?

Ankle links are fibrous links that connect stereocilia from the same row, as well as adjacent rows, at the base of the hair bundle. They are present in the mouse cochlear hair bundles from P2 and start to disappear on P9, and they play a critical role in early postnatal hair bundle development (**Goodyear et al., 2005**). In the case of *Ush2a*$^{\Delta TM/\Delta TM}$ mice, because basal lateral links similar to ankle links are still present, I hypothesise that in the absence of the long b-isoform of usherin, the hair bundles are sufficiently weakened during the first postnatal week to slowly degrade, leading to late-onset, progressive auditory defects. Furthermore, because usherin and adgrv1 don't interact directly (**Chen et al., 2014**), these two proteins may form different types of links at the base of the stereocilia. The putative *usherin links* could play a role in supporting adgrv1 links and reinforcing the tension between adjacent stereocilia at their base during their final phase of postnatal development and maturation, prior to hearing onset. They could also connect stereocilia exclusively from the

same row or exclusively from adjacent rows. However, it could be that in normal mice, it is more difficult to detect these usherin links or to distinguish them from adgrv1 links, as usherin might be expressed in lower quantities than adgrv1 in the cochlear hair bundles, just as in the hair bundles of chicken vestibular hair cells (**Grati et al., 2012**).

Gene therapy as a cure for Usher syndrome?

In the gene therapy project I participated in, although there was a spectacular restoration of the vestibular function in *Ush1g*$^{-/-}$ mice, hearing restoration was only partial. This raises the question of whether the viral injection was done early enough. If an injection were done at an embryonic stage, would the hearing restoration be increased? It is essential such a hypothesis be tested, as the timing of the viral injection is a crucial factor if we were to apply the method to *Ush2a*$^{\Delta TM/\Delta TM}$ mice. If we were to test virally mediated gene therapy on *Ush2a*$^{\Delta TM/\Delta TM}$ mice, the initial hypothesis is that P3 would be too late an age to inject animals and hope for good auditory restoration, as ankle links are already well established at this age, and the effects of the absence of the long b-isoform of usherin could already be felt by the developing hair bundle. Although it is true for all USH genes, when it comes to USH2 proteins such as usherin for example, it is essential the virus be injected as early as possible, as USH2 proteins make part of a transient structure in the cochlea, i.e. the ankle link complex, that only exists between P2 and P9. Although difficult to carry out, *in utero* injections could provide a solution to the time constraints related to the use of virally mediated gene therapy to treat Usher syndrome in mice.

An alternative to virally mediated gene therapy, could be the use of nuclease-based technologies, such as the CRISPR/Cas9-mediated homology directed repair (HDR). The

CRISPR/Cas9-mediated HDR has been successfully used to correct the progressive hearing loss phenotype in C57BL/6NTac mice, caused by the *Cdh23*^{ahl} allele (**Mianné et al., 2016**). The study showed that hearing thresholds in "repaired" *Cdh23*^{ahl} mice were normal for low and mid-high frequencies, and that IHC and OHC hair bundle morphology was normal, as late as 9 months of age. The use of this technique should allow researchers to use the C57BL/6N mice strains (common in most research laboratories) to investigate the long-term effects of genetic mutations causing auditory dysfunction, without having to resort to time-consuming backcrossing strategies, for example.

It should be noted however, that research on CRISPR/Cas9-mediated HDR, as a means to treat genetic auditory disorders, is still however in its initial phase, while research on treatment *via* virally mediated gene therapy is at a much more advanced stage, offering a safer option for treating Usher syndrome at this moment and time. The results obtained

Determining a robust genotype/phenotype correlation is essential for better diagnosis of USH patients

It is generally assumed that USH2A patients suffer from congenital moderate to severe hearing loss. Yet this is not what was observed in the *Ush2a*$^{\Delta TM/\Delta TM}$ mouse model. To my knowledge, this is the first USH mouse model which does not replicate the human auditory phenotype at early postnatal stages. However, I believe that the progressive nature of the hearing loss in *Ush2a*$^{\Delta TM/\Delta TM}$ mice is consistent with what has been observed in some USH2A patients (**Van Aarem et al., 1996; Pennings et al., 2003; Sadeghi et al., 2004**). It has indeed been shown that USH2A may manifest as a non-progressive (**Reisser et al., 2002; Liu et al., 2007; Keats and Lentz, 2013; Zou et al., 2015**) or a progressive (**Van Aarem et al.,**

1996; Pennings et al., 2003; Sadeghi et al., 2004) hearing impairment. Our results in *Ush2a*$^{\Delta TM/\Delta TM}$ mice may in fact show that the auditory phenotype in USH2A patients might depend on the nature of their *USH2A* mutation, specifically, on the persistence or absence of the usherin short isoform. The variable expressivity in USH2A patients could also be down to the effects of a modifier gene, such as *PDZD7.* Modifier genes, the effects of which can be seen at the transcriptional, cellular or organismal level, are capable of altering the expression of another gene, which can then affect the penetrance and the expressivity of the disease-causing mutation (**Nadeau, 2001**). It remains to be determined whether PDZD7 is in part responsible for the variable phenotype in USH2A.

To try and establish a mutation/phenotype correlation in USH2A patients, I analysed the available data in the scientific literature. Unfortunately, the information in the published studies was almost always incomplete. In most cases, when data concerning the evolution of the auditory phenotype was available, no reference was made to the type of mutation in the patients. In other cases, when the nature of the mutation was available, no information concerning the presence or not of progressive hearing loss was available. The gene coding for usherin was first reported in humans a little over 20 years ago (**Kimberling et al., 1995**), and the lack of systematically complete information is not totally surprising, because although a lot has been described and the role of usherin now far better understood, I believe two decades is still a relatively short time period to gain sufficient perspective. Clinical data will definitely become more complete as research advances, and as medical practice adapts to these advances.

USH1 patients are understandably the priority when it comes to testing treatments such as gene therapy, as they suffer from the most severe form of hearing loss, have severe vestibular dysfunction, and retinitis pigmentosa. However, although USH2 patients do not have any vestibular dysfunction and suffer from a less severe hearing impairment than USH1 patients, the progressive nature of the hearing loss observed in certain patients leaves a window of opportunity where gene therapy could potentially be used to prevent further damage. For example, patients who are diagnosed with moderate hearing loss at birth, and will undergo a progressive aggravation of the hearing impairment, could be considered potential candidates for gene therapy.

USH1 patients suffer from congenital severe to profound deafness and balance problems, and are therefore easier to diagnose, treat, and follow directly from birth, compared to USH2 or USH3 patients. USH2 patients, are often only diagnosed during their teenage years, once the progressive retinitis pigmentosa begins (**Keats and Lentz, 2013**), and are hence generally not considered for early genetic screening tests. This means that until the visual defects appear, hearing loss could, in some cases, have already worsened. Although there are financial constraints related to the application of high-throughput genetic testing, advances in technology are helping to reduce the cost of such services. By undertaking regular hearing threshold, masking tuning curve, and maybe just as importantly, genetic screening tests, in congenitally deaf patients, I am convinced this will help establish a robust genotype/phenotype correlation, and as a consequence, help in the early detection of those USH2A patients who fall under the “progressive” category. This will allow them to receive adapted treatment and care.

Perspectives

My PhD work has shed light on the role usherin plays within the ankle link complex in cochlear hair cells, but several questions still remain unanswered. What role does the transmembrane isoform of usherin play in the synaptic region of cochlear hair cells, where it has been reported to colocalise with adgrv1 and whirlin (**van Wijk et al., 2006**)? Does the short isoform of usherin also localise to the synaptic region, and if so what role does it play? On a more general note, what is the exact role of the a-isoform of usherin during the development of the hair bundle, and at more mature stages?

A lot also remains to be done to determine the nature of the basal lateral links looking like ankle links observed in the *Ush2a*$^{\Delta TM/\Delta TM}$ mice, and how these links might influence and/or interact with other lateral links of the hair bundle. Indeed, the work done on *Ush2a*$^{-/-}$ mice (**Zou et al., 2015**) showed that both adgrv1 and pdzd7 were mislocalised all along the stereocilia in OHC and IHC hair bundles, and although this was not the case in *Ush2a*$^{\Delta TM/\Delta TM}$ mice, scanning electron micrographs in these mice did reveal, in some hair bundles, what seemed to be an increased number of lateral links towards the apical end of OHC stereocilia. Are these supernumerary links the consequence of a compensatory mechanism that strengthens a weakened hair bundle or does usherin play a role in restricting the amount of lateral links along the length of the stereocilia? Analysis of transmission electron micrographs of *Ush2a*$^{\Delta TM/\Delta TM}$ cochlear hair bundles could provide useful insight, and help verify some of these unanswered questions.

Finally, to confirm whether the late onset defects that are observed in *Ush2a*$^{\Delta TM/\Delta TM}$ mice are due to early developmental deficiencies, as I have hypothesised, it would be interesting to test auditory function in conditional mutant mice that lose the long b-isoform

of usherin after the period of hair bundle development. To obtain these mice, *Ush2a*$^{exon69flox/exon69flox}$ mice would have to be crossed with *Myo15-cre* transgenic mice carrying the *cre* recombinase gene driven by the *myosin-15* gene promoter, which in the inner ear, deletes the DNA segment flanked by the lox (loci of recombination) sites only in hair cells, between the ages of P0 and P2 (**Caberlotto et al., 2011b**). With this technique, and depending on the protein turnover rate, complete removal of the protein has been observed between P8 and P30. An absence of late onset auditory defects in these conditional mutant mice, such as the ones observed in the *Ush2a*$^{\Delta TM/\Delta TM}$ mice, would indicate that the source of the hearing loss lies within the early developmental stages before P8, which would provide precious information for therapeutic strategies in USH2A patients.

Conclusion

If the 1980's can be described as the decade during which the biophysical and biochemical properties of the mechano-electrical transduction process were extensively investigated, and the 1990's as the decade during which the first deafness genes were discovered, the turn of the century has seen researchers use ever-improving biochemical and genetic tools to discover and thoroughly characterise the nature, and the functional role of a vast number of molecular components of the auditory system. My PhD work, which has been fully integrated in this context, has shown that the removal of the long b-isoform of usherin in mice does not result in the disruption of ankle links, and is associated with a delayed progressive auditory phenotype, reminiscent of what is observed in some USH2A patients. This knowledge should contribute to the development of promising therapeutic strategies, such as virally mediated gene therapy, and CRISPR/Cas9-mediated HDR.

BIBLIOGRAPHY

A

Adato A, Lefèvre G, Delprat B, Michel V, Michalski N, Chardenoux S, Weil D, El-Amraoui A, Petit C (2005) Usherin, the defective protein in Usher syndrome type IIA, is likely to be a component of interstereocilia ankle links in the inner ear sensory cells. Hum Mol Genet 14:3921–3932.

Agrawal Y, Carey JP, Della Santina CC, Schubert MC, Minor LB (2009) Disorders of balance and vestibular function in US adults. Arch Intern Med 169:938–944.

Ahmad J, Khan SN, Khan SY, Ramzan K, Riazuddin S, Ahmed ZM, Wilcox ER, Friedman TB, Riazuddin S (2005) DFNB48, a new nonsyndromic recessive deafness locus, maps to chromosome 15q23-q25.1. Hum Genet 116:407–412.

Ahmed ZM, Goodyear R, Riazuddin S, Lagziel A, Legan PK, Behra M, Burgess SM, Lilley KS, Wilcox ER, Riazuddin S, Griffith AJ, Frolenkov GI, Belyantseva IA, Richardson GP, Friedman TB (2006) The Tip-Link Antigen, a Protein Associated with the Transduction Complex of Sensory Hair Cells, Is Protocadherin-15. J Neurosci 26:7022–7034 Available at: http://www.jneurosci.org/cgi/doi/10.1523/JNEUROSCI.1163-06.2006.

Ahmed ZM, Riazuddin S, Bernstein SL, Ahmed Z, Khan S, Griffith AJ, Morell RJ, Friedman TB, Riazuddin S, Wilcox ER (2001) Mutations in the novel protocadherin PCDH15 cause Usher syndrome type 1F. Am J Hum Genet 69:25–34.

Akil O, Seal RP, Burke K, Wang C, Alemi A, During M, Edwards RH, Lustig LR (2012) Restoration of Hearing in the VGLUT3 Knockout Mouse Using Virally Mediated Gene Therapy. Neuron 75:283–293.

Alagramam KN, Murcia CL, Kwon HY, Pawlowski KS, Wright CG, Woychik RP (2001a) The mouse Ames waltzer hearing-loss mutant is caused by mutation of Pcdh15, a novel protocadherin gene. Nat Genet 27:99–102.

Alagramam KN, Yuan H, Kuehn MH, Murcia CL, Wayne S, Srisailpathy CR, Lowry RB, Knaus R, Van Laer L, Bernier FP, Schwartz S, Lee C, Morton CC, Mullins RF, Ramesh A, Van Camp G, Hageman GS, Woychik RP, Smith RJ (2001b) Mutations in the novel protocadherin PCDH15 cause Usher syndrome type 1F. Hum Mol Genet 10:1709–1718.

Askew C, Rochat C, Pan B, Asai Y, Ahmed H, Child E, Schneider BL, Aebischer P, Holt JR (2015) Tmc gene therapy restores auditory function in deaf mice. Sci Transl Med 7:1–12.

Assad JA, Hacohen N, Corey DP (1989) Voltage dependence of adaptation and active bundle movement in bullfrog saccular hair cells. Proc Natl Acad Sci U S A 86:2918–2922 Available at: papers2://publication/uuid/6D1FE7CB-D951-4A63-BA31-E392791AC76A.

Assad JA, Shepherd GMG, Corey DP (1991) Tip-link integrity and mechanical transduction in vertebrate hair cells. Neuron 7:985–994.

B

Balaban CD, Hoffer ME, Gottshall KR (2012) Top-down approach to vestibular compensation: Translational lessons from vestibular rehabilitation. Brain Res 1482:101–111 Available at: http://dx.doi.org/10.1016/j.brainres.2012.08.040.

Belyantseva I a, Boger ET, Naz S, Frolenkov GI, Sellers JR, Ahmed ZM, Griffith AJ, Friedman TB (2005) Myosin-XVa is required for tip localization of whirlin and differential elongation of hair-cell stereocilia. Nat Cell Biol 7:148–156.

Beurg M, Fettiplace R, Nam J-H, Ricci AJ (2009) Localization of inner hair cell mechanotransducer channels using high-speed calcium imaging. Nat Neurosci 12:553–558.

Bhattacharya G, Miller C, Kimberling WJ, Jablonski MM, Cosgrove D (2002) Localization and expression of usherin: A novel basement membrane protein defective in people with Usher's syndrome type IIa. Hear Res 163:1–11.

Bitner-Glindzicz M et al. (2000) A recessive contiguous gene deletion causing infantile hyperinsulinism, enteropathy and deafness identifies the Usher type 1C gene. Nat Genet 26:56–60.

Blazejczyk M, Sobczak A, Debowska K, Wisniewska MB, Kirilenko A, Pikula S, Jaworski J, Kuznicki J, Wojda U (2009) Biochemical characterization and expression analysis of a novel EF-hand Ca2+ binding protein calmyrin2 (Cib2) in brain indicates its function in NMDA receptor mediated Ca2+ signaling. Arch Biochem Biophys 487:66–78 Available at: http://dx.doi.org/10.1016/j.abb.2009.05.002.

Boëda B, El-Amraoui A, Bahloul A, Goodyear R, Daviet L, Blanchard S, Perfettini I, Fath KR, Shorte S, Reiners J, Houdusse A, Legrain P, Wolfrum U, Richardson G, Petit C (2002) Myosin VIIa, harmonin and cadherin-23, three Usher I gene products that cooperate to shape the sensory hair cell bundle. EMBO J 21:6689–6699.

Bolz H, von Brederlow B, Ramírez a, Bryda EC, Kutsche K, Nothwang HG, Seeliger M, del C-Salcedó Cabrera M, Vila MC, Molina OP, Gal a, Kubisch C (2001a) Mutation of CDH23, encoding a new member of the cadherin gene family, causes Usher syndrome type 1D. Nat Genet 27:108–112.

Bolz H, von Brederlow B, Ramírez A, Bryda EC, Kutsche K, Nothwang HG, Seeliger M, del C-Salcedó Cabrera M, Vila MC, Molina OP, Gal A, Kubisch C (2001b) Mutation of CDH23, encoding a new member of the cadherin gene family, causes Usher syndrome type 1D. Nat Genet 27:108–112.

Bork JM et al. (2001) Usher syndrome 1D and nonsyndromic autosomal recessive deafness DFNB12 are caused by allelic mutations of the novel cadherin-like gene CDH23. Am J Hum Genet 68:26–37.

Brandt T (2000) Management of vestibular disorders. J Neurol 247:491–499 Available at: http://www.ncbi.nlm.nih.gov/pubmed/10993488.

C

Caberlotto E, Michel V, Boutet de Monvel J, Petit C (2011a) Coupling of the mechanotransduction machinery and stereocilia F-actin polymerization in the cochlear hair bundles. Bioarchitecture 1:169–174.

Caberlotto E, Michel V, Foucher I, Bahloul A, Goodyear RJ, Pepermans E, Michalski N, Perfettini I, Alegria-Prévot O, Chardenoux S, Do Cruzeiro M, Hardelin J-P, Richardson GP, Avan P, Weil D, Petit C (2011b) Usher type 1G protein sans is a critical component of the tip-link complex, a structure controlling actin polymerization in stereocilia. Proc Natl Acad Sci U S A 108:5825–5830.

Chen Q, Zou J, Shen Z, Zhang W, Yang J (2014) Whirlin and PDZ Domain-containing 7 (PDZD7) Proteins Are Both Required to Form the Quaternary Protein Complex Associated with Usher Syndrome Type 2. J Biol Chem 289:36070–36088 Available at: http://www.jbc.org/cgi/doi/10.1074/jbc.M114.610535.

Cheung ELM, Corey DP (2006) Ca 2 1 Changes the Force Sensitivity of the Hair-Cell Transduction Channel. Biophys J 90:124–139 Available at: http://www.pubmedcentral.nih.gov/articlerender.fcgi?artid=1367012&tool=pmcentrez&rendertype=abstract\nhttp://dx.doi.org/10.1529/biophysj.105.061226.

Chien WW, Isgrig K, Roy S, Belyantseva I a, Drummond MC, May L a, Fitzgerald TS, Friedman TB, Cunningham LL (2015) Gene Therapy Restores Hair Cell Stereocilia Morphology in Inner Ears of Deaf Whirler Mice. Mol Ther 8:1–9 Available at: http://www.nature.com/doifinder/10.1038/mt.2015.150.

Corey DP, Hudspeth a J (1979) Response latency of vertebrate hair cells. Biophys J 26:499–506 Available at: http://www.pubmedcentral.nih.gov/articlerender.fcgi?artid=1328566&tool=pmcentrez&rendertype=abstract.

Corey DP, Hudspeth a J (1983) Kinetics of the receptor current in bullfrog saccular hair cells. J Neurosci 3:962–976.

Crawford BYAC, Evans MG, Fettiplace R (1989) Adaptation of transducer.

Crawford BYAC, Evans MG, Fettiplacet R (1991) July 1990). :369–398.

D

Davenport SL, O'Nuallain S, Omenn G, Wilkus R (1978) Usher Syndrome in Four Hard-of-hearing Siblings. Pediatrics 62:578–583.

Denk W, Holt JR, Shepherd GMG, Coreytt DP (1995) Calcium imaging of single stereocilia in hair cells: Localization of transduction channels at both ends of tip links. Neuron 15:1311–1321.

Deveze A, Bernard-Demanze L, Xavier F, Lavieille JP, Elziere M (2014) Vestibular compensation and vestibular rehabilitation. Current concepts and new trends. Neurophysiol Clin 44:49–57 Available at: http://dx.doi.org/10.1016/j.neucli.2013.10.138.

Di Palma F, Holme RH, Bryda EC, Belyantseva I a, Pellegrino R, Kachar B, Steel KP, Noben-Trauth K (2001) Mutations in Cdh23, encoding a new type of cadherin, cause stereocilia disorganization in waltzer, the mouse model for Usher syndrome type 1D. Nat Genet 27:103–107.

Doherty D, Chudley AE, Coghlan G, Ishak GE, Innes AM, Lemire EG, Rogers RC, Mhanni AA, Phelps IG, Jones SJM, Zhan SH, Fejes AP, Shahin H, Kanaan M, Akay H, Tekin M, Triggs-Raine B, Zelinski T (2012) GPSM2 mutations cause the brain malformations and hearing loss in Chudley-McCullough syndrome. Am J Hum Genet 90:1088–1093.

E

Eatock R a, Corey DP, Hudspeth a J (1987) Adaptation of mechanoelectrical transduction in hair cells of the bullfrog's sacculus. J Neurosci 7:2821–2836.

Ebermann I, Phillips JB, Liebau MC, Koenekoop RK, Schermer B, Lopez I, Schäfer E, Roux AF, Dafinger C, Bernd A, Zrenner E, Claustres M, Blanco B, Nürnberg G, Nürnberg P, Ruland R, Westerfield M, Benzing T, Bolz HJ (2010) PDZD7 is a modifier of retinal disease and a contributor to digenic Usher syndrome. J Clin Invest 120:1812–1823.

Ebermann I, Scholl HPN, Charbel Issa P, Becirovic E, Lamprecht J, Jurklies B, Millán JM, Aller E, Mitter D, Bolz H (2007) A novel gene for Usher syndrome type 2: Mutations in the long isoform of whirlin are associated with retinitis pigmentosa and sensorineural hearing loss. Hum Genet 121:203–211.

Ezan J, Lasvaux L, Gezer A, Novakovic A, May-Simera H, Belotti E, Lhoumeau A-C, Birnbaumer L, Beer-Hammer S, Borg J-P, Le Bivic A, Nürnberg B, Sans N, Montcouquiol M (2013) Primary cilium migration depends on G-protein signalling control of subapical cytoskeleton. Nat Cell Biol 15:1107–1115 Available at: http://www.ncbi.nlm.nih.gov/pubmed/23934215.

F

Fanning AS, Anderson JM (1999) Protein modules as organizers of membrane structure. Curr Opin Cell Biol 11:432–439.

Furness DN, Hackney CM (1985) Cross-links between stereocilia in the guinea pig cochlea. Hear Res 18:177–188 Available at: http://www.ncbi.nlm.nih.gov/pubmed/4044419.

Furness DN, Katori Y, Nirmal Kumar B, Hackney CM (2008) The dimensions and structural attachments of tip links in mammalian cochlear hair cells and the effects of exposure to different levels of extracellular calcium. Neuroscience 154:10–21.

G

Garcia JA, Yee AG, Gillespie PG, Corey DP (1998) Localization of myosin-Ibeta near both ends of tip links in frog saccular hair cells. J Neurosci 18:8637–8647 Available at: http://www.jneurosci.org/cgi/content/abstract/18/21/8637\npapers2://publication/uuid/773E9EA4-0571-4290-9673-DCEF5974FA82.

Géléoc GSG, Holt JR (2014) Sound strategies for hearing restoration. Science 344:1241062 Available at: http://www.pubmedcentral.nih.gov/articlerender.fcgi?artid=4148779&tool=pmcentrez&rendertype=abstract.

Gentry HR, Singer AU, Betts L, Yang C, Ferrara JD, Sondek J, Parise L V. (2005) Structural and biochemical characterization of CIB1 delineates a new family of EF-hand-containing proteins. J Biol Chem 280:8407–8415.

Ghaffari R, Aranyosi AJ, Freeman DM (2007) Longitudinally propagating traveling waves of the mammalian tectorial membrane. Proc Natl Acad Sci U S A 104:16510–16515 Available at: http://www.pnas.org/content/104/42/16510.full.

Ghaffari R, Farrahi S, Aranyosi AJ, Richardson GP, Freeman DM (2011) Tectorial membrane traveling waves underlie impaired hearing in Tectb mutant mice. AIP Conf Proc 1403:85–89 Available at: http://dx.doi.org/10.1038/ncomms1094.

Gibson F, Walsh J, Mburu P, Varela A, Brown K, A., Antonio M, Beisel K, W., Steel K, P., Brown SD, M. (1995) A type VII myosin encoded by the mouse deafness gene shaker-1. Nature 374:62–64 Available at: http://www.nature.com/doifinder/10.1038/374062a0\nhttp://www.ncbi.nlm.nih.gov/pubmed/7870172.

Gillespie PG, Cyr JL (2004) Myosin-1c, the hair cell's adaptation motor. Annu Rev Physiol 66:521–545.

Goodyear R, Richardson G (1999) The ankle-link antigen: an epitope sensitive to calcium chelation associated with the hair-cell surface and the calycal processes of photoreceptors. J Neurosci 19:3761–3772.

Goodyear RJ, Forge A, Kevin Legan P, Richardson GP (2010) Asymmetric distribution of cadherin-23 and protocadherin-15 in the kinocilial links of avian sensory hair cells. J Comp Neurol 518:4288–4297.

Goodyear RJ, Legan PK, Wright MB, Marcotti W, Oganesian a, Coats S a, Booth CJ, Kros CJ, Seifert R a, Bowen-Pope DF, Richardson GP (2003) A receptor-like inositol lipid phosphatase is required for the maturation of developing cochlear hair bundles. J Neurosci 23:9208–9219.

Goodyear RJ, Marcotti W, Kros CJ, Richardson GP (2005) Development and properties of stereociliary link types in hair cells of the mouse cochlea. J Comp Neurol 485:75–85.

Grati M, Kachar B (2011) Myosin VIIa and sans localization at stereocilia upper tip-link density implicates these Usher syndrome proteins in mechanotransduction. Proc Natl Acad Sci:11476–11481 Available at: http://www.ncbi.nlm.nih.gov/pubmed/21709241.

Grati M, Shin J-B, Weston MD, Green J, Bhat M a., Gillespie PG, Kachar B (2012) Localization of PDZD7 to the Stereocilia Ankle-Link Associates this Scaffolding Protein with the Usher Syndrome Protein Network. J Neurosci 32:14288–14293.

Grillet N, Xiong W, Reynolds A, Kazmierczak P, Sato T, Lillo C, Dumont RA, Hintermann E, Sczaniecka A, Schwander M, Williams D, Kachar B, Gillespie PG, M??ller U (2009) Harmonin Mutations Cause Mechanotransduction Defects in Cochlear Hair Cells. Neuron 62:375–387.

H

Hacohen N, Assad J a, Smith WJ, Corey DP (1989) Regulation of tension on hair-cell transduction channels: displacement and calcium dependence. J Neurosci 9:3988–3997 Available at: http://www.ncbi.nlm.nih.gov/pubmed/2555460.

Hamann J et al. (2015) International Union of Basic and Clinical Pharmacology. XCIV. Adhesion G protein-coupled receptors. Pharmacol Rev 67:338–367 Available at: http://www.pubmedcentral.nih.gov/articlerender.fcgi?artid=4394687&tool=pmcentrez&rendertype=abstract.

Holme RH, Kiernan BW, Brown SDM, Steel KP (2002) Elongation of hair cell stereocilia is defective in the mouse mutant whirler. J Comp Neurol 450:94–102.

Holt JR, Gillespie SKH, Provance DW, Shah K, Shokat KM, Corey DP, Mercer JA, Gillespie PG (2002) A chemical-genetic strategy implicates myosin-1c in adaptation by hair cells. Cell 108:371–381.

Howard J, Hudspeth a J (1987) Mechanical relaxation of the hair bundle mediates adaptation in mechanoelectrical transduction by the bullfrog's saccular hair cell. Proc Natl Acad Sci U S A 84:3064–3068 Available at: http://www.pubmedcentral.nih.gov/articlerender.fcgi?artid=304803&tool=pmcentrez&rendertype=abstract.

Howard J, Hudspeth AJ (1988) Compliance of the hair bundle associated with gating of mechanoelectrical transduction channels in the Bullfrog's saccular hair cell. Neuron 1:189–199.

Hudspeth a J (1982) Extracellular current flow and the site of transduction by vertebrate hair cells. J Neurosci 2:1–10.

Hudspeth a J, Corey DP (1977) Sensitivity, polarity, and conductance change in the response of vertebrate hair cells to controlled mechanical stimuli. Proc Natl Acad Sci U S A 74:2407–2411.

Hudspeth a J, Jacobs R (1979) Stereocilia mediate transduction in vertebrate hair cells (auditory system/cilium/vestibular system). Proc Natl Acad Sci U S A 76:1506–1509.

J

Jacobs RA, Hudspeth AJ (1990) Ultrastructural correlates of mechanoelectrical transduction in hair cells of the bullfrog's internal ear. Cold Spring Harb Symp Quant Biol. 55:547-61

Johnson KR, Zheng QY, Weston MD, Ptacek LJ, Noben-Trauth K (2005) The Mass1frings mutation underlies early onset hearing impairment in BUB/BnJ mice, a model for the auditory pathology of Usher syndrome IIC. Genomics 85:582–590.

Jørgensen F, Ohmori H (1988) Amiloride blocks the mechano-electrical transduction channel of hair cells of the chick. J Physiol. 403:577-88

K

Kachar B, Parrakal M, Kurc M, Zhao Y, Gillespie PG (2000) High-resolution structure of hair-cell tip links. Proc Natl Acad Sci 110:12155–12155 Available at: http://www.pnas.org/cgi/doi/10.1073/pnas.1311228110.

Kamiya K, Michel V, Giraudet F, Riederer B, Foucher I, Papal S, Perfettini I, Le Gal S, Verpy E, Xia W, Seidler U, Georgescu M-M, Avan P, El-Amraoui A, Petit C (2014) An unusually powerful mode of low-frequency sound interference due to defective hair bundles of the auditory outer hair cells. Proc Natl Acad Sci U S A 111:9307–9312 Available at: http://www.pubmedcentral.nih.gov/articlerender.fcgi?artid=4078795&tool=pmcentrez&rendertype=abstract.

Kane KL, Longo-Guess CM, Gagnon LH, Ding D, Salvi RJ, Johnson KR (2012) Genetic background effects on age-related hearing loss associated with Cdh23 variants in mice. Hear Res 283:80–88 Available at: http://www.pubmedcentral.nih.gov/articlerender.fcgi?artid=3277672&tool=pmcentrez&rendertype=abstract.

Kanjhan R, Hryciw DH, Yun CC, Bellingham MC, Poronnik P (2006) Postnatal developmental expression of the PDZ scaffolds Na +-H+ exchanger regulatory factors 1 and 2 in the rat cochlea. Cell Tissue Res 323:53–70.

Kawashima Y, Géléoc GSG, Kurima K, Labay V, Lelli A, Asai Y, Makishima T, Wu DK, Santina CC Della, Holt JR, Griffith AJ (2011) Mechanotransduction in mouse inner ear hair cells requires transmembrane channel – like genes. J Clin Invest 121:4796–4809.

Kazmierczak P, Sakaguchi H, Tokita J, Wilson-Kubalek EM, Milligan RA, Müller U, Kachar B (2007) Cadherin-23 and protocadherin-15 interact to form tip-link filaments in sensory hair cells. Nature 449:87–91 Available at: http://www.nature.com/doifinder/10.1038/nature06091.

Keats JB, Lentz J (2013) Usher Syndrome Type I. NCBI Bookshelf.

Kennedy HJ, Evans MG, Crawford AC, Fettiplace R (2003) Fast adaptation of mechanoelectrical transducer channels in mammalian cochlear hair cells. Nat Neurosci 6:832–836.

Kikkawa Y, Mburu P, Morse S, Kominami R, Townsend S, Brown SDM (2005) Mutant analysis reveals whirlin as a dynamic organizer in the growing hair cell stereocilium. Hum Mol Genet 14:391–400.

Kim KX, Beurg M, Hackney CM, Furness DN, Mahendrasingam S, Fettiplace R (2013) The role of transmembrane channel-like proteins in the operation of hair cell mechanotransducer channels. J Gen Physiol 142:493–505 Available at: http://eutils.ncbi.nlm.nih.gov/entrez/eutils/elink.fcgi?dbfrom=pubmed&id=24127526&retmode=ref&cmd=prlinks\npapers2://publication/doi/10.1085/jgp.201311068.

Kim KX, Fettiplace R (2013) Developmental changes in the cochlear hair cell mechanotransducer channel and their regulation by transmembrane channel-like proteins. J Gen Physiol 141:141–148 Available at: http://www.pubmedcentral.nih.gov/articlerender.fcgi?artid=3536526&tool=pmcentrez&rendertype=abstract.

Kimberling WJ, Weston MD, Möller C, van Aarem a, Cremers CW, Sumegi J, Ing PS, Connolly C, Martini a, Milani M (1995) Gene mapping of Usher syndrome type IIa: localization of the gene to a 2.1-cM segment on chromosome 1q41. Am J Hum Genet 56:216–223.

Kroese AB, Das A, Hudspeth AJ (1989) Blockage of the transduction channels of hair cells in the bullfrog's sacculus by aminoglycoside antibiotics. Hear Res. 3:203-17

Kros CJ, Marcotti W, van Netten SM, Self TJ, Libby RT, Brown SDM, Richardson GP, Steel KP (2002) Reduced climbing and increased slipping adaptation in cochlear hair cells of mice with Myo7a mutations. Nat Neurosci 5:41–47.

Kros CJ, Rüsch A, Richardson GP (1992) Mechano-Electrical Transducer Currents in Hair Cells of the Cultured Neonatal Mouse Cochlea. Proceedngs Biol Sci R Soc.

Kurima K et al. (2002) Dominant and recessive deafness caused by mutations of a novel gene, TMC1, required for cochlear hair-cell function. Nat Genet 30:277–284.

L

Lamb JS, Chadwick RS (2011) Dual traveling waves in an inner ear model with two degrees of freedom. Phys Rev Lett 107:1–4.

Lane PW (1963) Whirler Mice - A Recessive Behavior Mutation in Linkage Group VIII. J Hered.

Le Calvez S, Avan P, Gilain L, Romand R (1998) CD1 hearing-impaired mice. I: Distortion product otoacoustic emission levels, cochlear function and morphology. Hear Res 120:37–50.

Lee HY, Raphael PD, Park J, Ellerbee AK, Applegate BE, Oghalai JS (2015) Noninvasive in vivo imaging reveals differences between tectorial membrane and basilar membrane traveling waves in the mouse cochlea. Proc Natl Acad Sci 112:3128–3133 Available at: http://www.pnas.org/lookup/doi/10.1073/pnas.1500038112.

Lefevre G, Michel V, Weil D, Lepelletier L, Bizard E, Wolfrum U, Hardelin J-P, Petit C (2008) A core cochlear phenotype in USH1 mouse mutants implicates fibrous links of the hair bundle in its cohesion, orientation and differential growth. Development 135:1427–1437 Available at: http://dev.biologists.org/cgi/doi/10.1242/dev.012922.

Liu X, Bulgakov O V, Darrow KN, Pawlyk B, Adamian M, Liberman MC, Li T (2007) Usherin is required for maintenance of retinal photoreceptors and normal development of cochlear hair cells. Proc Natl Acad Sci U S A 104:4413–4418.

Lopez-Poveda E a., Johannesen PT (2012) Behavioral estimates of the contribution of inner and outer hair cell dysfunction to individualized audiometric loss. JARO - J Assoc Res Otolaryngol 13:485–504.

Lumpkin EA, Hudspeth AJ (1995) Detection of Ca2+ entry through mechanosensitive channels localizes the site of mechanoelectrical transduction in hair cells. Proc Natl Acad Sci U S A 92:10297–10301.

Lumpkin EA, Marquis RE, Hudspeth AJ (1997) The selectivity of the hair cell's mechanoelectrical-transduction channel promotes Ca2+ flux at low Ca2+ concentrations. Proc Natl Acad Sci U S A 94:10997–11002 Available at: papers2://publication/uuid/85DC40FD-49C4-42C4-AB37-6EDB0CE48E57.

M

Mathur PD, Zou J, Zheng T, Almishaal A, Wang Y, Chen Q, Wang L, Vashist D, Brown S, Park A, Yang J (2015) Distinct expression and function of whirlin isoforms in the inner ear and retina: An insight into pathogenesis of USH2D and DFNB31. Hum Mol Genet 24:6213–6228.

Mburu P et al. (2003) Defects in whirlin, a PDZ domain molecule involved in stereocilia elongation, cause deafness in the whirler mouse and families with DFNB31. Nat Genet 34:421–428.

McGee J, Goodyear RJ, McMillan DR, Stauffer E a, Holt JR, Locke KG, Birch DG, Legan PK, White PC, Walsh EJ, Richardson GP (2006) The very large G-protein-coupled receptor VLGR1: a component of the ankle link complex required for the normal development of auditory hair bundles. J Neurosci 26:6543–6553.

Meyer A, Petit C, Safieddine S (2013) Thérapie génique des surdités humaines. Medecine/Sciences 29:883–889.

Mianné J, Chessum L, Kumar S, Aguilar C, Codner G, Hutchison M, Parker A, Mallon A-M, Wells S, Simon MM, Teboul L, Brown SDM, Bowl MR (2016) Correction of the auditory phenotype in C57BL/6N mice via CRISPR/Cas9-mediated homology directed repair. Genome Med 8:16 Available at: http://genomemedicine.com/content/8/1/16.

Michalski N, Michel V, Bahloul A, Lefèvre G, Barral J, Yagi H, Chardenoux S, Weil D, Martin P, Hardelin J-P, Sato M, Petit C (2007) Molecular characterization of the ankle-link complex in cochlear hair cells and its role in the hair bundle functioning. J Neurosci 27:6478–6488.

Michalski N, Michel V, Caberlotto E, Lefevre GM, Van Aken AFJ, Tinevez JY, Bizard E, Houbron C, Weil D, Hardelin JP, Richardson GP, Kros CJ, Martin P, Petit C (2009) Harmonin-b, an actin-binding scaffold protein, is involved in the adaptation of mechanoelectrical transduction by sensory hair cells. Pflugers Arch Eur J Physiol 459:115–130.

Michel V, Goodyear RJ, Weil D, Marcotti W, Perfettini I, Wolfrum U, Kros CJ, Richardson GP, Petit C (2005) Cadherin-23 is a component of the transient lateral links in the developing hair bundles of cochlear sensory cells. Dev Biol 280:281–294.

Møller A, Jannetta P (1983) Interpretation of brainstem auditory evoked potentials: results from intracranial recording in humans. Scand Audiol 12:125–133.

Mustapha M, Chouery E, Chardenoux S, Naboulsi M, Paronnaud J, Lemainque A, Mégarbané A, Loiselet J, Weil D, Lathrop M, Petit C (2002) DFNB31, a recessive form of sensorineural hearing loss, maps to chromosome 9q32-34. Eur J Hum Genet 10:210–212.

N

Nadeau JH (2001) Modifier genes in mice and humans. Nat Rev Genet 2:165–174.

Nakayama J, Hamano K, Iwasaki N, Nakahara S, Horigome Y, Saitoh H, Aoki T, Maki T, Kikuchi M, Migita T, Ohto T, Yokouchi Y, Tanaka R, Hasegawa M, Matsui A, Hamaguchi H, Arinami T (2000) Significant evidence for linkage of febrile seizures to chromosome 5q14-q15. Hum Mol Genet 9:87–91 Available at: http://www.ncbi.nlm.nih.gov/pubmed/10587582.

Narayanan P, Chatterton P, Corey DP, James M, Perrin BJ (2015) Length regulation of mechanosensitive stereocilia depends on very slow actin dynamics. Nat Commun 6:1–24 Available at: http://dx.doi.org/10.1038/ncomms7855.

Nikkila H, McMillan DR, Nunez BS, Pascoe L, Curnow KM, White PC (2000) Sequence similarities between a novel putative G protein-coupled receptor and Na+/Ca2+ exchangers define a cation binding domain. Mol Endocrinol 14:1351–1364.

Noben-Trauth K, Johnson KR (2009) Inheritance patterns of progressive hearing loss in laboratory strains of mice. Brain Res 1277:42–51 Available at: http://www.pubmedcentral.nih.gov/articlerender.fcgi?artid=2700199&tool=pmcentrez&rendertype=abstract.

O

Ohmori H (1985) Mechano-electrical transduction currents in isolated vestibular hair cells of the chick. J Physiol 359:189–217 Available at: http://www.pubmedcentral.nih.gov/articlerender.fcgi?artid=1193371&tool=pmcentrez&rendertype=abstract.

P

Pearsall N, Bhattacharya G, Wisecarver J, Adams J, Cosgrove D, Kimberling W (2002) Usherin expression is highly conserved in mouse and human tissues. Hear Res 174:55–63.

Peng AW, Effertz T, Ricci AJ (2013) Adaptation of Mammalian Auditory Hair Cell Mechanotransduction Is Independent of Calcium Entry. Neuron 80:960–972 Available at: http://dx.doi.org/10.1016/j.neuron.2013.08.025.

Pennings RJE, Huygen PLM, Weston MD, van Aarem A, Wagenaar M, Kimberling WJ, Cremers CWRJ (2003) Pure tone hearing thresholds and speech recognition scores in Dutch patients carrying mutations in the USH2A gene. Otol Neurotol 24:58–63.

Pepermans E, Michel V, Goodyear R, Bonnet C, Abdi S, Dupont T, Gherbi S, Holder M, Makrelouf M, Hardelin J-P, Marlin S, Zenati A, Richardson G, Avan P, Bahloul A, Petit C (2014) The CD2 isoform of protocadherin-15 is an essential component of the tip-link complex in mature auditory hair cells. EMBO Mol Med 6:984–992 Available at: http://www.pubmedcentral.nih.gov/articlerender.fcgi?artid=4119359&tool=pmcentrez&rendertype=abstract.

Petit C (2001) Usher Syndrome : From Genetics to Pathogenesis. 000.

Pickles JO, Comis SD, Osborne MP (1984) Cross-links between stereocilia in the guinea pig organ of Corti, and their possible relation to sensory transduction. Hear Res 15:103–112.

R

Randy McMillan D, Kayes-Wandover KM, Richardson JA, White PC (2002) Very large G protein-coupled receptor-1, the largest known cell surface protein, is highly expressed in the developing central nervous system. J Biol Chem 277:785–792.

Reichenbach T, Stefanovic A, Nin F, Hudspeth AJ (2012) Waves on Reissner's Membrane: A Mechanism for the Propagation of Otoacoustic Emissions from the Cochlea. Cell Rep 1:374–384.

Reisser CF V, Kimberling WJ, Otterstedde CR (2002) Hearing loss in Usher syndrome type II is nonprogressive. Ann Otol Rhinol Laryngol 111:1108–1111.

Riazuddin S et al. (2012) Alterations of the CIB2 calcium- and integrin-binding protein cause Usher syndrome type 1J and nonsyndromic deafness DFNB48. Nat Genet 44:1265–1271 Available at: http://dx.doi.org/10.1038/ng.2426.

Ricci a J, Wu YC, Fettiplace R (1998) The endogenous calcium buffer and the time course of transducer adaptation in auditory hair cells. J Neurosci 18:8261–8277 Available at: http://www.ncbi.nlm.nih.gov/pubmed/9763471.

Ricci a. J, Fettiplace R (1998) Calcium permeation of the turtle hair cell mechanotransducer channel and its relation to the composition of endolymph. J Physiol 506:159–173.

Ricci AJ (2005) The Transduction Channel Filter in Auditory Hair Cells. J Neurosci 25:7831–7839 Available at: http://www.jneurosci.org/cgi/doi/10.1523/JNEUROSCI.1127-05.2005.

Ricci AJ, Fettiplace R (1997) The effects of calcium buffers on mechanoelectrical transduction in turtle hair cells. Biophys J 72:Wpo98–Wpo98 Available at: //a1997we74701508.

Russell IJ, Richardson GP, K??ssl M (1989) The responses of cochlear hair cells to tonic displacements of the sensory hair bundle. Hear Res 43:55–69.

S

Sadeghi M, Cohn ES, Kelly WJ, Kimberling WJ, Tranebjoerg L, Möller C (2004) Audiological findings in Usher syndrome types IIa and II (non-IIa). Int J Audiol 43:136–143.

Sakai T, Umeki N, Ikebe R, Ikebe M (2011) Cargo binding activates myosin VIIA motor function in cells. Proc Natl Acad Sci U S A 108:7028–7033 Available at: http://www.pubmedcentral.nih.gov/articlerender.fcgi?artid=3084129&tool=pmcentrez&rendertype=abstract.

Schneider E, Märker T, Daser A, Frey-Mahn G, Beyer V, Farcas R, Schneider-Rätzke B, Kohlschmidt N, Grossmann B, Bauss K, Napiontek U, Keilmann A, Bartsch O, Zechner U, Wolfrum U, Haaf T (2009) Homozygous disruption of PDZD7 by reciprocal translocation in a consanguineous family: A new member of the Usher syndrome protein interactome causing congenital hearing impairment. Hum Mol Genet 18:655–666.

Schneider ME, Dose AC, Salles FT, Chang W, Erickson FL, Burnside B, Kachar B (2006) A new compartment at stereocilia tips defined by spatial and temporal patterns of myosin IIIa expression. J Neurosci 26:10243–10252 Available at: http://www.jneurosci.org/cgi/content/abstract/26/40/10243\npapers2://publication/doi/10.1523/JNEUROSCI.2812-06.2006.

Self T, Mahony M, Fleming J, Walsh J, Brown SD, Steel KP (1998) Shaker-1 mutations reveal roles for myosin VIIA in both development and function of cochlear hair cells. Development 125:557–566.

Sheng M, Sala C (2001) PDZ domains and the organization of supramolecular complexes. Annu Rev Neurosci:1–29.

Siemens J, Lillo C, Dumont R a, Reynolds A, Williams DS, Gillespie PG, Müller U (2004) Cadherin-23 is a component of the tip link in hair-cell stereocilia. Nature 428:950–955.

Skradski SL, White HS, Pt\kiek LJ (1998) Genetic Mapping of a Locus (mass1) Causing Audiogenic Seizures in Mice. Genomics 49:188–192 Available at: http://linkinghub.elsevier.com/retrieve/pii/S0888754398952296.

Strupp M, Thurtell MJ, Shaikh AG, Brandt T, Zee DS, Leigh RJ (2011) Pharmacotherapy of vestibular and ocular motor disorders, including nystagmus. J Neurol 258:1207–1222.

T

Tarchini B, Jolicoeur C, Cayouette M (2013) A Molecular Blueprint at the Apical Surface Establishes Planar Asymmetry in Cochlear Hair Cells. Dev Cell 27:88–102 Available at: http://dx.doi.org/10.1016/j.devcel.2013.09.011.

Tilney LG, Cotanche DA, Tilney MS (1992) Actin filaments, stereocilia and hair cells of the bird cochlea. VI. How the number and arrangement of stereocilia are determined. Development. 1:213-2

Toriello H, Reardon W, Gorlin RJ (2004) Hereditary Hearing Loss and Its Syndromes (Oxford Monographs on Medical Genetics) 2nd Edition

Trautwein P, Hofstetter P, Wang J, Salvi R, Nostrant A (1996) Selective inner hair cell loss does not alter distortion product otoacoustic emissions. Hear Res 96:71–82 Available at: http://www.ncbi.nlm.nih.gov/entrez/query.fcgi?cmd=Retrieve&db=PubMed&dopt=Citation&list_uids=8817308.

V

Van Aarem A, Pinckers AJLG, Kimberling WJ, Huygen PLM, Bleeker-Wagemakers EM, Cremers CWRJ (1996) Stable and progressive hearing loss in type 2A Usher's syndrome. Ann Otol Rhinol Laryngol 105:962–967.

van Wijk E, Pennings RJE, te Brinke H, Claassen A, Yntema HG, Hoefsloot LH, Cremers FPM, Cremers CWRJ, Kremer H (2004) Identification of 51 novel exons of the Usher syndrome type 2A (USH2A) gene that encode multiple conserved functional domains and that are mutated in patients with Usher syndrome type II. Am J Hum Genet 74:738–744.

van Wijk E, van der Zwaag B, Peters T, Zimmermann U, te Brinke H, Kersten FFJ, Märker T, Aller E, Hoefsloot LH, Cremers CWRJ, Cremers FPM, Wolfrum U, Knipper M, Roepman R, Kremer H (2006) The DFNB31 gene product whirlin connects to the Usher protein network in the cochlea and retina by direct association with USH2A and VLGR1. Hum Mol Genet 15:751–765.

Verpy E, Leibovici M, Michalski N, Goodyear RJ, Houdon C, Weil D, Richardson GP, Petit C (2011) Stereocilin connects outer hair cell stereocilia to one another and to the tectorial membrane. J Comp Neurol 519:194–210.

Verpy E, Leibovici M, Zwaenepoel I, Liu XZ, Gal A, Salem N, Mansour A, Blanchard S, Kobayashi I, Keats BJ, Slim R, Petit C (2000) A defect in harmonin, a PDZ domain-containing protein expressed in the inner ear sensory hair cells, underlies Usher syndrome type 1C. Nat Genet 26:51–55.

Vollrath M a, Eatock RA (2003) Time course and extent of mechanotransducer adaptation in mouse utricular hair cells: comparison with frog saccular hair cells. J Neurophysiol 90:2676–2689 Available at: http://www.ncbi.nlm.nih.gov/pubmed/12826658.

Von Bekesy G (1954) Some electro-mechanical properties of the organ of Corti. Ann Otol Rhinol Laryngol. 2:448-68

W

Walsh T, Shahin H, Elkan-Miller T, Lee MK, Thornton AM, Roeb W, Abu Rayyan A, Loulus S, Avraham KB, King MC, Kanaan M (2010) Whole exome sequencing and homozygosity mapping identify mutation in the cell polarity protein GPSM2 as the cause of nonsyndromic hearing loss DFNB82. Am J Hum Genet 87:90–94 Available at: http://dx.doi.org/10.1016/j.ajhg.2010.05.010.

Webb SW, Grillet N, Andrade LR, Xiong W, Swarthout L, Della Santina CC, Kachar B, Müller U (2011) Regulation of PCDH15 function in mechanosensory hair cells by alternative splicing of the cytoplasmic domain. Development 138:1607–1617.

Weil D, Blanchard S, Kaplan J, Guilford P, Gibson F, Walsh J, Mburu P, Varela A, Levilliers J, Weston MD (1995) Defective myosin VIIA gene responsible for Usher syndrome type 1B. Nature 374:60–61.

Weil D, El-Amraoui A, Masmoudi S, Mustapha M, Kikkawa Y, Lainé S, Delmaghani S, Adato A, Nadifi S, Zina Z Ben, Hamel C, Gal A, Ayadi H, Yonekawa H, Petit C (2003) Usher syndrome type I G (USH1G) is caused by mutations in the gene encoding SANS, a protein that associates with the USH1C protein, harmonin. Hum Mol Genet 12:463–471.

Weston MD, Eudy JD, Fujita S, Yao S, Usami S, Cremers C, Greenberg J, Ramesar R, Martini a, Moller C, Smith RJ, Sumegi J, Kimberling WJ, Greenburg J (2000) Genomic structure and identification of novel mutations in usherin, the gene responsible for Usher syndrome type IIa. Am J Hum Genet 66:1199–1210 Available at: http://www.pubmedcentral.nih.gov/articlerender.fcgi?artid=1288187&tool=pmcentrez&rendertype=abstract.

Weston MD, Luijendijk MWJ, Humphrey KD, Möller C, Kimberling WJ (2004) Mutations in the VLGR1 gene implicate G-protein signaling in the pathogenesis of Usher syndrome type II. Am J Hum Genet 74:357–366.

Wolfrum U (2003) The cellular function of the usher gene product myosin VIIa is specified by its ligands. Adv Exp Med Biol. 533:133-42

Wu YC, Ricci AJ, Fettiplace R (1999) Two components of transducer adaptation in auditory hair cells. J Neurophysiol 82:2171–2181.

X

Xiong W, Grillet N, Elledge HM, Wagner TFJ, Zhao B, Johnson KR, Kazmierczak P, M??ller U (2012) TMHS is an integral component of the mechanotransduction machinery of cochlear hair cells. Cell 151:1283–1295.

Y

Yagi H, Tokano H, Maeda M, Takabayashi T, Nagano T, Kiyama H, Fujieda S, Kitamura K, Sato M (2007) Vlgr1 is required for proper stereocilia maturation of cochlear hair cells. Genes to Cells 12:235–250.

Yang J, Liu X, Zhao Y, Adamian M, Pawlyk B, Sun X, McMillan RD, Liberman MC, Li T (2010) Ablation of whirlin long isoform disrupts the USH2 protein complex and causes vision and hearing loss. PLoS Genet 6:9.

Z

Zhao B, Wu Z, Grillet N, Yan L, Xiong W, Harkins-Perry S, M??ller U (2014) TMIE is an essential component of the mechanotransduction machinery of cochlear hair cells. Neuron 84:954–967.

Zhao Y, Yamoah EN, Gillespie PG (1996) Regeneration of broken tip links and restoration of mechanical transduction in hair cells. Proc Natl Acad Sci U S A 93:15469–15474.

Zou J, Mathur PD, Zheng T, Wang Y, Almishaal A, Park AH, Yang J (2015) Individual USH2 Proteins Make Distinct Contributions to the Ankle Link Complex during Development of the Mouse Cochlear Stereociliary Bundle. Hum Mol Genet:1–48.

Zou J, Zheng T, Ren C, Askew C, Liu XP, Pan B, Holt JR, Wang Y, Yang J (2014) Deletion of PDZD7 disrupts the Usher syndrome type 2 protein complex in cochlear hair cells and causes hearing loss in mice. Hum Mol Genet 23:2374–2390.

Abstract

Usher syndrome (USH) is characterised by a sensorineural congenital deafness and a progressive loss of vision by retinitis pigmentosa. During my PhD, my main focus of study was a gene responsible for Usher syndrome type 2, *USH2A*. This gene codes for usherin, a protein associated with the fibrous links located at the base of the hair bundle of cochlear, and vestibular hair cells. In mice, these transitory links start to disappear as of postnatal day 9 (P9), and the molecular complex with which they are associated is composed of usherin, adgrv1 (an adhesion G protein coupled receptor), whirlin, and pdzd7 (two submembranous PDZ domain-containing scaffold proteins). Previous work has shown that the interaction in between these 4 proteins is essential for the development of the hair bundle, the structure responsible for the initiation of the mechano-electrical transduction (MET) process in the hair cells.

During my thesis, I studied the short term and long term effects of the absence of the longest of the 2 usherin isoforms, the transmembrane b-isoform, in mice carrying a mutation in the *Ush2a* gene ($Ush2a^{\Delta TM/\Delta TM}$). In these mice, I measured mechano-electrical currents, auditory brainstem responses, undertook auditory masking tests, and analysed scanning electron micrographs of cochlear hair bundles. Through this work, I showed that basal lateral links similar to ankle links could be observed on P4, and that MET currents were normal on P7. The absence of the long b-isoform of usherin actually has very little effect on the morphology or the function of the cochlear hair bundle in mice, until 3 or 4 months of age. As of 4 months old however, $Ush2a^{\Delta TM/\Delta TM}$ mice suffer from a progressive hearing loss, and frequency selectivity defects, mainly cause by a dysfunction of outer hair cells. These results will further add to the debate on whether the hearing loss in Usher syndrome type 2A is progressive or not. Hearing loss in USH2A patients is generally considered non progressive, but several studies have given indication to the contrary. My work has shown that in mice, deafness caused by mutations to the *Ush2a* gene can also follow a progressive pattern. The potential existence of this temporal window in USH2A patients whose hearing impairment is less severe at birth, but gets worse over time, could allow clinicians to use gene therapy as curative treatment for patients who fall into this category.

Résumé

Le syndrome d'Usher (USH) associe une surdité neurosensorielle congénitale et une perte progressive de la vision par rétinite pigmentaire. Pendant ma thèse, l'essentiel de mon travail a porté sur un gène responsable du syndrome d'Usher de type 2, *USH2A*. Ce gène code pour l'usherine, une protéine associée aux liens fibreux interstéréociliaires situés à la base de la touffe ciliaire des cellules ciliées de la cochlée et du vestibule. Ces liens transitoires disparaissent autour du 9^{e} jour post-natal (P9) chez la souris, et le complexe moléculaire associé à ces liens inclut l'usherine, adgrv1 (un récepteur membranaire couplé aux protéines G), la whirline, et pdzd7 (deux protéines sous-membranaires d'échafaudage contenant des domaines PDZ). Des travaux précédents ont montré que l'interaction de ces quatre protéines était nécessaire à un développement correct de la touffe ciliaire, qui lui-même conditionne la transduction mécano-électrique opérée par les cellules ciliées.

Pendant ma thèse, j'ai étudié les effets, à court terme et à long terme, de l'absence de la plus longue des 2 isoformes connues de l'usherine, l'isoforme-b transmembranaire, sur des souris mutantes pour le gène *Ush2a* (*Ush2a*$^{\Delta TM/\Delta TM}$). Chez ces souris, j'ai effectué des mesures de courants de transduction mécano-électrique, des enregistrements des potentiels évoqués auditifs (PEA), des tests de masquage auditif, et une analyse morphologique des cellules ciliées par imagerie au microscope électronique à balayage. Ainsi, j'ai pu montrer que les liens interstéréociliaires basaux étaient présents à P4 et que les courants de transduction mécano-électrique étaient normaux à P7. L'absence de l'isoforme-b de l'usherine n'a, en fait, que très peu de conséquences morphologiques et fonctionnelles sur la touffe ciliaire des cellules ciliées de la cochlée durant les 3 ou 4 premiers mois de vie chez la souris. A partir de l'âge de 4 mois cependant, les souris *Ush2a*$^{\Delta TM/\Delta TM}$ souffrent d'une perte progressive de l'audition et d'anomalies de la sélectivité dans l'analyse des fréquences du son, dues surtout à un dysfonctionnement des cellules ciliées externes. Ces résultats viennent alimenter le débat sur le caractère progressif de la surdité du syndrome d'Usher de type 2A. La surdité des patients USH2A est considérée comme étant le plus souvent non progressive, mais plusieurs études ont révélé que certains patients souffrent en fait d'une surdité progressive. Mon travail a permis de montrer que chez la souris, la surdité en rapport avec des mutations d'*Ush2a* peut également être progressive. L'existence potentielle d'une fenêtre temporelle chez les patients USH2A dont la surdité moins sévère à la naissance, va ensuite s'aggraver, pourrait permettre d'envisager dans le futur un traitement curatif précoce du déficit auditif de ces patients, par thérapie génique.